UCONN LIBRARY

University of Connecticut
OpenCommons@UConn

Doctoral Dissertations | University of Connecticut Graduate School

5-2-2018

Modulating Aged Macrophages and Osteoprogenitors with a Calcium Phosphate Drug Delivery System

Jumana Alhamdi
University of Connecticut - Storrs, jumana.alhamdi@uconn.edu

Follow this and additional works at: https://opencommons.uconn.edu/dissertations

Recommended Citation
Alhamdi, Jumana, "Modulating Aged Macrophages and Osteoprogenitors with a Calcium Phosphate Drug Delivery System" (2018). *Doctoral Dissertations*. 1778.
https://opencommons.uconn.edu/dissertations/1778

Modulating Aged Macrophages and Osteoprogenitors with a Calcium Phosphate Drug Delivery System

Jumana Rajeh Alhamdi, PhD, University of Connecticut, 2018

ABSTRACT

Older adults suffer from weakened and delayed bone healing due to age-related alterations in bone cells and in the immune system. Given the interaction between the immune system and skeletal cells, therapies that address deficiencies in both the skeletal and the immune system are required to effectively treat bone injuries of older patients. The sequence of macrophage activation observed in healthy tissue repair involves a transition from a pro-inflammatory state followed by a pro-reparative state. In older patients, inflammation is slower to resolve and impedes healing. The goal of this dissertation was to design a novel drug delivery system for temporal guidance of the polarization of macrophages using bone grafting materials. A biomimetic calcium phosphate coating (bCaP) physically and temporally separated the pro-inflammatory stimulus interferon-gamma (IFNγ) from the pro-reparative stimulus simvastatin (SIMV). Effects on both human (THP-1) and aged mouse bone marrow macrophages were tested. Sequential M1-to-M2 activation was achieved with both cell types. Successful osteogenic differentiation of human osteoprogenitors derived from older patients was confirmed with the delayed delivery of SIMV from bCaP. These results suggest that this novel immunomodulatory drug delivery system holds potential for controlling macrophage activation to maximize older patient bone healing. In vitro studies prove our hypothesis and show successful macrophage phenotype modulation and improved in vitro osteogenesis in preparation for future in vivo studies.

Modulating Aged Macrophages and Osteoprogenitors with a Calcium Phosphate Drug Delivery System

Jumana Rajeh Alhamdi

B.S., University of Baghdad, 2009

M.S., University of California San Diego, 2014

A Dissertation

Submitted in Partial Fulfillment of the

Requirements for the Degree of

Doctor of Philosophy

at the

University of Connecticut 2018

APPROVAL PAGE

Doctor of Philosophy Dissertation

Modulating Aged Macrophages and Osteoprogenitors with a Calcium Phosphate Drug Delivery System

Presented by

Jumana Rageh Alhamdi, M.S.

Major Advisor _____
Liisa T. Kuhn

Associate Advisor _____
Marja M. Hurley

Associate Advisor _____
Sangamesh G. Kumbar

Associate Advisor _____
Lakshmi S. Nair

University of Connecticut

2018

Acknowledgements

First and foremost, I would like to start by thanking my advisor, Dr. Liisa Kuhn, without whom this work would not have been possible. It has been an honor to be her student. I thank her for supporting and encouraging me to stay positive even when research was a struggle. No matter how many meetings were scheduled, grants due, papers to review, conferences to chair, classes to teach, seminars to host or family events to attend, I always felt I could knock on Dr. Kuhn's door and she would make the time to answer my questions. To feel like this much of a priority kept me motivated and encouraged me to continue my research. Dr. Kuhn made me a better writer, taught me to ask the right scientific questions, to speak up with confidence when it comes to science and always provided me with positive quotes like "rejection is redirection", "FAIL: First Attempt In Learning". I am also thankful for the excellent example she has provided as a successful woman in engineering and professor.

I would like to also thank my committee members, Drs. Hurley, Kumbar, and Nair, whom have provided many helpful discussions about my work, which have helped shaping this dissertation and improved the quality of the research. I thank them for providing their insight through rigorous discussion of my data and how it fits into the bigger picture. I am fortunate to have such a group of intelligent scientists, who are also student advocates, on my committee. I would also like to thank Dr. Kara Spiller from Drexel University for her valuable input in the design and interpretation of my studies with macrophages. I appreciate all their contributions of time, ideas, and input to make my Ph.D. experience more productive.

I also appreciate the help given by my UConn friends whom have fostered this wonderful learning environment. I'm especially grateful to Dr. Kelly Hawley for her help with the human macrophages and for her support during the last few stressful months. I would like to express my appreciation for the fun environment that Assistant Professor Alix Deymier and Dr. Brian Wingender brought to the lab and for their support.

I owe special thanks to my husband, Dr. Sinan Alhamdi, for his continued love, support and understanding during my pursuit of Ph.D degree that made the completion of this thesis possible. He moved 3 times with me, and was always there to support me when I didn't think I could make it to the end of this long road. Thank you for everything you've done, thank you for supporting my research, brining me dinner when I worked late nights and never complained about me spending so much time in the laboratory. Thank you for those weekends when you drove me to work so we would spend more time together. You have been patient when I'm frustrated, you celebrate with me when even the littlest things go right, and you are there whenever I needed you to listen. I greatly value your contribution and deeply appreciate your belief in me. Thank you for being such wonderful husband and friend.

Finally, I acknowledge the people who mean a lot to me, my parents, Rageh and Entsar, for showing faith in me and giving me liberty to choose what I desired. I thank my father who raised me with a love for science and taught me ambition, desire to help others, and to always work hard until the end to celebrate the rewords. I thank my mother for the selfless love, care, pain and sacrifice she did to shape my life. Although you hardly understood what I researched, you were willing to listen. Thank you for being there to encourage me every step of the way and for your willingness to give of yourselves so that your children can succeed. I would never be able to pay back the love and affection showered upon me by my parents. Also, I express my thanks to my father in law, Ali, my mother in law, Shoaa, and my sisters, Ruaa, Rand and Zainab, for their love and moral support.

رسالة شكر وتقدير

أولاً وقبل كل شيء، أود أن أبدأ بتوجيه الشكر إلى أستاذتي الدكتورة ليسا كوون التي لم يكن لهذا العمل أن يتم دون إشرافها وتوجيهها. لقد كان شرفاً أن أكون طالبتها. واود ايضا ان أشكرها على دعمها وتشجيعها لي للبقاء واثقةً من نفسي حتى في أوقات كون البحث صراعا. على رغم العديد من الاجتماعات التي تمت، والحاجة إلى إنهاء كتابة طلب المنح، والأوراق العلمية التي تحتاج المراجعة، والمؤتمرات التي أحتاجت ترؤسها، والدروس التي تحتاج التدريس، والحلقات الدراسية التي تحتاج الإستضافة، أو الأحداث العائلية التي تتطلب الحضور، كنت دائماً أشعر أن بامكاني أن أطرق باب الأستاذة كوون، وأنها سوف ستأخذ من وقتها الثمين جزءاً للإجابة على أسألتي. لقد أبقاني شعوري بتلك الأهمية بالنسبة لها متحفزةً ومتشجعةً على مواصلة بحثي. لقد جعلتني الأستاذة كوون كاتباً أفضل، وعلمتني أن أطرح السؤال العلمي الصحيح، والتحدث بثقة عندما يتعلق الأمر بالعلم، وقدمت لي دائما مع نصائح إيجابية مثل "رفض الفكرة ليس سوى إعادة توجيه" و"الفشل هو الخط الأول في التعلم". وأنا أيضاً ممتنة للمثال الرائع الذي قدمته لي كامرأة ناجحة في الهندسة وكأستاذه.

أود أيضاً أن أشكر الأساتذة الدكتور هرلي، والدكتور كمبار، والدكتور ناير أعضاء لجنة المناقشة لهذا البحث والذين أبدوا العديد من الملاحظات المفيدة حول عملي، والتي ساعدت في تشكيل هذه الأطروحة وتحسين نوعية البحث. أشكرهم جداً على تقديم رؤيتهم من خلال مناقشات دقيقة حول البيانات التي استخدمتها وكيفية تناسبها مع الأطار الأكبر للبحث. أنا محظوظة أن يكون لدي مثل هذه المجموعة من العلماء الأذكياء في لجنة المناقشة، والذين هم أيضا من المهتمين بالطلبة ونجاحهم. وأود أيضاً أن أشكر الدكتورة كارا سبيلر من جامعة دريكسل على مدخلاتها وتوجيهاتها القيمة من أجل إكمال تصميم وتنفيذ الدراسة حول الخلايا اللمفيه الكبير أنا أقدر كل مساهماتهم بالوقت، والأفكار، والمدخلات لجعل تجربة الدكتوراه بالنسبة لي تجربة أكثر غنىً.

كما أقدر المساعدة التي قدمها أصدقائي في جامعة كونكتيكت الذين عززوا تلك البيئة التعليمية الرائعة. أنا ممتنة بشكل خاص للدكتورة كيلي هاولي لمساعدتها في العمل على الخلايا اللمفيه الكبير البشريه ودعمها خلال الأشهر المجهدة القليلة الماضية. أود أن أعرب عن تقديري للبيئة الممتعة التي جلبتها الدكتورة ألكس ديميرو الدكتور براين ويندنجر لمختبر البحث ودعمهم المستمر.

أنا مدينة بشكر خاص لزوجي، الدكتور سنان الحمدي، لحبه المستمر، ودعمه، وتفهمه لظروفي أثناء سعيي للحصول على شهادة الدكتوراه والتي جعلت أمر إنهاء هذه الرسالة أمراً ممكناً. لقد انتقل ثلاث مراتٍ من أجلي، وكان دائماً موجوداً لدعمي عندما كنت أعتقد أني لن أستطيع الوصول إلى نهاية مطاف هذا الطريق الطويل. أشكرك على كل ما قمت به، وشكراً لك على دعم بحثي، وجلب العشاء لي عندما كنت أعمل إلى وقتٍ متأخر من الليل، ولم تشكِ أبداً من قضائي الكثير من الوقت في المختبر. أشكرك على عطلات نهاية الإسبوع تلك عندما كنت تأخذني بسيارتك للعمل لكي نقضي المزيد من الوقتِ معاً. لقد كنت صبوراً جداً معي عندما كنت أشعر بالإحباط، وكنت تحتفل معي عندما تحدث أصغر الأشياء بشكلٍ صحيح، وكنت هناك دائماً كلما كنتُ في حاجة لك للإستماع لي. أنا أقدر كثيراً مساهمتك في حياتي وإيمانك بي وفي عملي. شكراً لك على كونك هذا الزوج والصديق الرائع.

وأخيرا، أحب أن أشير للناس الذين يعنون الكثير بالنسبة لي، وهم والديّ ، المهندس راجح وإنتصار، اللذان أظهرا الإيمان بي ومنحاني الحرية في اختيار ما أريد. أشكر والدي الذي زرع فيّ حب العلم وعلمني الطموح، والرغبة في مساعدة الآخرين، والعمل دائماً بجد حتى النهاية للإحتفال بالمكافآت. أشكر والدتي على الحب الذي ليس له حدود، والرعاية، والتضحية التي قامت بها لتشكيل حياتي. فإنكِ كنتِ دوماً على إستعداد للاستماع لي. أشكركم على وجودكم لتشجيعي على كل خطوة على الطريق، وعلى إستعدادكم لتقديم كل مايمكن لكم لتمكين أبناؤكم على النجاح. لن أكون قادرةً أبداً على رد مقدار الحب والمودة التي غمرها والدي علي. كما أتقدم بالشكر إلى عمي المهندس علي الحمدي، و خالتي الغالية شعاع، وأخواتي رؤى ورند وزينب، على حبهم ودعمهم المعنوي.

Table of Contents

List of Figures

compared to cells cultured on AntiA-bCaP-PEM30-FGF2 (+A/+F) at 4 h, 1, 2, and 3 days of culture. (C) Percent LIVE® stained area of RAW cells on bCaP coating showing access to AntiA on day 3 of culture (** $P < 0.01$, **** $P < 0.001$),). (D) Fluorescent LIVE stained images of cells cultured on bCaP-FGF2 (-A/+F) as compared to cells cultured on AntiA-bCaP-FGF2 (+A/+F) at 4 h, 1, 2, and 3 days of culture. Scale bar = 100 μm.

Figure 2.5: Scanning electron microscopy of bCaP with AntiA. (Column A) SEM of AntiA-bCap(24)-PEM before cell culture. (Column B) SEM of AntiA-bCap(24)-PEM coated disk and incubated in cell medium for 4hrs and 3 days without cells. (Column C) 4hrs and Day3 LIVE staining +A/+F AntiA-bCaP(24)-PEM-MC3T3-E1. (Column D) 4hrs and Day-3 LIVE staining +A/+F AntiA-bCaP(24)-PEM-RAW.

Figure 2.6: SEM imaging of AntiA-bCaP coated disks (Column A) SEM of AntiA-bCap(24) before cell culture. (Column B) SEM of AntiA-bCap(24) coated disk and incubated in cell medium for 4hrs and 3 days without cells. (Column C) 4hrs and Day3 LIVE staining +A/+F AntiA-bCaP(24)-MC3T3-E1. (Column D) 4hrs and Day-3 LIVE staining +A/+F AntiA-bCaP(24)- RAW.

Figure 2.7 : SEM images of bCaP (48hrs). (Column A) bCap(48) before cell culture with AntiA and without AntiA. (Column B) 4hrs and Day3 LIVE staining –A/+F-bCaP(48)-MC3T3-E1, bCa(48) coating after 4hrs and 3 days of cell culture –A/+F and correspondent SEM imaging. (Column C) 4hrs and Day3 LIVE staining +A/+F-bCaP(48)-MC3T3-E1 and SEM images of the coating after 4hrs and 3 days of cell culture.

Figure 3.1: Evaluation of the kinetics of THP-1 macrophage access to the cytotoxic AntiA molecule below the biomimetic calcium phosphate (bCaP) barrier coating. (A) Schematic representation of the bCaP coating and AntiA location. (B) Quantified percent LIVE® stained

area of THP-1 cells on bCaP coating (**** $P < 0.001$). (C) Fluorescent LIVE® stained images of cells cultured on bCaP alone (-A) as compared to cells cultured on bCaP-AntiA (+A) at over time in culture. Scale bar = 100 μm.

Figure 3.2: Gene expression of human THP-1 macrophages cultured on bCaP as compared to non-tissue culture-treated polystyrene (PS) on day 1 and day 6 of culture. (A-C) M1 macrophage markers. (D and E) M2 macrophage markers. qRT-PCR data presented as fold change over the housekeeping gene GAPDH. * $P < 0.05$.

Figure 3.3: Simvastatin dose response study. Gene expression of human THP-1 macrophages cultured on bCaP with either 2 or 10 μg SIMV beneath the bCaP with LPS and IFNγ in the media for the first three days. (A-C) M1 macrophage markers and (D and E) M2 macrophage markers. (F) Schematic representation of the experimental configuration. qRT-PCR data presented as fold change over the housekeeping GAPDH and normalized to M0 macrophages cultured on bCaP without drug. * $P < 0.05$.

Figure 3.4: IFNγ dose response study in combination with 10 μg SIMV. Gene expression of human THP-1 macrophages cultured on bCaP with IFNγ on the exterior and SIMV below the bCaP barrier layer. (A- C) M1 macrophage markers. (D and E) M2 macrophage markers. Data presented as fold change over the housekeeping gene GAPDH. * $P < 0.05$.

Figure 3.5: Gene expression for THP-1 cultured on bCaP surface with or without 250 ng IFNγ or 10 μg SIMV or both over 6 days. (A-C) M1 macrophage markers and (D and E) M2 macrophage markers. (F) Schematic representation of the sequential delivery system. * $P < 0.05$.

Figure 3.6: Gene expression of old murine bone marrow derived macrophages over time when cultured on bCaP with 250 ng IFNγ on the exterior and 10 μg SIMV below the bCaP barrier

layer as compared to culture on the bCaP layer only. (A-C) M1 markers. (D and F) M2 markers. * $P < 0.05$.

Figure 3.7: A comparison of the gene expression of primary bone marrow macrophages from young adult and old mice during culture on bCaP with 10 μg SIMV below the bCaP barrier layer. The M1 stimuli LPS and IFNγ were in the culture medium for the first 3 days. (A-C) M1 macrophage markers. (D, E) M2 macrophage markers. Data normalized to GAPDH and then expressed as fold change over M0 macrophages cultured on bCaP. * $P < 0.05$.

Figure 4.1: Age-related changes in osteoprogenitors (A) RT-qPCR cytokines gene expression. older human osteoprogenitors, 73 years old, as compared to younger cells, 44 years old. Data presented as fold-change over 4hrs baseline. Statistical analysis was performed using GraphPad software. t: test analysis of each gene of young vs old was performed and a $P < 0.05$ was considered significantly different. (B) β-Galactosidase (SABG) senescent staining of Osteoprogenitors obtained from 78 Years old female bone chip cells culture Scale bar=200um.

Figure 4.2: RT-qPCR cytokines gene expression of inflammatory cytokines of 66 years old human osteoprogenitors treated with SIMV-A. (A). Day 3 gene expression of inflammatory cytokines with SIMV-A given at 4hrs and continues twice a week until day 21. (B). Day 6 gene expression of inflammatory cytokines with SIMV-A given at day 3 continues twice a week until day 21. (C) Day 10 gene expression of inflammatory cytokines with SIMV-A given at day 7 continues twice a week until day 21. Data presented as fold-change compared to 4hrs baseline. Statistical analysis was performed using GraphPad software. t: test analysis of each time point was performed and a $P < 0.05$ was considered significantly different.

Figure 4.3: XO staining of human osteoprogenitor 66 years old , passage 2 seeded cells at 15,000 cells/cm^2, treated with SIMV-A at various timing. Green frame indicates the start time of

SIMV-A treatment. A) 0.5nM of simvastatin was pipetted after 4hrs of culture and continued twice a week until day 30. B) 0.5nM of simvastatin was pipetted on day 3 of culture and continued twice a week until day 30. C) 0.5nM or 10 nM of simvastatin was pipetted with osteogenic medium on day 7 of culture and continued twice a week until day 30. Scale bar 100 um.

Figure 4.4: Calcium content and gene expression of human osteoprogenitor 66 years old treated with SIMV-A at various timing showing enhanced osteogenesis by delayed SIMV-A as measured by (A) Calcium content on day 30 of culture. (B, C, D) Osteogenic genes (*BSP*, *OCN* and *BMP-2*) with low dose ,0.5nM, given at day 7 as compared to higher dose given at the same time. Data presented as fold-change compared to day 7 baseline. Statistical analysis was performed using GraphPad software. Two way ANOVA multiple comparison analysis was performed and a $P < 0.05$ was considered significantly different (*$P < 0.05$, ****P= < 0.0001).

Figure 4.5: Human osteoprogenitor 62 years old seeded on bCaP coated disks (C) or (S) 2 μg or 10 μg SIMV-bCaP. (A) AlamarBlue cell proliferation assay (B) Gene expression anti-inflammatory markers (*IL1β, IL6* and *TNFα*) and pro-reparative *IL10*. Data presented as fold-change compared to control. Statistical analysis was performed using GraphPad software. Two way ANOVA multiple comparison analysis of each gene was performed and a $P < 0.05$ was considered significantly different.

Figure 4.6: Osteogenic gene expression of Older human osteoprogenitor (62 YO) with delayed delivery of 2 μg or 10 μg SIMV from bCaP. (A) *COL1A1*. (B) *BSP* and (C) *OCN*. QPCR presented in fold change over day 7 (baseline) using 2-ΔΔCT. Statistical analysis was performed using GraphPad software. Unpaired t: test analysis of each time point was performed and a $P < 0.05$ was considered significantly different.

List of Abbreviations

MCSF	Macrophage colony-stimulating factor
GCSF	Granulocyte colony-stimulating factor
SDF 1	Stromal cell-derived factor-1
IGF	Insulin-like growth factor
IL6	Interleukin 6 gene
IL10	Interleukin 10 gene
IL1β	Human Interleukin 1- beta gene
Il1β	Mouse Interleukin 1- beta gene
TNFα	Tumor necrosis factor alpha gene
MSCs	Mesenchymal stem cells
TGF-β	Transforming growth factor-beta
PDGF	Platelet Derived Growth Factor
FGF-2	Fibroblast growth factor-2
IGF	insulin-like growth factor
BMPs	Bone morphogenetic proteins
VEGF	Vascular endothelial growth factor
RANK	Receptor activator of nuclear factor kappa-β
RANKL	Receptor activator of nuclear factor kappa-β ligand
OPG	Osteoprotegerin
RUNX2	Runt-related transcription factor 2
hASCs	Human adipose stem cells

mRNA	Messenger Ribonucleic acid
DNA	Deoxyribonucleic acid
FDA	Food and Drug Administration
BMD	Bone Mass Density
M1	Proinflammatory macrophages
M2	Pro- regenerative macrophages
LPS	Lipopolysaccharide
JAK	Janus kinase
ICAM-1	Intercellular Adhesion Molecule 1
bCaP(24)	Nanocrystalline calcium phosphate made with SBFX5
bCaP (48)	Nanocrystalline calcium phosphate made with 24 h in Solution A
SBFx5	Simulated body fluid with 5x normal ionic concentrations
PEM	Polyelectrolyte multilayer
PLGlut	Poly-L-Glutamic acid
PLLys	Poly-L-Lysine
-A/+F	No AntiA, with FGF-2
+A/-F	With AntiA, no FGF-2
+A/+F	AntiA and FGF-2
AntiA	Antimycin A
TCPsb	Tissue culture plastic sand blasted disk inserts
ELISA	Enzyme-linked immunosorbent assay
FBS	Fetal bovine serum
MC3T3-E1	Mouse osteoprogenitor cells

RAW	RAW 264.7 mouse monocyte-macrophage cell-line
THP-1	Human monocyte-macrophage cell-line
SEM	Scanning electron microscopy
PBMC	Peripheral blood mononuclear cell
PMA	Phorbol-12-myristate 13-acetate
hPB	human peripheral blood
M-BMM	Mouse Bone Marrow Derived Macrophages
SIMV	Simvastatin HMG-CoA reductase inhibitors therapeutic agent for cardiovascular disease
GAPDH	Glyceraldehyde 3-phosphate dehydrogenase
CCL1	Human Chemokine ligand 1 gene
CXCL10	C-X-C motif chemokine 10 is a protein that in humans is encoded by the *Cxcl10* gene.
CXCL11	C-X-C motif chemokine 11 is a protein that in humans is encoded by the *Cxcl11* gene.
Cxcl11	C-X-C motif chemokine 10 is a protein that in mouse is encoded by the *Cxcl11* gene.
CD163	Cluster of Differentiation 163, a protein that in humans is encoded by the CD163 gene [Hemoglobin-Haptoglobin Scavenger Receptor]
CCL17	Human Chemokine ligand 17 (also known as TARC) gene
Ccl17	Mouse Chemokine ligand 17 (also known as TARC) gene
CD193	C-Type Mannose Receptor 1, also termed as MRC1 (C-type mannose receptor 1)
Nos2	Nitric oxide synthases are a family of enzymes catalyzing the production of nitric oxide from L-arginine
Arg1	Gene encodes the protein arginase
SASP	Senescence-associated secretory phenotype
SA-β-gal	Senescence-associated β-galactosidase
TGFα	Transforming Growth Factor Alpha

MCP1	Monocyte Chemotactic Protein-1
COL1A1	Human Collagen Type I Alpha 1 Chain gene
BSP	Human Bone sialoprotein gene
OCN	Human Osteocalcin gene

Chapter 1

Background and Specific Aims

1.1 Introduction

Bone is a unique organ that constantly remodels to maintain strong structure for daily forces applied to it. Our bones are a very important component of the oral and skeletal system and functionally interact with many other organs and tissues including bone marrow, lymphoid tissue, kidneys, adipose tissue, endocrine pancreas, brain and gonads [1]. Bone homeostasis is a continuous process composed of a balance between bone resorption and bone formation that is necessary to maintain structural integrity in response to loading, to repair damaged bone and to maintain normal physiological mineral levels.

After the first few decades of life, there will be rapid decline in bone formation while bone resorption stays constant causing bone fragility and reduction in bone's ability to heal [2-4]. Fractures and bone trauma can occur in people of any age; however, the number of broken bones increases with advanced age. In the older patients a combination of osteoporosis, decreased in bone density, and increased incidence of fall results in more bone injuries than younger patients [5, 6]. In addition to estrogen deficiency and inadequate intake of calcium and vitamin D, there are biological changes that occur in the older human associated with oxidative stresses and telomere shortening including cellular senescence, fat increase, chronic inflammation and reduced ability to fight infection [7].

The growing older population, anticipated to reach more than 25% in 2060 in the US [8], makes it essential to develop therapeutic bone repair strategies specifically geared towards the

older person, in addition to treatments for the younger person. Understanding the bone regeneration capacity in the older patient is essential when developing therapeutic strategies for bone regeneration designed specifically to heal older bone in a timely manner. Therefore this chapter will focus on reviewing bone repair and healing affected by aging as well as strategies involved in localized delivery of biomolecules to counter age related decline of bone repair processes.

This chapter begins by describing the immune system as related to bone repair, then the effect of the aging process on immune system with detailed information about how macrophages, bone homeostasis and repair are affected by age-associated inflammation. Existing strategies for countering the age-related decline of bone regeneration processes are described, particularly those involving localized delivery of molecules. In general, this dissertation focused on the development of a novel, biomimetic, a sequential delivery system capable of modulating macrophage phenotypes that could also stimulate osteogenesis of older human osteoprogenitors.

1.1.1 Bone Repair and Osteoimmunology

1.1.1.1 Bone Repair phases

Bone heals and repairs itself in two ways; primary (direct) fracture healing requires fixation, or secondary (indirect) fracture healing. Flat bone (craniofacial bones) heals via intramembranous healing while long bones heals via endochondral ossification. The majority of bones heal via the secondary (indirect) fracture healing which consists of both endochondral and intramembranous bone healing [9]. The indirect bone healing process involves events that

orchestrate five sequential and overlapping phases including hematoma formation, inflammation, soft callus formation, hard callus formation, and bone remodeling [10]. At the cellular level, the key players in the overall repair process include: inflammatory cells, vascular cells, osteoprogenitors, and osteoclast. After bone injury, the very first response is hematoma formation which initiates the acute inflammatory stage. This step is critical to bone healing because the hematoma initiates the signaling cascade that leads to successful bone formation [10].

The hematoma and inflammation phases involve immune cells from the peripheral blood, bone marrow cells and the invasion of inflammatory cells. The same pro-inflammatory stimuli that activate the clotting forming hematoma cascade also activate neutrophils, monocytes, and macrophages [11]. This cellular response results in the secretion of a wide range of cytokines and growth factors including macrophage colony stimulating factor (M-CSF), granulocyte colony-stimulating factor (GCSF), stromal cell-derived factor-1 (SDF 1), interleukins-1 and -6 (IL1 and 6), and tumor necrosis factor-α (TNF-α) [3, 12, 13]. The secretion of these factors facilitate the recruitment of additional inflammatory cells, and enhance the migration and invasion of essential mesenchymal stem cells (MSCs) [14, 15]

In endochondral ossification, after the inflammatory phase, cartilaginous tissue will then form soft callus involving chondrocytes and fibroblasts to provide mechanical support to the fracture and act as a template for the bony callus. Chondrocytes are derived from mesenchymal progenitors their function appears by the synthesis of the cartilaginous matrix [16]. After all granulation tissues are replaced by cartilage, the chondrocytes undergo hypertrophy and mineralize the cartilaginous matrix before apoptosis. The proliferation and differentiation of both

fibroblast and chondrocyte are stimulated by the coordinated expression of growth factors including Transforming growth factor-beta (TGF-β2 and -β3), Platelet Derived Growth Factor (PDGF), fibroblast growth factor-1 (FGF-1), insulin-like growth factor (IGF) , and BMP family (BMP-2, -4, -5 and -6) [16]. These factors will then activate bone cells osteoblast to start the hard callus formation phase (forming mineralized bone matrix). The hard callus formation begins by the removal of the soft callus with revascularization [12].

The hard callus can form in the absence of a cartilaginous template in intramembranous bone formation. During intramembranous ossification, compact and spongy bone forms directly from sheets of undifferentiated mesenchymal cells. The flat bones of the face, most of the cranial bones, and the clavicles are formed via intramembranous ossification. The process begins by inflammatory and mesenchymal cells migration to the injury site [17]. These MSCs will first proliferate and condense into compact nodules then they begin to differentiate into specialized cells (osteoprogenitors and then osteoblasts), early osteoblasts appear in a cluster called the ossification center. The osteoblasts secrete osteoid, uncalcified matrix consisting of collagen precursors and other organic proteins (type 1 collagen, bone sialoprotein and osteocalcin [18]), which calcifies with alkaline phosphatase enzyme [19], thereby entrapping the osteoblasts within the mineralized matrix. Once entrapped, the osteoblasts will then differentiate into osteocytes or mature bone cells [19]. As osteoblasts transform into osteocytes, osteoprogenitors in the surrounding connective tissue differentiate into new osteoblasts at the edges of the growing bone. At this point new bone formation is slowed and the compact MSCs surrounding the area of new bone formation will form the periosteum [20].

1.1.1.2 The Immune System

The immune system is a host defense system that spread throughout the body and involves many types of cells, organs, proteins, and tissues. The immune system is typically divided into two categories: innate and adaptive immunity. Both systems work closely together and take on different tasks. Innate immunity refers to nonspecific defense mechanisms that come into play immediately or within hours of an antigen's appearance or injury in the body. These mechanisms include physical barriers such as skin, chemicals in the blood, and immune system cells that attack foreign cells in the body. Adaptive immunity refers to antigen-specific immune response [21].

The majority of macrophages (innate immune cell) differentiate from circulating peripheral-blood mononuclear cells (PBMcs) that rapidly infiltrate the injury site or in response to inflammation [22-24]. Depending on the stage of healing at the injured site, inflammatory macrophages are polarized toward appropriate activation pathways that help to initiate and carry on the healing process. First, macrophages exhibit the pro-inflammatory phase, or cell recruitment phase, described as classically activated macrophages (commonly referred to as M1) [25]. Soon after cell recruitment phase, these M1 macrophages will be polarized to pro-reparative phase described as alternative activated macrophages (commonly referred to as M2 macrophages) to carry on the regeneration process [26]. M2 macrophages can be further subdivided into a series of distinct phenotypes, each with diverse functions ranging from tissue deposition to tissue remodeling [27, 28].

Successful macrophage activation outcomes can be measured by specific gene expression of each phenotype depending on macrophage source [29, 30]. M1 macrophages are usually

activated by IFN-γ and/or lipopolysaccharide (LPS) while M2 macrophages are activated by interleukins IL-4, IL-13 or IL-10 [29, 31]. M2a macrophages are characterized by their ability to inhibit inflammation and contribute to the stabilization of angiogenesis [32]. The differences between two main subtypes of M2 macrophages, namely "M2a" macrophages stimulated by IL-4 and "M2c" macrophages stimulated by IL-10, are not well understood. In fact, temporal gene expression analysis of human wound healing showed that M2c-related genes were upregulated at early times after injury, while M2a-related genes appeared at later stages or were downregulated after injury [27]. Overall, the polarization phenotype adopted by a macrophage can have a major influence over healing progression and outcome almost in all tissue repair process [33-36].

1.1.1.3 Osteoimmunology: The Communication between the skeletal and immune systems

At the molecular level, bone healing is driven by three main factors: pro-inflammatory cytokines and growth factors, pro-osteogenic factors, and angiogenic factors. The cross-talk between the inflammatory cells and osteoprogenitors introduced the term osteoimmunology which can be defined as an emerging field of research dedicated to the investigation of the interactions between the immune and skeletal systems [37]. These interactions are not only mediated by the release of cytokines and chemokines , by either inflammatory cells or bone cells, but also by direct cell-cell contact.

After a bone injury, a variety of inflammatory cells infiltrate the injured site to initiate and stimulate the healing process. Inflammatory macrophages are essential components of the innate immune systems also present throughout all bone healing phases secreting essential cytokines to promote vascularization, directed other cells migration, differentiation, and mediate

the overall healing process [38-40]. Various cytokines secreted by inflammatory cells play an important role in both formation and resorption. It has been demonstrated that Macrophages promote or suppress osteoclast activity through the secretion of TNF-α, IL-1, IL-6, and IFN-γ [41, 42]. In addition, TNF-*α* and IL-1 promote resorption activity of osteoclasts by increasing M-CSF. M-CSF can bind to its receptor and stimulate differentiation via the actions of Receptor activator of nuclear factor kappa-κ ligand (RANKL) and osteoprotegerin (OPG), as a soluble decoy receptor for RANKL, which are a crucial regulator of osteoclastogenesis attributed to osteoclast differentiation and activation [43-48].

On the other hand, IL-10 has been considered as an important regulator of bone homeostasis, in homeostatic and inflammatory conditions. It has been demonstrated in multiple studies that IL-10 could directly inhibit osteoclasts formation by its direct action on osteoclast precursors [49-52] and by reducing nuclear factor of activated T cells (NFATC) expression [53, 54]. In fact, enhanced osteoclastogenesis has been observed in cultures of bone marrow macrophages lacking IL-10 [55]. The molecular mechanism of this inhibition indicated that IL-10 upregulated OPG expression but downregulated expression of the RANKL [56].

Moreover, IL-10 can promote osteoblastic differentiation by the inhibition of TGF-β1 production in murine bone marrow cells [57, 58]. Furthermore, it has been demonstrated there is a reduction of osteoblasts generation in bone marrow cell cultures obtained from IL-10 deficient mice with a reduction in bone mass, bone formation and increased bone mechanical fragility [59]. The study also emphasized that cytokines and inflammatory mediators, including TNF-α, IFN-γ, and *IL6*, had negative effects on the differentiation, proliferation, and function of osteoblasts in general [59]. Furthermore, *IL10* can downregulate the synthesis of

proinflammatory cytokines and chemokines, such as IL-1, *IL6*, TNF-α and downregulate the synthesis of nitric oxide, gelatinase, and collagenase [60].

Interleukin 1beta (IL-1β), a cytokine secreted by macrophages, have the ability to stimulate osteoblasts proliferation and production of mineralized bone matrix and accelerate endochondral ossification process in mice [61]. Furthermore, in vitro study showed that IL-6 inhibits bone nodule formation using rat calvarial cells and concluded that IL-6 may inhibit osteoblast differentiation [62]. Another cytokine that showed an effect on bone is IL-4. IL-4 enhanced osteocalcin gene expression and alkaline phosphatase (ALP) activity but reduced Runt-related transcription factor 2 (RUNX2) gene expression and bone nodule formation of human adipose stem cells (hASCs) [63].

It can be concluded from the above studies there is a well-recognized link between the bone and the immune system and in recent years there has been a major effort to elucidate and understand this link. The co-regulation of the skeletal and immune systems emphasizes the extreme complexity of such an interaction. Their interdependency must be considered in designing therapeutic approaches for better bone repair outcome. In other words, it is necessary to think of the osteoimmune system as a complex physiological system involving the immune response and the host defense when implanting bone scaffold as well as the effect of specific molecules used to enhance the bone repair on the immune system and vice versa.

1.1.2 Age-Related Alterations to Bone and Bone Healing Processes

Age affects the microscopic and macroscopic structure of bone and leads to a reduction of total bone mass. It's well known that older bones are thinner and fragile with increased risk of bone

fractures and vertebral bone compression failures. The reduced volume and strength of older bone creates challenges for orthopaedic and maxilla-facial craniofacial surgeons and prosthodontists (the dentists that place dental implants). With increasing age of the patient, surgeons conducting bone grafting procedures often utilize more plates and screws to stabilize the injured bone during healing. The overall length of hospital stay increases with patient age and the lack of activity further leads to a decline in patient health [64]. Since the structural changes to bone with age result from cellular and molecular changes, this next section provides a detailed description of those a*lterations* and thereby provides new focus areas for biomaterials research to address the source of the age-related bone frailty.

1.1.2.1: Effects of Age on bone cells: Osteoblasts, Osteoclasts and Osteocytes

There are very few reports of age-specific functional changes to osteoblasts and osteoclasts; however, there is evidence for a reduced generation of osteoblasts and an increased generation of osteoclasts by the long-lived stem cells in bone as will be discussed in the next section. Osteocytes, also long-lived, are derived from terminally differentiated osteoblasts and are prone to aging related changes associated with estrogen reduction [65, 66]. Osteocytes also increasingly die with advancing age [67-69]. The reasons are many in addition to acute estrogen deficiency: increased oxidative stresses due to increased production of hydrogen peroxide and several other reactive oxygen species, treatment with glucocorticoids and an age-related increase of endogenous glucocortoids, and reduced physical activity. Their increased death with age has profound effects on bone because of their role in remodelling. Osteocyte death is directly associated with reduced bone strength in human patients that experience vertebral compression

fractures [70]. There are several mechanisms that contribute to the change in bone structure associated with osteocyte death. Osteocytes release factors that inhibit bone remodeling and their lack of production elevates resorption [71-73]. Dying osteocytes also release several factors that promote osteoclastogenesis including chemoattractants, prostaglandins, receptor activator for nuclear factor-kB (NF-kB) ligand and proinflammatory cytokines [74]. A reduction in bone vascularity and hydration is seen after osteocyte death, which reduces the strength of the materials bone are made of, such as the carbonated apatite crystals and collagen and proteoglycans [75]. The complicated signaling of the dying osteocyte has been summarized well [76]. Localized delivery strategies directed at supporting survival of the osteocyte could thus positively impact bone repair outcomes.

1.1.2.2: Effects of Age on Mesenchymal Stromal Cells

Mesenchymal stromal progenitor cells, found in stromal tissues throughout the body, abbreviated as MSCs in this dissertation, are one of the key cells that contribute to bone regeneration. They produce factors that orchestrate immune cells involved in the healing process and differentiate into bone cells. An early promulgator of the trophic effects of stem cells from production of biomolecules was Dr. Arnold Caplan [77]. Early phases of successful bone healing include recruitment and proliferation of a sufficient number of MSCs along with a supportive blood supply. The number of MSCs obtained by marrow aspiration have been shown to decline with increased age of the donor bone marrow [78], indicating fewer MSCs are available to contribute to the healing process with age. A study that quantified the number of MSCs from young and old human bone showed there is a decrease in osteoprogenitor cell number in 60 year old female patients as compared to younger patients [79]. The decline in

osteoprogenitor cell number resulted in decreased mineralization, protein levels of bone matrix and calcium content [78, 79].

Further studies have confirmed the decrease in MSC number, responsiveness to signaling molecules, differentiation potential, and proliferative capacity in MSC derived from humans [80, 81] and animals [82-84]. With advanced age, MSCs differentiate more into adipocytes, rather than into osteoblasts, and differentiation and responsiveness of MSCs to signaling molecules become impaired in patients of advanced age compared to MSCs derived from younger bone [85]. There is clear evidence that the decrease of osteoblastogenesis and the age-related changes in overall bone strength is due to the accumulation of bone marrow fat [86-88]. A general overview of the molecular and cellular alterations within bone that occur with age are summarized in Figure 1.

Peffers *et al.* [89] used a systems biology technique to investigate the mRNA and DNA protein alterations in human MSCs with age. Their study found evidence of alteration in both transcriptional and post-transcriptional levels in a number of transcription factors and alterations in energy metabolism and cell survival. Similar studies have been done to investigate gene expression changes in aged mouse MSCs and revealed significant stage-specific changes of genes associated with differentiation, cell cycle and growth factors [90]. Measurements of oxidative damage, ROS levels and nuclear proteins p21 and p53, which are markers of the aging process, were all increased in MSCs from older animals or humans [78]. Additional details about the alteration of MSCs with aging can be found in reviews by Kuang *et al.* [91], Bellantuono *et al.* [92] and Sui *et al* [93].

Overall, alterations with age give rise to an impaired role of MSCs during bone regeneration in older patients. The identification of age-associated changes to MSCs provides insights on how to improve their function during bone healing. Autogenous MSCs from older patients used for stem cell therapies will likely benefit from being delivered to the wound site in scaffolds containing growth factors that address their deficiencies in proliferation or survival, as well as an osteoinductive agent.

1.1.2.3: Growth Factors Associated with Bone Formation and Regeneration Decrease with Age

Growth factors are soluble signaling molecules secreted by cells involved in bone repair such as inflammatory cells, fibroblasts, endothelial cells, MSCs and osteoblasts**.** The role of the following growth factors in bone repair is well established: bone morphogenetic proteins (BMPs), fibroblast growth factor (FGF), insulin-like growth factors (IGFs), platelet-derived growth factor (PDGF), transforming growth factor-β (TGF-β1 and TGF-β2) and vascular endothelial growth factor (VEGF). The complicated interplay of many growth factors and their role in bone healing has been described well previously [11]. The sequence of growth factors present in the wound depends on the healing stage; for example, platelets release TGF-β1, PDGF, IGF-I and VEGF immediately after the bone injury and this causes other cells nearby to start to also secrete TGF-β and PDGF in response to the platelets. This cascade of reactions is explained in the review by Barnes et al. [94]. BMPs may also stimulate the production of other growth factors important for bone regeneration; for example, BMP-2 stimulates the production of IGF and VEGF [95]. With regards to biomaterials delivery systems, each growth factor has a

specific role, at a specific time, in the regeneration process making it essential that each factor is presented in a biomimetic manner during healing in order to perform its role successfully.

The regulatory effect of BMPs on bone and the importance of this factor during bone repair has been extensively reviewed by multiple scholars [96]. BMPs play a critical role in regulating cell growth, differentiation, and apoptosis of osteoblasts, chondrocytes and MSCs [97]. One change that occurs with aging is that an increased dose of BMP-2 must be used to obtain the same amount of bone within the same amount of time as a younger person or animal. Sixteen month old rats needed to be given six times more BMP-2 in order to form the same amount of ectopic bone as three month old rats [98]. Meyer *et al.* [99] showed 6 week old rats with fractures were restored to normal bone biomechanics after 4 weeks, while 1 year old rats took 26 weeks post-fracture to reach normal bone biomechanics. Old rats in that study also had lower BMP-2 mRNA levels as compared to younger rats. The need for higher doses in older patients means that delivery systems for older patients must be designed to achieve highly localized delivery, so that the off-target effects that occur with diffusion of BMP-2 away from the bone injury site is minimized.

PDGF stimulates directed cell movement toward a gradient of PDGF, known as chemotaxis, as well as stimulating cell proliferation [100, 101]. It is another important growth factor contributing to the bone healing process. PDGF is synthesized early during normally healing human bone fractures by various cell types like platelets, monocytes, macrophages, endothelial cells, and osteoblasts [102]. A more detailed description about the role of PDGF in bone can be found in Hollinger *et al.* [103] and Caplan *et al.* [104]. Like other factors related to

initiating the process of wound healing, aging has been found to alter the temporal profile of PDGF production and its receptors in mice within acute incisional wounds [105]. That study showed a delay and reduction in PDGF production and its receptors with increasing animal age that delays wound healing. These studies indicate that PDGF supplementation would be an advantageous strategy for older patients when administered early in order to kick-start the wound healing process, but not continuously which would impair wound healing.

FGF-2 is present during the early stages of fracture healing and guides angiogenesis and causes MSC proliferation [106-108]. FGFs are produced by many cell types such as monocytes, macrophages, mesenchymal cells, osteoblasts, and chondrocytes. In mice, disruption of a receptor for FGF-2, FGFR2, results in progressive osteopenia and decreased bone formation rates like that seen in older patients, suggesting FGF-2 changes are in part responsible for loss of bone mass in the elderly [109, 110]. Indeed, with age, FGF-2 and FGFR1 mRNA and protein in MSCs has been found to decrease with age [111], causing impairment in a number of essential signaling pathways involved in the bone repair process. These studies further support the conclusions summarized in Figure 1.

IGFs play an important role in normal bone development with null mutations of the genes encoding IGF-1 and 2 causing growth retardation, abnormalities in the growth plate, and decreased bone calcification in newborn mice [112]. IGF-I and TGF-β1 are essential growth factors needed during the early stage of fracture healing and their level is has been found to be reduced with aging. Nicolas *et al.* [113] showed a linear decline in the skeletal content of IGF-I as well as a decrease TGF-β1 content using samples of femoral cortical bone from mainly men

and some women between the ages of 20-64 yr. The circulating serum level of IGF-1 was reduced in women of age 70 or older who had experienced femoral bone mass reduction with aging [114], and in both elderly men and women who had a reduction in BMD [115]. Furthermore, the age-related decline in IGF-1 level reduced mechanical strength in human tibial posterior cortex bone samples which caused increased bone fracture rates [116].

To summarize, the aging process causes decreased production of TGF-β1, PDGF, IGF-I, FGF-2, BMP-2 and VEGF involved in wound healing and specifically bone repair. The decreased presence of nearly every key growth factor involved in bone homeostasis, repair and regeneration contributes to age-related bone disease and slowed or difficult bone healing in the older patient. Increasing cell production of growth factors in older patients or locally delivering either growth factors or drugs that lead to an increase in one or more growth factors is thus is an efficacious strategy to counter aging deficiencies and thereby enhance healing of elderly bone.

1.1.3 Inflammaging and senescent cells Affect Bone Healing in Older Patients

1.1.3.1: Age-associated Increase of Pro-inflammatory Molecules Impedes Bone Healing

No matter what the age is, after bone injury, an inflammation stage with marked cytokine production is necessary for initiation and progression of the normal healing process. The major source of cytokines are immune cells known as macrophages, except during aging when the inflamm-aging process results in a low-grade pro-inflammatory environment all the time from senescent cells throughout the body[117]. In bone, both macrophages formed from blood monocytes recruited to the injury site and resident bone macrophages are present throughout all

of the fracture healing phases. They alter phenotype to promote various steps of tissue regeneration such directing MSC migration, proliferation, and differentiation, vascularization and remodeling as reviewed by [38, 40, 118, 119]. Understanding the relationship between macrophages and the skeletal system is essential for developing optimal therapeutic approaches to treat fractures in the elderly.

The polarization of macrophages into the so-called "pro-inflammatory M1" and "pro-reparative M2" phenotypes are both delayed in elderly patients and impair fracture healing of bone as reviewed in more detail by [120]. With age, the ratio of pro- inflammatory to anti-inflammatory cytokines produced by macrophages increases and negatively impacts bone repair processes. TNF-α is significantly increased in M1 macrophages from aged rats as compared to those from young rats [121, 122]. TNF-α directly induces the marrow precursor cell differentiation into osteoclasts [123] and thus this helps to tip the homeostatic balance in bone towards resorption. There is also a decrease in systemic interferon-gamma (IFNγ) concentrations after fracture in older patients compared to young [124], which further increases resorption because IFNγ inhibits osteoclastic bone resorption [41, 42]. Aging bone marrow macrophages are more susceptible to oxidative stresses and they proliferate less in response to signals from granulocyte macrophage colony-stimulating factor (GM-CSF) [125]. M2 macrophages promote the ossification phase and studies in young mice show that the M2 phenotype can be increased with administration of interleukin 4 and 13 in fractures as a means to improve bone formation [126]. Modulating macrophages through delivery of cytokines is thus a strategy that could be pursued in older humans or animals to increase bone repair rates.

Cauley *et al.* [127] examined the circulating levels of pro-inflammatory cytokines (e.g. IL-6, TNF-α, and IL-1) and their contribution to fractures in older humans. The study showed a strong correlation between high serum levels of inflammatory markers with incidence of fractures during a 5.8-yr follow-up period. Those with a higher level of inflammatory markers had the highest risk and history of fracture. Since IL-1 and IL-6 are potent promoters of osteoclast differentiation and activation[128, 129], their increase with age increases bone resorption and fracture risk. TNF-α both stimulates bone resorption and inhibits new bone formation thus increasing fracture risk. The inducible nitric oxide synthesis pathway (iNOS) which inhibits the production of new osteoblasts and induces osteoblast apoptosis is activated through the effects of TNF-α and IL-1 and further increases the higher activity of bone resorbing cells relative to bone forming cells. The pro-inflammatory environment in the body of the older patient thus contributes to increased fracture risk and the accelerates progressive loosening of total joint replacements that occurs in response to implant debris [130]. A low-grade pro-inflammatory environment is a serious health concern because increased circulating cytokine levels have been shown to be strong, independent risk factors of morbidity and mortality in elderly populations [131].

1.1.3.2: Cellular Senescence

Aging is a result of predictable cellular death associated with a predetermined cellular lifespan known as the Hayflick limit [132]. The progressive decline in cellular function and eventual cell death is a result of cells wearing out from continued use and exposure to disease, oxidative stresses, DNA damage, altered chromatin structure, oncogene activation and telomere

dysfunction as reviewed by others [133-135]. These inducers cause cell senescence which is irreversible cell cycle arrest in which cells no longer divide, but remain viable and metabolically active. In experiments with genetically altered mice in which senescent cells could be selectively killed, the negative effects of these cells and their association with many diseases of old age were proven [136].

Senescent cells accumulate in multiple tissues in the body. They are present in old mouse bones and bone marrow [137]. Senescent cells no longer function normally, but their inability to replicate is a better alternative than developing cancer from the cellular abnormality. Senescent cells are actually protective if present in cancerous growths [138, 139].

1.1.3.3: Effects of Cellular Senescence

Changes in Systemic Levels of Growth Factors and Cytokines

A subset of senescent cells develop a senescence associated secretory phenotype (SASP) and secrete numerous pro-inflammatory cytokines (e.g. Interleukin(IL)-1, -6, -8), chemokines and extracellular matrix degrading proteases [140]. Senescent cells thus contribute to the chronic low-level inflammation that develops in older people termed inflamm-aging [117]. Inflammation goes up, but expression of pro-regenerative growth factors and extracellular matrix components required for wound healing and tissue regeneration is down-regulated[105]. Healing of bone and other tissues is negatively impacted by these changes. The negative effects of senescent cell secretions and the reduction of pro-regenerative factors in the blood of older animals has been clearly demonstrated in mouse experiments in which the blood circulation of young and old mice is connected [141, 142]. This surgical technique is known as heterochronic

parabiosis. Connection of an old mouse to the blood of a young mouse has been reported to reverse impaired age-related pathologies of aged mice including cardiac hypertrophy, slowed healing of muscle and bone injuries, and decline of hepatocyte proliferation [141, 142]. These experiments support the idea that reductions in normal tissue function and the regenerative potential with advanced age are most likely caused by the presence of factors elevated or reduced as part of the aging process. An efficacious therapeutic strategy for older patients will thus supplement or knock-down levels of particular molecules identified to be altered with increasing age, while not negatively impacting the normal healing process that utilizes these same molecules.

Changes in the immune system

Aging results in changes to the total number and activity of immune cells, both those involved in innate immunity (e.g. monocytes, macrophages, natural killer cells and dendritic cells), as well as immune cells involved in adaptive immunity that respond to antigens (e.g. B- and T-lymphocytes) [143]. With increasing age, more hematopoietic stem cells become granulocytes, macrophages and dendritic cells, than B- and T- lymphocytes, thereby reducing the ability to fight infection [144]. In normal wound healing, neutrophils are the first cells to a wound site, but with age they become slower to arrive at an infection site, despite the fact their production rate remains the same with advancing age [144]. The slowed neutrophil response gives rapidly dividing bacteria an undesirable head start in older patients.

Macrophages have impaired phagocytosis and reduced cytokine production in response to bacteria derived lipopolysaccharide (LPS) [145, 146]. The increased background levels of proinflammatory cytokines (IL-6 and TNF-alpha) decrease their sensitivity to stimuli and prolong inflammation once initiated [147]. Aged mice (both BALB/c and FVB/N) were found to have an enhanced inflammatory response similar to older humans, as measured by cytokine and chemokine production or neutrophil infiltration, compared with young mice indicating that mice can be use a model for aging studies [148]. In addition, transfer of macrophages from young mice to old mice was able to reverse impaired wound healing in aged mice [149-151], reinforcing the potential gains from therapies focused on shifting the immune system of older patients back to a more youthful state. The wide ranging effects of senescence and aging on the immune system have been previously summarized [117, 144]. Overall, the older person's altered immune system make them more prone to infection, prolonged pathological inflammatory responses, slower wound healing and less reactive to vaccination. These immune system deficiencies provide the motivation to develop local delivery systems from biomaterials for immunomodulation. Schematic representation of the age-related alteration with age can be found in Figure 1.1.

1.1.3 Strategies to Date for Modulating Inflammation During Bone Healing

Given the essential role of macrophages in the bone repair process, they represent an attractive therapeutic target for improving bone repair outcomes especially in compromised bone of older individuals. Several strategies for local delivery of cytokines have been developed to modulate macrophages phenotype to accelerate wound healing in mice. For example, the effect

of local co-delivery of IFNγ with IL-4 to macrophage and the influence of each phenotype on the peripheral nerve regeneration using polysulfone nerve-bridging tubes filled with agarose hydrogel [152]. Another study designed silk films embedded with IFNγ or IL4 to promote M1 or M2a polarization [153]. Similarly, osmotic pump has been used to deliver IL4 to mitigate orthopedic implant wear particle-associated inflammation [154]. In addition, the sequential delivery of immunomodulatory cytokines, IFNγ and IL-4, was studied to facilitate the transition of M1-to-M2 macrophages and enhance bone vascularization in vivo in subcutaneous mouse model using decellularized bone scaffolds with biotin–streptavidin interactions [155]. Dexamethasone was delivered as an alternative to cytokines to promote M2 polarization and reduces fibrous encapsulation using microdialysis tubing [156].

Preventing the activity of pro-inflammatory factors that are at elevated levels due to aging is an alternate strategy to increase bone healing activity in older patients. Patients with chronic periodontitis received systemic doses of an inhibitor to TNFα and that resulted in lowered serum level of inflammatory markers and improved outcomes [157]. Quite different results were obtained when this strategy was tested in young mice. Inhibition of endogenous TNF, by either systemic delivery of anti-TNF or local injection of recombinant murine *IL10* at the fracture site, reduced callus mineralization leading to poor bone bridging across the fracture site [121]. In the young animals, local rhTNF treatment was only effective to improve mice fracture healing when administered within 24 h of injury when only neutrophils were present [158]. This provides evidence that strategies being developed to address the altered physiology in older patients should be tested in aged rodent models or run the risk of not showing a positive effect.

1.1.4 Effect of Statins on Bone Healing and as an Immunomodulatory agent

There is a well-recognized link between the bone and the immune system and in recent years there has been a major effort to identify molecules that can target both bone and immune cells [159, 160]. Several molecules that were initially identified and studied in the immune system and other applications have been shown to have an essential effect also on bone mineral density (BMD) and bone healing, such as nonsteroidal anti-inflammatory drug (NSAID), cyclo-oxygenase selectivity (COX), aspirin and statins [161-165]. Statins, HMG-CoA reductase inhibitors, are common cholesterol-lowering drugs. Simvastatin, which belongs to the statin family, is administered in the lactone form, which is a prodrug [166-168]. It is rapidly hydrolyzed in its first pass through the liver from the inactive lactone to the hydroxy acid active form, which has considerable similarity to the structure of acetyl CoA (Fig. 1.2).

Literature suggests that statins may have potential novel therapeutic effect for diverse conditions, ranging from sepsis and inflammatory diseases to chronic wounds and dementia and osteoporosis [169, 170]. Statins have been shown to exhibit pro-reparative properties by reducing the release of specific chemokines, cytokines and adhesion molecules, as well as modulating T-cell activity. Statins inhibit the transendothelial migration of leukocytes by decreasing the expression of adhesion molecules, such as Intercellular Adhesion Molecule 1 (ICAM-1), lymphocyte function-associated antigen-1 and monocyte chemotactic protein-1 [171, 172]. Moreover, statins further prevent inflammation by inhibiting chemokine release and Th1-type chemokine receptors on T cells [173, 174].

The anti-inflammatory activity of statins results in reduced synovial inflammation and cartilage degradation in rabbit experimental osteoarthritis [175]. Studies on the

immunomodulatory effects of lovastatin on rats with experimental autoimmune encephalitis found a decrease in IFN-γ and *IL6*, with an increase in the anti-inflammatory cytokine *IL10*. Further studies on neuro-inflammatory disorders found that statins inhibited the expression of inducible nitric oxide synthase and proinflammatory cytokines TNF-α and IFN-γ, suggesting promise for diseases such as multiple sclerosis [176]. Simvastatin was extensively studied for its role as anti-inflammation drug and that by inhibiting the production of multiple cytokines such as TNF-α , IL-1β, *IL6* and IL-17 with induction of regenerative cytokines such as *IL10*, IL-4 and IL-27 [177-181]. In this thesis, Simvastatin was used to modulate inflammatory macrophages derived from either mouse or human. More detailed review of simvastatin anti-inflammatory effect could be found in chapter 3.

1.1.5 Delivery of Simvastatin in Bone Repair

Beyond simvastatin's inhibition of cholesterol synthesis, many observational studies have reported a positive effect of oral use simvastatin on fracture risk bone mineral density (BMD) in older individuals. Simvastatin use was associated with a significant reduction in the risk of hip fracture and other non-spine fracture in older patients [182, 183]. One to five years usage of oral simvastatin resulted in a significant increase in BMD, both on the spine and femoral hip, specifically in postmenopausal women [164, 184, 185]. These studies provided useful information about the relation between simvastatin use and fracture risk and BMD among older women. However there are multiple side effects associated with all systemic administered drugs, simvastatin side effects includes muscle breakdown, liver problems, allergic reactions, diarrhea,

headache, and increased blood sugar levels [186]. Therefore local delivery from a biomaterial delivery system would overcome side effects of simvastatin.

Studies have also shown a promising effect of locally delivered simvastatin beta-hydroxy acid on bone formation. For example, 20 ug of beta-hydroxy acid simvastatin was loaded in Poly(e-caprolactone) (PCL) spiral scaffolds implanted in rats critical size cranial defects. The study showed tissue integration within the implant and mineralized bone restoration with simvastatin loaded scaffold compared to control [187]. Jeon et al. compared sustained release of 1 ug simvastatin hydroxy acid versus 5 ug intermittent release from PLGA microparticles on the young male rat calvarial defect. Histological evaluation, 28 days post-implantation showed 32.3% increase in bone thickness and a 74.1% greater bone area with intermittent release than sustained delivery [188].

Simvastatin, pro-drug form, was delivered on titanium threaded screw coated with biomimetic calcium phosphate showed greater increase in bone area in ovariectomized rat tibia fracture [189]. MSCs sheet combined with 0.5 mg simvastatin were locally delivered from calcium sulfate (CS) to osteotomy model in rat tibia and resulted in more callus formation around the fracture site at 2 weeks, and complete bone union at 8 weeks[190] . Skoglund et al. compared systemic subcutaneous injections of 20 mg/day simvastatin or 0.1 mg/kg simvastatin directly delivered to mouse femur fracture from an osmotic mini-pump. Local delivery of low dose of simvastatin showed better improvement of biomechanical parameters and bone formation [191]. Alpha-tricalcium phosphate particles loaded with multiple dose of simvastatin delivered locally on adult rat calvarias defect was tested for its osteogenic and inflammatory effect. High dose, 0.5 mg, of simvastatin caused more inflammation, while lower, 0.1 mg, dose

suppressed inflammation, induced significantly higher bone volumes than the higher dose. Simvastatin treatment is dose dependent, too high dose of simvastatin could have negative effect on bone formation as well as inflammation [192-194]. Therefore, systemic or local administration of high doses of simvastatin might block new bone formation due to accumulation of excessive dose on systemic and cellular level.

1.1.6 Calcium Phosphate Delivery Systems Advantages over Polymers

Calcium phosphates are widely used as synthetic bone grafts providing several advantages such as their osteoconductivity, biocompatibility and injectability [195, 196]. Moreover, their intrinsic porosity allow for the incorporation of drugs and active biomolecules in the coatings providing highly localized delivery of the drug to the targeted site of injury [197]. Unlike biodegradable polymer drug delivery systems, bCaP can provide a safe environment for the cells with no harmful acidic byproducts seen with some polymer degradation and dissolution processes. The byproduct from polymer use may cause a release an acid product that catalyzes further degradation providing uncontrolled released of drug that could negatively impact the wound microenvironment [198]. We have seen first-hand, in our own in vitro testing, the benefits of using novel bCaP coatings on biomaterial as barrier layer for delayed and sequential delivery of bioactive molecular to macrophages.

1.1.7 Sequential Delivery Systems.

Multiple strategies of biomaterial drug delivery systems are being developed to provide multiple factors delivery mimicking the natural biological tissue regeneration process [199]. These strategies focused on biomaterials use for multiple regeneration therapeutics such as wound healing/infection, bone, cartilage, muscle, teeth and cancer, and have shown some efficacy both *in vitro* [200-202], and *in* vivo [203] . The use of a biomimetic calcium phosphate (bCaP) barrier layer with a poly-L-Lysine (PLLys) and poly-L-Glutamic acid (PLGlut) PEM successfully provided pure sequential delivery of two factors to osteoprogenitors in vitro and in vivo[204, 205] .

Several materials have been used to locally modulate bone healing with simvastatin in combination with hormones and growth factors. For example; the sequential delivery of PDGF and simvastatin were locally delivered from a double-walled PDLLA-PLGA microspheres on rat maxillary molars [206]. However, this study was limited in terms of providing information about the effect of SIMV combined with another factor on older compromised bone. The combined effects of simvastatin and FGF-2 were investigated in vitro on the proliferation and differentiation of MC3T3-E1 [207]. Cellulose acetate microspheres were also used in vitro for alternating delivery of simvastatin hydroxyacid and PTH [208]. These studies used a young cell line which failed to predict the effect of SIMV on primary older cells. Furthermore, these approaches were limited by the co-delivery profile provided to the cells and the lack of timely-control over the factors being delivered. Therefore, there is a need for delivery system offer control over the sequence of delivery when modulating inflammatory macrophages for better healing outcome.

1.1.8 Importance of Controlling the Timing of Immunomodulatory Therapies:

Inflammatory response, the first stage of healing after tissue injury, is one of the requisite phases for successful healing. Blocking the initial inflammatory response can disrupt the delicate balance between macrophage subsets and may result in negative outcome. It is proven that the administration of nonsteroidal anti-inflammatory drugs such as cyclooxygenase-1 (COX-1 or 2) early times after injury impairs overall healing outcomes as well as osteointegration of dental implant [209, 210]. Overall, mounting evidence supports that timely-controlled inflammation is required for bone healing. During prolonged inflammation, the continuous infiltration of M1 macrophages are detrimental to the overall healing process. In fact, prolonged local or systemic delivery of M1-polarizing agents, 7 days starting at the time of fracture, compromised normal healing in adult rats [211, 212]. On the other hand, the early injection of M2a or M2c macrophages directly after in to a mouse wound injury inhibited healing [213].

1.1.9 Gap in Knowledge.

Bone regeneration and repair is markedly reduced in older patients. Previously, most bone regeneration strategies focused on healing younger bone, however these strategy is not as effective for treating the injuries of aged patients. A strategy to address repair of bone injuries in older patients must take into consideration the age-related loss of bone quality and inflammaging and alterations relative to young cell behavior. Furthermore, most studies to date focused on addressing one single cell type or modulating one single molecule within a tissue which is not an effective strategy to overcome complex, multifactorial aging effects. The use of high doses of a single osteoinductive molecule to accomplish bone repair in older patients and animals is not the

best strategy to overcome the reduced healing capacity because it leads to unwanted side effects such as an inflammatory response to the growth factor or off-target effects. Local delivery of multiple therapeutic molecules that can address the many types of physiological alterations with age will offer the best means of accomplishing robust bone regeneration in older patients. Therapeutic approaches of the future should be tailored to the older patient's bone structure, physiology and resolve the impaired immunity, enhanced inflammation, and reduced number and osteogenic differentiation potential of MSCs associated with the presence of senescent cells to expedite bone healing in the elderly. This dissertation research therefore focused on the design of a biomaterials drug delivery system that may be used one day to improve bone regeneration outcomes. The delivery system is based on a thin layer of biomimetic calcium phosphate: bone-like apatite with unique delivery profile that allows for stepwise sequential delivery to macrophages.

1.2 Hypothesis

The overarching hypothesis is that sequential, localized delivery of anti-inflammatory/osteogenic simvastatin will modulate macrophage transitions and improve osteogenesis.

1.3 Specific Aims

There is an age-related alteration in macrophage response after injury that prevents wound healing initiation and resolution [124]. The long-term goal of our research is to enhance older bone regeneration by modulating the innate immune system via local sequential delivery of

immunomodulatory cytokines or delayed-localized delivery of anti-inflammatory molecules from novel biomaterial coating that can be applied to commercially available bone graft substitutes.

AIM #1: Develop a delivery system for sequential or delayed delivery of biomolecules to osteoprogenitors or macrophages using a biomimetic calcium phosphate (bCaP) coating. ***Sub-Hypothesis:*** If bCaP serves as barrier layer to delay access to a cytotoxic compound, antimycin A, then cells (osteoprogenitors or macrophages) should show a delayed cell death rather than immediate cell death.

- 1A: Demonstrate delayed access of RAW264.7 macrophage to cytotoxic antimycin-A (AntiA) covered with a bCaP coating. Cells cultured directly on the bCaP coated disks and viability will be measured with LIVE staining over time (from 4 hr to 5 days). The Kuhn lab previously demonstrated that incorporation of bCaP-PEM was used for sequential delivery of two factors to osteoprogenitors. Here we tested the ability of the bCaP-PEM to sequential deliver factors to macrophages and studied the differences between using bCaP-PEM as compared to bCaP coating.
- 1B: Visualize the change in bCaP coating integrity as a function of incubation time with macrophages by scanning electron microscopy (SEM) imaging to discover the mechanism of cell access to the compound covered by a bCaP coating.

AIM #2: Determine if the sequential delivery of IFNγ followed by Simvastatin from bCaP can modulate macrophage phenotype. ***Sub-Hypothesis:*** If bCaP sequentially delivers M1 stimulating IFNγ followed by M2 stimulating SIMV, then macrophage phenotype should show a transition from M1 to M2 over time as measured by gene expression.

- 2A: Determine the effect of the biomaterial bCaP coating itself on M1 to M2 of THP-1 cells.
- 2B: The M1/M2 transition of the young THP-1 human monocyte cell line will be modulated by the sequential delivery of IFNγ followed by SIMV from bCaP.
- 2C: The M1/M2 transition of the old mouse primary bone marrow macrophages in vitro and in vivo was modulated by the sequential delivery of IFNγ followed by SIMV from bCaP.

AIM #3: Determine if delayed local delivery of Simvastatin from bCaP can improve in vitro osteogenesis. ***Sub-Hypothesis:*** If pro-inflammatory cytokines in older cells negatively impact osteogenic differentiation, then delivery of anti-inflammatory SIMV, after the pro-inflammatory phase, will modulate cytokines produced by osteoprogenitors and increase osteogenesis.

- 3A: The optimal timing for delivery of beta-hydroxy acid SIMV to increase osteogenesis of osteoprogenitor cells from older human was investigated as measured by cytokine production and differentiation. In vitro studies using osteoprogenitors obtained from older human bone chips were conducted to determine the effective delayed access dose.
- 3B: Demonstrated delayed delivery of SIMV from bCaP modulates cytokine production and increases differentiation of osteoprogenitors from older human bone chip.

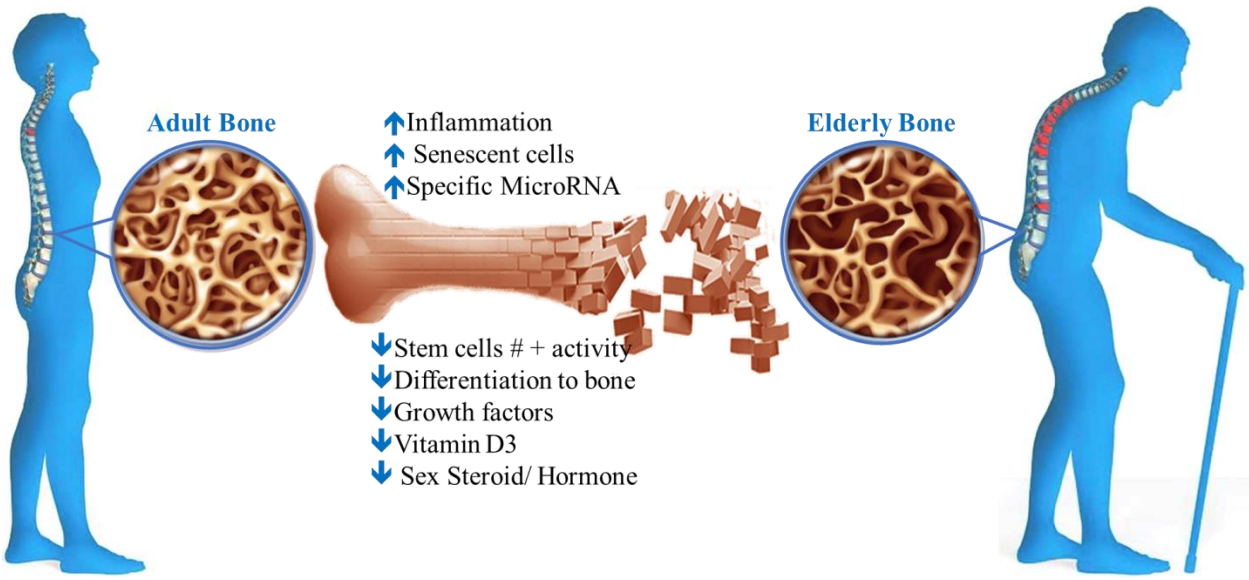

Figure 1.1: Illustration of age-related alterations that have an effect on reducing bone cell contributions to the healing process and impact on overall bone structure with advanced age. (Source: modified from [214]).

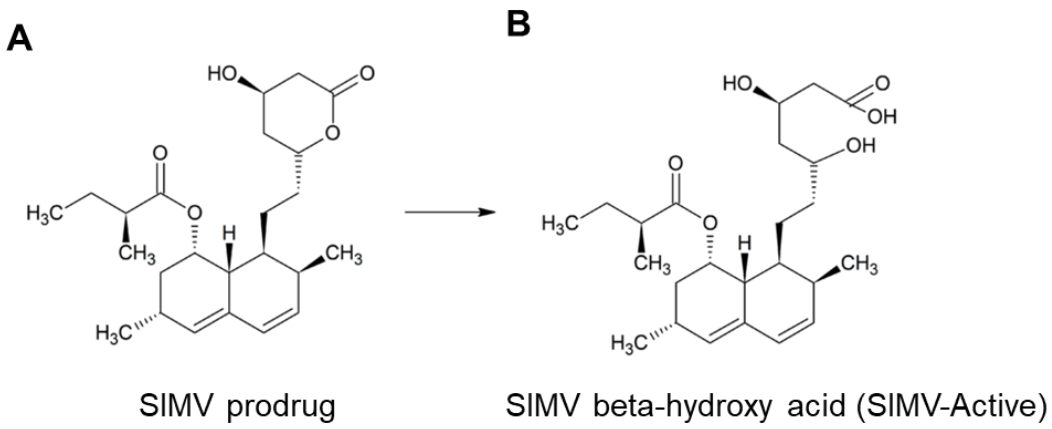

Figure 1.2: Simvastatin structure. (A) Simvastatin in prodrug structure, (B) open ring beta hydroxy acid form of simvastatin .

Chapter 2

A bCaP Delivery System for Sequential Delivery of Biomolecules to Macrophages and Osteoprogenitors

2.1 Introduction

Highly localized, sequential delivery of multiple factors is needed to trigger multiple phases of tissue regeneration and to avoid conflicting messages to progenitor stem cells. A sequential, cell-mediated delivery system was recently developed in our laboratory for the delivery of two different bioactive factors using a biomimetic calcium phosphate (bCaP) barrier layer and a poly-L-Lysine/poly-L-Glutamic acid polyelectrolyte multilayer (PEM) film [204]. The study proved that bCaP-PEM could sequentially deliver two factors in vitro to osteoprogenitor cells with 3 days gap between the delivery of the two factors. It was also shown that the delivery of the factors was based on the cell-interaction with the materials and not based on the diffusion of the factors out. However, the possibility of bCaP-PEM to provide sequential delivery to other cell types and the tunability of delivery kinetics were unknown.

It is critical for new drug delivery systems to offer specific tunability and customize the delivery profile to best match the cellular needs around the implant to achieve successful tissue regeneration. For example, during bone fracture healing, sequential and overlapping stages of regeneration can be distinguished during the healing process [215]. During the early healing phases (hematoma formation and inflammation), the skeletal and immune system are closely interacting through common cell precursors and molecular mediators [216, 217]. Although the whole cascade of healing is complex, it is reported that macrophages are present throughout all bone healing phases [218, 219]. They are part of the acute phase response triggered by tissue

injury and thus represent one of the earliest cells migrating to the site of injury [9, 220]. Given the importance of macrophages impact on the healing process, targeting both osteoprogenitors and macrophages with a multiple drug delivery approach is a necessity for successful bone repair outcomes.

The natural processes of tissue development or tissue repair involve the sequential synthesis, secretion, and assembly of different matrix components, growth factors, and other proteins to guide cell process. There is a clear positive effect from delivering two factors to enhance tissue repair over delivering one factor [201, 221]. Several scholars examined the synergic effect of local delivery of two growth factors on bone healing especially bone morphogenetic proteins (BMPs) combined with other growth factors. For example, a blend of BMP-7 with insulin-like growth factor-I (IGF-I) [222], BMP-7 with BMP-2 [223-227], BMP-2 with IGF-1 [228-230], BMP-2 with Cobalt ions [231], as well as BMP-2 with fibroblast growth factor (FGF-2) [205, 232], were all examined and found to achieve better bone healing outcomes. Another strategy was developed to promote dentoalveolar regeneration by the combined delivery of PDGF-Simvastatin [206].

Combinations of growth factors that aid different steps of regeneration are thus anticipated to synergistically enhance tissue regeneration. Several different types of delivery systems for multiple growth factors have been developed as potential therapeutics for wound healing/infection, bone, cartilage, muscle, teeth, and cancer, and have shown some efficacy in vitro [200, 201, 203, 233]. The sequential delivery of immunomodulatory cytokines was also used to facilitate the transition of macrophage phenotypes and enhance vascularization [155]. The co-delivery profile in most of these delivery systems due to uncontrolled diffusion through the biomaterial resulted in bad healing outcomes [155]. The drawback of the previous systems

motivated this work to offer highly localized delivery targeting both osteoprogenitors and macrophages using biomimetic calcium phosphate (bCaP) to avoid off target dosing or prolonged exposure to the biomolecule.

Calcium phosphate coatings have a great potential as a carrier for a drug in orthopedics as well as in maxillofacial surgery due to their biocompatibility, osteoconductivity, and easy preparation. bCaP coatings techniques were first developed in 1990 by Kokubo and his colleagues [234]. bCaP can be deposited by the immersing of a substrate or scaffold in a supersaturated solution of CaP under physiological conditions of temperature (37°C) and pH (7.4) to nucleate bone-like carbonated apatite. The method has been improved and refined by several scholars [235-239]. Recently a biomimetic calcium phosphate bone substitute has been developed for local delivery of biomolecules in sustained slow release of the drugs to the site of injury [240-252].

This chapter examined the use of a thin layer of bCaP coating to provide sequential delivery of two factors: one factor above and one factor below the thin bCaP layer to orchestrate reparative activities of both macrophages and osteoprogenitors. The tunability of the bCaP-PEM system [204] was also investigated in this chapter by removing the PEM film and using one or two bCaP layers. The bCaP layer was altered by increasing time in the simulated body fluid solutions used to produce the coating [253, 254]. In addition, because the monocytes/macrophages are one of the first cell-types that would interact with the coating [9, 220], cell culture studies with murine-derived RAW 264.7 macrophage or MC3T3-E1 osteoprogenitor were conducted to best mimic the natural cell combination around the bone

implant. It was hypothesized that removing the PEM film leaving bCaP only or increasing bCaP thickness would result in sequential delivery of multiple factors to macrophages.

This chapter reports the in vitro assessment of the sequential delivery of two factors with opposing action (proliferation (FGF-2) or cytotoxic (AntiA)) delivered either from bCaP or bCaP-PEM coatings with alternations made to the system by removing the PEM portion or varying the bCaP thickness. This study showed that the delivery kinetics from bCaP-PEM can be tuned by removing the PEM layer or modulating bCaP thickness. In addition, changes in factor delivery kinetics resulting from changing the cell type cultured on the coating. The macrophages (RAW 264.7) can dissolve the bCaP crystal to access the embedded factor while the osteoprogenitors (MC3T3-E1) made their way through the cracks in the crystal junction to access the embedded factor. Variety of cell type should be considered when designing cell mediated growth factor delivery systems.

2.2 Materials and Methods

2.2.1 Material Fabrication

2.2.2.1: bCaP application

The bCaP deposition procedure followed previously reported method [204]. Briefly, ultra violet light-sterilized sandblasted tissue culture polystyrene disks (TCPsb) (NUNC, Rochester, NY) 22 mm in diameter were coated with bCaP mineral crystals via extended immersion in SBFx5 solutions [238, 253, 255]. bCaP was formed by immersion of TCPsb disks in solution-A for 24 hours at 37 C followed by dehydration with series of graded alcohol solutions. The dried disks were then immersed in a second solution (Solution-B) for another 24 hours at 50 C also followed by a dehydration step. Solutions A and B salts concentrations are summarized in Table 2.1. To alter the bCaP coating thickness, the time of incubation in solution B was varied from 24 hr to 48 hr and replaced with fresh solution every 24 hr. All SBFx5 solution reagents were used as received from Sigma-Aldrich.

2.2.2.2: PEM bilayer coating

Layer-by-layer PEM was applied by automated alternate dipping in poly-glutamic and poly-lysine solutions with saline rinses between following previously reported method [204]. Briefly, TCPsb disks coated with bCaP were held vertically in a custom 3-D printed sample holder and automatically dipped into PEM solutions and saline rinses using a histology staining machine (Varistain 24-4, Thermo Shandon, Loughborough, UK). The automatic PEM bi-layer process included an adsorption of poly-L-Glutamic acid (PLGlut) (1 mg/ml, Sigma P4761, St. Louis, MO) for 10 min followed by 1 min in seven saline rinses. This was followed by

adsorption of (poly L Lysine) (PLLys, Sigma P2636, St. Louis, MO) for 10 min followed by 1 min in seven saline rinses. This cycle was repeated to achieve 30 bilayers of PEM coating on 2-D disks.

2.2.2.3: Bioactive Factor Absorption

Prior to bCaP and PEM coating, 10 μl of 40mM AntiA dissolved in ethanol (213 μg/disk) was applied for 10 minutes on one side of the TCPsb disks and then the disk with AntiA was rinsed three times with saline. After that, (AntiA adsorption and bCaP and PEM coating) were applied, a carrier free recombinant human FGF-2 (R & D Systems, Minneapolis, MN) in saline was applied to the coated disks. Disks were incubated for 1 hr in 0.5 ml (375 ng/ml) of FGF-2 solution to allow binding to the surface and then rinsed three times with saline. Previous studies had determined that the final dose of FGF-2 was 120 ng/disk by Enzyme-linked immunosorbent assay (ELISA) on the post-binding and rinse solutions [204].

2.2.2 Characterization

Cell Culture Assays

MC3T3-E1 mouse calvarial osteoprogenitor cells (ATCC, Manassas, VA) or macrophages RAW 264.7 (ATCC, Manassas, VA) were cultured in Alpha-Minimal Essential Medium (α-MEM, No. 12571, Gibco BRL, Invitrogen) supplemented with 10% fetal bovine serum (FBS), 100 U/ml penicillin and 100 μg/ml streptomycin sulfate. The medium was refreshed three times a week until cells reached 80% confluency and passages 10–30 were

routinely used. For passaging and seeding, MC3T3-E1 cells were removed from the flasks by treatment with 0.25% Trypsin-EDTA (Sigma, St. Louis, MO) for 3 minutes. Macrophages were gently scraped from the flasks using a sterile cell scraper (Sigma, St. Louis, MO). Cells were counted using an automated cell counter (Bio-Rad, TC20) with trypan blue staining prior to cell seeding on coated disks. Prior to cell seeding, coated disks were UV sterilized for 10 min on each side and then incubated α-MEM medium for 35 minutes in non-treated tissue culture 12-well plates (Corning Inc., Corning, NY). MC3T3-E1s were seeded at 4×10^4 cells/cm^2 in culture medium while RAW 264.7 and THP-1 cells were seeded at 3×10^4 cells/cm^2 and incubated at 37°C and 5% CO_2.

LIVE® staining (Invitrogen Life Technologies, Grand Island, NY) was performed on both cells following the manufacturer's protocol. At various time points after cell seeding, coated disks were transferred to a new 12-well plate (Corning Inc., Corning, NY) and washed with phosphate buffered saline solution (PBS) to remove non-adherent cells and incubated at room temperature for 30 minutes in LIVE® staining reagents. After 30 min of incubation, disks were flipped over for imaging at 100X magnification using an inverted microscope (TE300, Nikon) equipped with a camera (Diagnostic Instruments), and imaging software (Spot Insight, Nikon).

Cell density was quantified as average percent fluorescent area via ImageJ software (U. S. National Institutes of Health, Bethesda, Maryland, US) as follows. Image analysis of 3 images per well with 3 replicates. Average percent fluorescently labelled area of 3 images taken per well was determined by standardized thresholding and ImageJ analysis. Percent cell death was calculated by subtracting the average percent live stained area of the AntiA group normalized by its respective AntiA-negative control from 100%. All experiments were repeated

at least three times. The CellTiter-Blue® (CTB) (Promega Corporation, WI, USA) cell viability assay was used on bCaP only disks (data are not shown here) for comparison to the live staining method. All experiments were repeated at least three times. Schematic representation of the experimental setup and coating method can be found in Figure 2.1.

Evaluation of Cell Access Mechanism:

Scanning electron microscopy (SEM) (JSM - 5900LV, Jeol USA Inc. Peabody, MA) was used to examine the coating before and after incubation in culture medium for 4 hr or 3 days with or without cells to determine the coating degradation mechanisms in the presence and absence of PEM coatings. Either MC3T3-E1 , RAW 264.7 cells were cultured on disks coated with AntiA-bCaP-FGF2, or AntiA-bCaP-PEM30-FGF2. LIVE® staining was performed to examine cell access kinetics and then cells were removed by incubation in Trypsin-EDTA (Sigma, St. Louis, MO).

For SEM preparation, the trypsin solution was removed, disks were washed three times with DI water and dried with a series of ethanol solutions. Disks with PEM coatings were critically point dried after ethanol dehydration using (LEICA EM CPD030, Leica Microsystems Inc. Buffalo Grove, IL, United States) to preserve the delicate surface structure of PEM film. After drying, disks were sputtered coated (vacuum DESK V, Denton Vacuum, LLC, NJ, United States) and imaged using SEM (SEM, TM-1000, Hitachi High-Technologies Corporation, Tokyo, Japan). SEM analysis was conducted on at least three samples per group.

2.2.3 Statistical Analysis

Statistical significances were determined using Graph Pad Prism software by unpaired t-tests if only two groups were in the study or by one-way ANOVA with Tukey post-tests for multiple comparisons in larger studies with P values ≥ 0.05 being considered statistically significant.

2.3 Results

2.3.1 Characterization of the Coatings bCaP vs. bCaP-PEM

MC3T3-E1 cell proliferation and viability on bCaP-coating was compared to cell cultured on bCaP-PEM30 to examine cell growth on the biomaterial coatings without any factors. Calcium phosphate layer (bCaP) enhanced cell proliferation over time compared to bCaP plus PEM. A significant decrease in percent LIVE® stained area of MC3T3-E1 cells was observed when cells cultured on bCaP-PEM (blue) as compared to cells cultured on bCaP-only (Gray) at day 1, 3 and 5 (Fig. 2.2 A, B).

To change the delivery profile from the bCaP-PEM system, PEM film was removed and cells were grown on bCaP coating as compared to cells cultured on bCaP -PEM film. MC3T3-E1 cells were either cultured on bCaP(24h) or bCaP (24h)-PEM coating with AntiA embedded beneath the bCaP coating and FGF2 on top of bCaP coating. MC3T3-E1s initially proliferated and then abruptly accessed the embedded AntiA on day 3 on AntiA-bCaP-PEM-FGF2 and then recovered (Fig 2.3 A, B). However, on bCaP(24h) coating without PEM, the AntiA was accessed by the cells on day 2 with less cell recovery over the time points studied compared to bCaP-PEM coating (Fig 2.3 C, D).

To further extend the timing of access between the two factors delivered to osteoprogenitors, bCaP barrier layer thickness was increased. Altering bCaP layer thickness was successfully achieved by changing the incubation time in solution B. Depositing thicker bCap layer resulted in no further delay in cells the access to the embedded factor. bCaP(48h) layer without PEM resulted in a more gradual access to the cytotoxic AntiA than bCaP(24h) but cell access was still detected on day 2 as measured by significant decrease in LIVE® staining on day 2 and the remaining time points in the study (Fig 2.3 E, F).

Studies with RAW 264.7 macrophages as compared to MC3T3-E1 mouse calvarial osteoprogenitors were conducted to investigate the possibility of altering the delivery kinetics of the factors by changing the cell type. Changing cell type to macrophages altered delivery kinetic of AntiA. RAW264.7 cells immediately accessed the embedded AntiA on disks coated with AntiA-bCaP-PEM-FGF2 observed by the significant decrease in LIVE® at 4 hrs and throughout the duration of the study (Fig. 2.4 A, B). Removing PEM film resulted in 2 days delay access by the macrophages (RAW 264.7) to the embedded AntiA on bCaP without PEM (Fig. 2.4 C, D).

2.3.2 Cell Access Mechanisms by SEM Imaging

SEM imaging was used before and after the cell culture on disks coated with bCaP and bCaP-PEM to investigate the mechanism followed by both cells type to access the embedded factor. SEM revealed that the incubation of bCaP-PEM coated disks in culture medium alone without cells resulted in changes in the surface structure of the cracks present in the coating indicating that the dissolution process opened the crystal junction between bCaP crystal (wider cracks were noticed) to facilitate cell access (Fig 2.5 A and B). The cracks were sharper after

MC3T3-E1 cultured on bCaP-PEM coated disk and wider when RAW cells cultured on bCaP-PEM coated disks (Fig 2.6 C). RAW cells did not have noticeable effect on the surface coating at 4hrs but changed the cracks structure on day3 (Fig 2.5 D).

SEM showed wider cracks between the crystal clusters of bCaP coating after the bCaP coated disks was incubated in cell culture medium (Fig 2.6 A, B). SEM revealed that RAW cells dissolved bCaP and created micro-openings in the bCaP coating to get access to the embedded AntiA on bCaP coating (Fig 2.6 D). SEM showed more cracks between the crystal junctions when a thicker layer of bCaP (48 hr long deposition time) was deposited and these cracks were even wider after MC3T3-E1 was cultured on the surface (Fig 2.7).

2.4 Discussion

Local delivery of single factor or combination of two factors using biomaterials has significantly progressed over the years reviewed by Kangwon Lee et al [199]. An ideal local delivery system should mimic the normal physiologic environment by controlling the timing and concentration of factors to be delivered. The ability of bCaP-PEM system [204] to tune factors delivery kinetic was investigated in this study for possible use of the system with multiple applications given the tunablity of the delivery offered by this study. The system ability to tune factor delivery was tested by the removal of PEM film or changing bCaP thickness.

PEM film caused decrease in cell viability as compared to cells grown on bCaP coatings without the PEM film. The reduced cells viability with bCaP-PEM is due to the effect of poly-L-Lysine within the coating. The PLLys is known to have slightly cytotoxic effect with time and concentration dependent assisted with MTT cytotoxicity evaluation assay [256, 257]. An

alternative strategy to delay cell access to embedded factor is by removing PEM layers and increase bCaP coating thickness.

bCaP coating thickness was either decreased or increased by changing the incubation time in solution B of the SBF during bCaP deposition. Increasing or decreasing the incubation time resulted in increase or decrease in the bCaP coating thickness [238, 239, 255]. Depositing a thicker bCaP(48h) layer did not change delivery kinetic observed by MC3T3-E-1. It is believed that increasing bCaP thickness have no effect on the access process of the cells as cells ability to penetrate the coating and access the embedded factors as compared to a thinner bCaP layer. It also believed that bCaP layer has nano-porous structure making the penetration of the cells through the pores easier to achieve with a thinner layer of bCaP [258-260].

Given the wide variety of cell types interacting with the biomaterial implanted in the body; an ideal biomaterial delivery system should have the ability to coordinate with the innate immune response. Macrophages are essential cells contribute in early phase of the regeneration process of any healing process. Macrophages are one of the very first cells interacting with the implanted materials [261] and have essential role in regulating tissue repair and tissue response to biomaterials [262-264]. Macrophages cell-type is known to have the ability of fast degradation or resorption of the coated material. RAW 264.7, a macrophages cell line, in particular have the ability to degrade non-cross-linked polyelectrolyte multilayer films [265]. In this study RAW 264.7 cells showed immediate no delay access to the embedded AntiA when cultured on bCaP-PEM and 2 days delay when cultured on bCaP without PEM. This change in delivery profile could be due (a) enhanced ability of macrophages to degrade the coating over osteoprogenitors; and (b) to the changes in bCaP surface morphology when covered with PEM. Previous study showed that bCaP crystallinity was reduced when bCaP coating covered with PEM film [204]

which enhanced and expedited the degradation process by the RAW cells. Varying cell type profoundly affected the surface coating and kinetics of delivery making this system valuable for applications to target specific cell type behavior.

For better assessment of cells mechanism of access to the embedded AntiA; SEM imaging was performed on coated disk before and after cell culture. Cells cultured on bCaP-PEM coated disk did not impact the surface coatings with both cell types. The dissolution process opened the crystal junction especially when bCaP coating without PEM was used. It was also noticed that the incubation in medium alone opened the cracks between the bCaP crystal junctions. Since incubation in medium made the cracks wider; it is believed that MC3T3-E1 were able to penetrate their processes through the wider cracks to access AntiA on day 2. RAW cells followed different approach by dissolving the bCaP coatings on day 3 of cell cultured on AntiA-bCaP . Macrophages have ability to produce factors that can dissolve the bCaP coating. RAW cells not only able to dissolve carbonate substrate, but also change in cells morphology was reported in response to the culture surface [266].

2.5 Conclusions

These studies proved that the drug delivery from bCaP-PEM system is governed by the interaction of the cells with the mineral-poly amino acid layered structure rather than by typical drug diffusion. Delivery kinetics could be tuned by removing PEM layers to best serve delayed delivery to macrophages. Removing PEM coating allowed earlier access by osteoprogenitor cells indicating PEM is an important component of the system when targeting this type of cells. Varying cell type profoundly affected the surface coating and tuned kinetics of delivery due to (i)

the enhanced ability of macrophages over osteoprogenitors to degrade the coating, and (ii) reduced bCaP crystallinity after the PEM coating procedure which caused expedited access to the second factor by RAW cells. Future work will be focused on the use of the bCaP system to modulate the innate immune cells with different biomolecular targeting both osteoprogenitor and macrophages behavior.

Table 2.1 Nominal chemical composition of Solutions A and B in mM.

Inorganic Salt	Solution A	Solution B	Reagent Chemical
$Na+$	733.5	733.5	Sodium chloride (NaCl)
$Mg^{2}+$	7.5	1.5	Magnesium Chloride, Hexahydrate ($MgCl_2 \bullet 6H_2O$)
$Ca^{2}+$	12.5	12.5	Calcium chloride dihydrate. ($CaCl_2 \bullet 2H_2O$)
Cl-	720	720	
HPO_4^{2}-	5	5	Sodium Hydrogen Phosphate ($Na_2HPO_4 \bullet 2H_2O$)
HCO_3-	21	10	Sodium Hydrogen Carbonate ($NaHCO_{3)}$

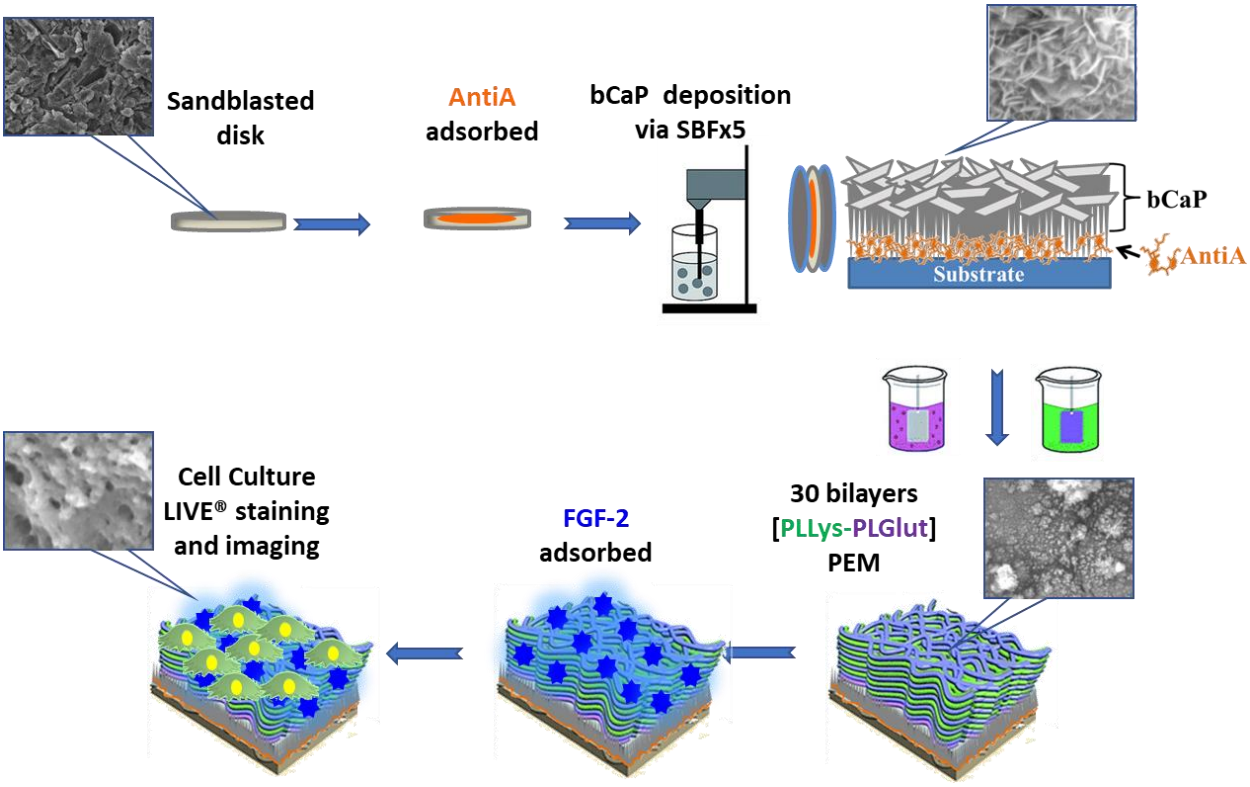

Figure 2.1. Schematic representation of disks coatings preparation and analysis.

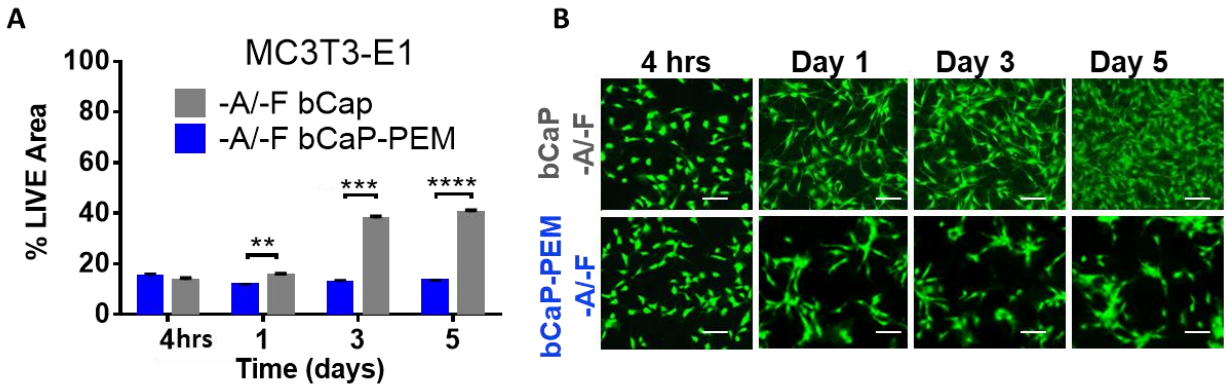

Figure 2.2: Osteoprogenitors cultured on bCaP coating or bCaP-PEM without any drug. (A) Percent of LIVE® stained area of MC3T3-E1s on bCaP (24h) (-A/-F) vs. bCaP (24h)-PEM (-A/-F) showing better cell growth and viability on bCaP coating as compared to the combination of bCaP-PEM. (B) Fluorescent LIVE® stained images of MC3T3-E1 cells on bCaP (24h) and bCaP (24h)-PEM.

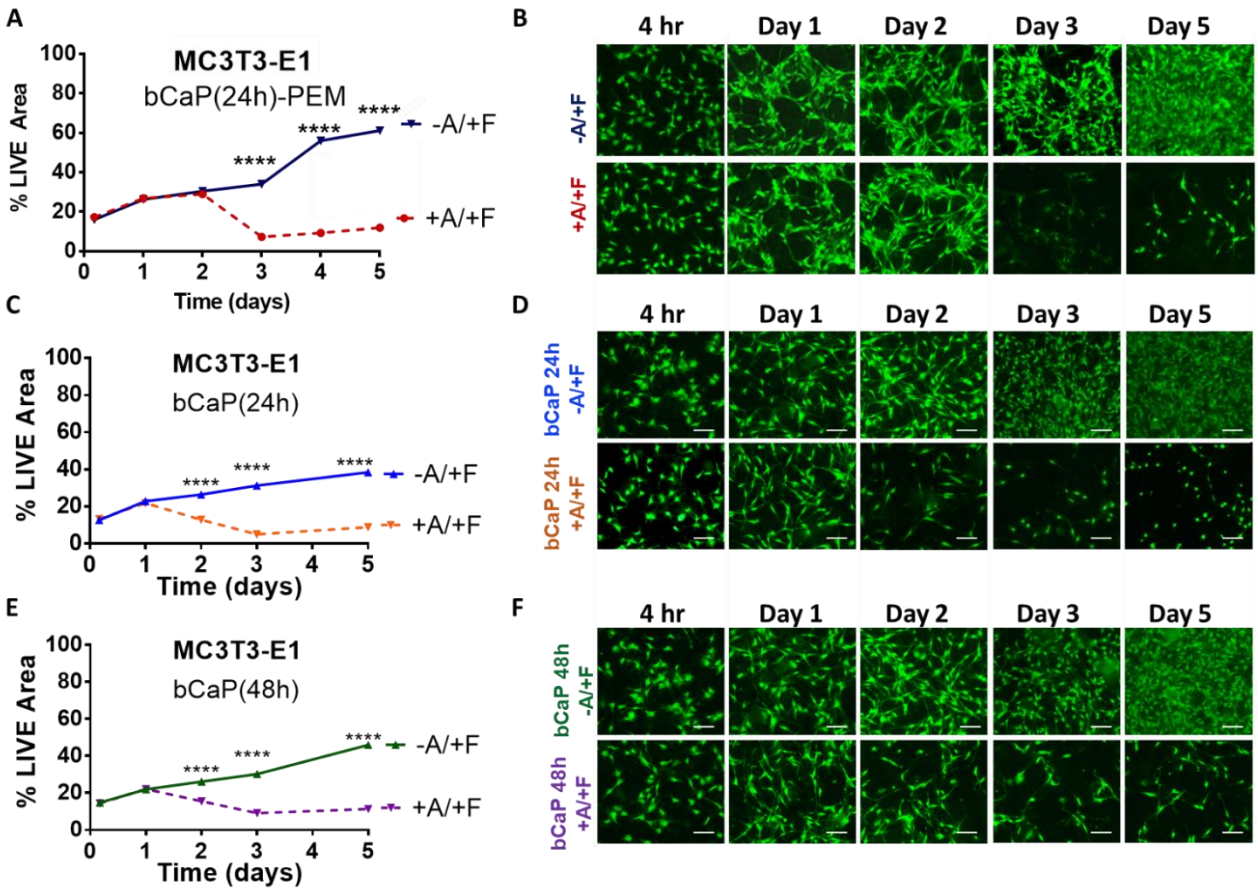

Figure 2.3: (A) % LIVE® stained area of MC3T3-E1s on bCaP24hr -FGF2 (-A/+F) vs .AntiA-bCaP24hr -FGF2 (+A/+F). (B) Fluorescent image of LIVE® staining of MC3T3-E1s on bCaP24hr -FGF2 (-A/+F) and on AntiA-bCaP24hr -FGF2 (+A/+F). (C) % LIVE® stained area of MC3T3-E1s on bCaP48hr -FGF2 (-A/+F) vs AntiA-bCaP48hr -FGF2 (+A/+F), D) fluorescent image of LIVE® stain of MC3T3-E1s on bCaP48hr -FGF2 (-A/+F) and on AntiA-bCaP48hr -FGF2 (+A/+F) , (**** $P < 0.001$). Scale bar = 100 μm.

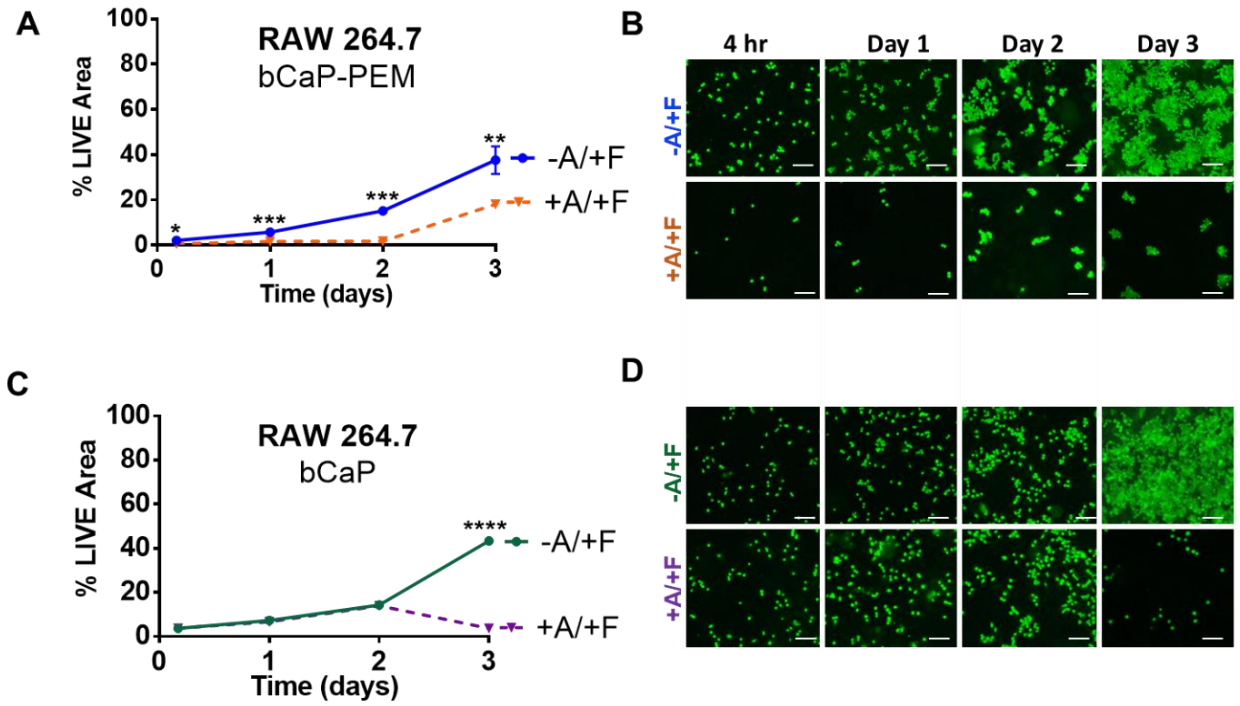

Figure 2.4: Tuning delivery kinetics by changing cell type and removing PEM coating **(**A) Percent LIVE® stained area of RAW 264.7 cells cultured on bCaP-PEM30-FGF2 (-A/+F) as compared to cells cultured on AntiA-bCaP-PEM30-FGF2 (+A/+F) showing RAW264.7 cells immediately accessing the embedded AntiA on 4hrs of culture (* $P \leq 0.05$, ** $P \leq 0.01$, *** $P \leq 0.001$). (B) Fluorescent LIVE stained images of cells cultured on bCaP-PEM30-FGF2 (-A/+F) as compared to cells cultured on AntiA-bCaP-PEM30-FGF2 (+A/+F) at 4 h, 1, 2, and 3 days of culture. (C) Percent LIVE® stained area of RAW cells on bCaP coating showing access to AntiA on day 3 of culture (** $P < 0.01$, **** $P < 0.001$),). (D) Fluorescent LIVE stained images of cells cultured on bCaP-FGF2 (-A/+F) as compared to cells cultured on AntiA-bCaP-FGF2 (+A/+F) at 4 h, 1, 2, and 3 days of culture. Scale bar = 100 μm.

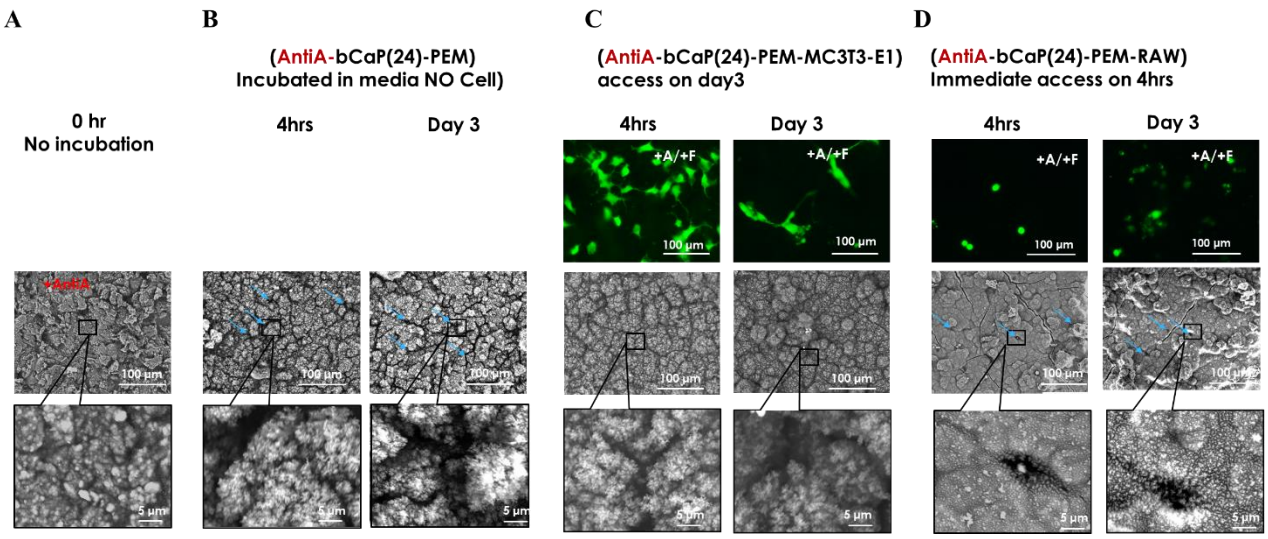

Figure 2.5: Scanning electron microscopy of bCaP with AntiA. (Column A) SEM of AntiA-bCap(24)-PEM before cell culture. (Column B) SEM of AntiA-bCap(24)-PEM coated disk and incubated in cell medium for 4hrs and 3 days without cells. (Column C) 4hrs and Day3 LIVE staining +A/+F AntiA-bCaP(24)-PEM-MC3T3-E1. (Column D) 4hrs and Day-3 LIVE staining +A/+F AntiA-bCaP(24)-PEM-RAW.

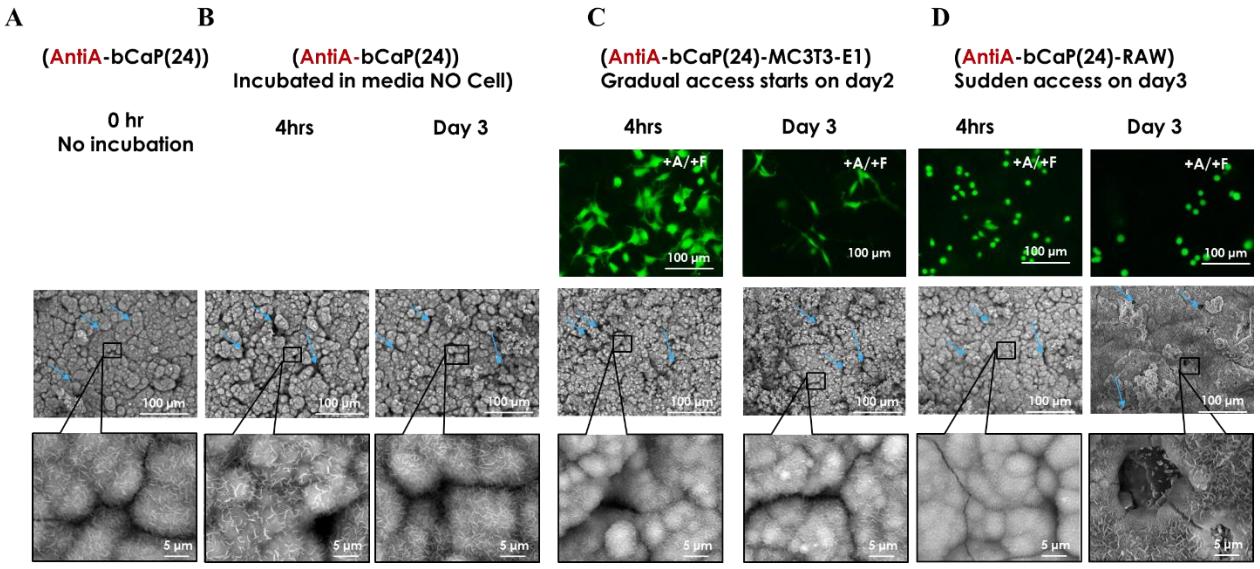

Figure 2.6: SEM imaging of AntiA-bCaP coated disks (Column A) SEM of AntiA-bCap(24) before cell culture. (Column B) SEM of AntiA-bCap(24) coated disk and incubated in cell

medium for 4hrs and 3 days without cells. (Column C) 4hrs and Day3 LIVE staining +A/+F AntiA-bCaP(24)-MC3T3-E1. (Column D) 4hrs and Day-3 LIVE staining +A/+F AntiA-bCaP(24)- RAW.

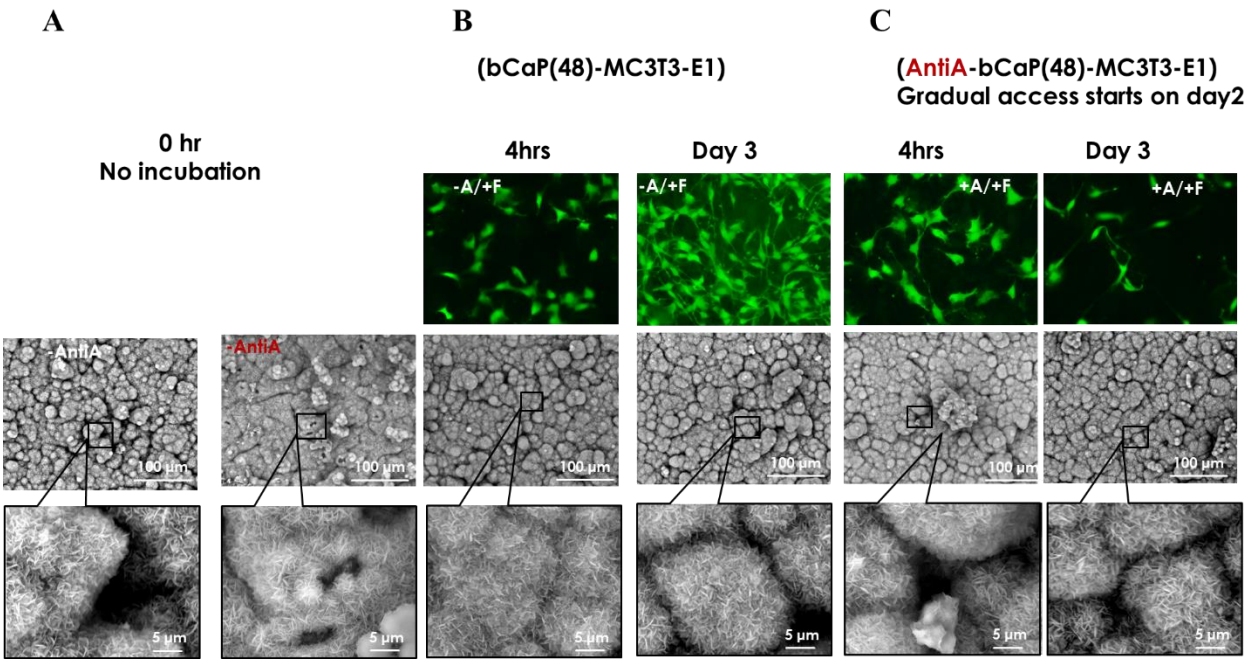

Figure 2.7 : SEM images of bCaP (48hrs). (Column A) bCap(48) before cell culture with AntiA and without AntiA. (Column B) 4hrs and Day3 LIVE staining –A/+F-bCaP(48)-MC3T3-E1, bCa(48) coating after 4hrs and 3 days of cell culture –A/+F and correspondent SEM imaging. (Column C) 4hrs and Day3 LIVE staining +A/+F-bCaP(48)-MC3T3-E1 and SEM images of the coating after 4hrs and 3 days of cell culture.

Chapter 3

Controlled M1-to-M2 Transition of Aged Macrophages from Calcium Phosphate Coatings

3.1 Introduction

Macrophages are present in nearly all tissues and are critical for tissue remodeling, homeostasis, and regeneration. Most tissues contain a population of resident macrophages that are able to dynamically adapt to changes in their microenvironment in order to orchestrate critical tissue-specific functions. After a bone injury, macrophages are among the first cells recruited from the bone marrow and peripheral blood to the site of injury, where they coexist with resident macrophages within the bone injury site [218]. Depending on the stage of healing at the injured site, macrophages become polarized toward an appropriate activation pathway that helps to regulate all phases of the healing process. First, macrophages exhibit a pro-inflammatory phenotype (commonly referred to as M1) [25]. M1 macrophages are critical for the initiation of angiogenesis and osteogenesis [26]. At later stages of healing, M1 macrophages transition to a pro-reparative phenotype (commonly referred to as M2) to guide the repair process to completion [26]. It is now known that M2 macrophages can be further subdivided into a series of distinct phenotypes, each with diverse functions ranging from tissue deposition to tissue remodeling [27]. Injuries with poor healing outcomes are associated with a stalled M1-to-M2 transition [267, 268]. Given the sequential and synergistic roles of M1 and M2 macrophages in the healing process, it has been proposed that biomaterial strategies that sequentially promote M1 and M2 activation will enhance healing compared to promotion of either phenotype alone or concurrent promotion of both types [26, 155, 269].

Many patients requiring bone repair treatments are older with chronic low levels of inflammation [117]. A few studies have examined the behavior of macrophages obtained from older mice and humans and seen an age-related impairment in macrophage polarization, cytokine production, phagocytic ability and have linked this to the impaired bone healing seen in older patients [122, 270, 271]. Age-related alterations in macrophage function and response to stimuli have been reported in old mouse bone marrow derived macrophages [125, 146, 272-274], as well as in human macrophages derived from peripheral blood monocytes taken from older patients over 65 years of age [275]. In general, macrophages from older humans and animals tend to secrete higher baseline levels of pro-inflammatory (M1) cytokines (e.g. *IL6* and TNFα), and respond more slowly to inflammatory stimuli as compared to macrophages from young humans and animals [276]. Decreased production of pro-reparative (M2) cytokines has been observed in macrophages from old mice [270]. There is also an increase in macrophage accumulation in dermal, adipose, thyroid and liver tissue in older humans and animals [271, 277-279]. In mice, it was demonstrated that transplanting bone marrow that contains the hematopoetic precursors for macrophages from 4-week-old young mice into 12-month-old adult mice improved fracture healing [280]. In addition, impaired cutaneous wound healing in aged mice was reversed when macrophages from young mice were transferred to aged mice [281]. Thus, a biomaterials delivery system with appropriately timed delivery of stimuli that can restore youthful macrophage polarization of endogenous macrophages could be a promising approach to enhance bone and tissue healing in the older population, but must consider the alterations to the macrophages present in the elderly tissue environment.

Several strategies for local delivery of molecules to modulate macrophage phenotype in young mice have been developed to accelerate tissue repair. M1 macrophages are usually

activated by interferon gamma (IFNγ) and/or lipopolysaccharide (LPS), while M2 macrophages are activated by interleukins IL-4, IL-13 or IL10 [29, 31], although it is likely that polarization stimuli in vivo are more complex and multifaceted. In a murine subcutaneous implantation model, the release of IFNγ enhanced vascularization relative to controls, but the dual delivery with IL-4 had no effect [155]. The lack of effect was attributed to the overlapping IFNγ and IL4 release profiles at the early phases, which caused simultaneous, not constructive, M1 and M2 activation. Indeed, too early of an increase of M2 macrophages can be detrimental as shown by impaired wound healing from administration of M2 macrophages at early times after injury [213], although this finding may be context-dependent [271]. Thus, a major goal of the present study was to design a biomaterial drug delivery system that sequentially delivers M1- and M2-promoting stimuli in distinct phases and to test the strategy in macrophage sfrom old mice.

In the present study, the applicability of a biomimetic calcium phosphate (bCaP) coating to serve as a highly localized delivery system to guide macrophage phenotype transitions was tested. The effect of in vitro sequential delivery of M1-stimulating IFNγ followed by the anti-inflammatory, M2-promoting simvastatin (SIMV) [177, 282-288] by bCaP was studied. Both human macrophages (THP-1 cell line), as well as primary mouse-bone marrow derived macrophages were tested. Macrophages were obtained from very old mice, 25-26 months old, that correlates to >85 human years [289]. The overall goal of the study was to test the hypothesis that the sequential delivery of IFNγ followed by SIMV from bCaP can sequentially polarize both young and aged macrophages, in vitro, from M1 to M2.

3.2. Materials and Methods

3.2.1. Application of bCaP coating with or without macrophage stimulating molecules

Simvastatin, (PHR1438, Sigma Aldrich), the M2-promoting molecule, was adsorbed directly on ultra violet light-sterilized, 22 mm, by placing 10 ul of ethanol containing 0, 2 or 10 μg SIMV on the side of the TCPsb disks to be cell-seeded and allowing it to dry for 10 min. A coating of bCaP was deposited to cover the SIMV or vehicle following a previously reported method [204]. Briefly, the disks were immersed in a 5x concentrated simulated body fluid solution in a two-step process leading to a crystalline, bone-like apatite coating [238, 253, 255]. After bCaP application, 0, 250 or 500 ng of the M1 stimulating molecule IFNγ (Cat#300-02, Peprotech Inc, NJ) in 0.5 ml PBS was adsorbed for one-hour on the outer surface of the bCaP coated disks and then rinsed with PBS. Disks were placed in 12 well non-treated tissue culture plastic cell culture dishes (Corning, USA, Cat# 351143) for the studies. Cells were also cultured directly on the non-treated polystyrene as a control for comparison to bCaP coated disks.

In the studies that determined the kinetics of macrophage access to a factor embedded below the bCaP layer, a cytotoxic dose of antimycin A (AntiA, Cat# A8674, Sigma, St. Louis, MO) was pipetted on to the TCPsb, allowed to adsorb and then covered with a layer of bCaP as described above. The dose of 213 μg/disk was applied by placing10 μl of a 40 mM solution in ethanol on the side of the TCPsb disks to be cell-seeded, allowed to dry for 10 minutes and then rinsed three times with saline prior to bCaP coating. No SIMV or IFNγ were used in the experiments with AntiA.

To determine the binding efficiency of IFNγ to the bCaP surface, a binding solution of 250 ng of IFNγ in 0.5 ml PBS was placed on bCaP coated disks for one hour and then collected

for enzyme-linked immunosorbent assay ELISA (PeproTech, Inc., New Jersey, Cat# 900-TM27). The disk was then rinsed twice with PBS with the first rinse removed immediately and the second one after 30 min. The difference between initial binding solution concentration and the concentration after 1 hr adsorption was used to determine the IFNγ bound on the disks. 100% binding efficiency of SIMV and Anti A was assumed based on their poor solubility and inability to detect the molecules by standard UV-VIS methods.

3.2.2 Cell culture

Young human peripheral blood derived macrophages: The monocyte cell line THP-1 (ATCC® TIB-202™) that is derived from human peripheral blood were used to obtain macrophages for the studies. THP-1 cells were expanded in ultra-low attachment flasks (Corning, USA, cat# CLS3814) in RPMI medium (Thermo Fisher Scientific, MA, USA) with 10% heat inactivated fetal bovine serum (FBS), and 100 U/ml penicillin and 100 μg/ml streptomycin sulfate. THP-1 at 0.6 million cells/ml were differentiated to macrophages through incubation in 100 mM phorbol-12-myristate 13-acetate (PMA) (Sigma, USA, P8139) for 24 hrs. Macrophages were then gently scraped off the ultra-low attachment culture flask and seeded at 1 x10^6 cell/ml on bCaP coated disks with or without the drugs/cytokines that had been incubated for 30 min in Roswell Park Memorial Institute (RPMI) medium (Thermo Fisher Scientific, MA, USA) prior to cell culture. In the SIMV dose determination studies, cells were cultured with 100ng/ml of both LPS and IFNγ in the medium to provide the M1 stimulation, and then refreshed on day 3 with drug free medium to evaluate the M2 effect of simvastatin.

Mouse Bone Marrow Derived Macrophages (BMDMs): The preparation of BMDMs from adult and old mice followed a previously described method [30]. Briefly, four male C57BL/6 mice that were either 6 months (adult) or 25 months old (old) were euthanized using CO_2 inhalation according to a protocol approved by the Institutional Animal Care Use Committee of University of Connecticut Health Center following recommendations of the Panel on Euthanasia of the American Veterinary Medical Association. Bone marrow of the dissected femurs and tibias were flushed with 5 mL DMEM (Gibco™ Invitrogen, CA, USA). The marrow was centrifuged for 5 mins and washed twice with medium and then cultured for five days in 100 mm non-treated tissue culture dish with 10% heat-inactivated FBS, 20 ng/mL monocyte colony stimulating factor (M-CSF) (PeproTech, Inc, NJ, USA, Cat# 300-25) and 100 U/mL penicillin and 100 μg/mL streptomycin. The cells were then gently scraped off the dish and re-suspended with media and plated at 0.5×10^6 cell/ml on bCaP coated disks with or without the drugs/cytokines that had been incubated for 30 min in RPMI medium prior to cell culture. Time points for analysis were restricted to day 1 and day 6 due to the difficulty of obtaining more than four of the very old mice at a time. Studies were repeated twice.

3.2.3 Characterization of macrophage phenotype transitions

Macrophage phenotype characterization: The expression of a panel of genes previously identified to be suitable for discriminating M1 and M2 macrophage phenotypes were evaluated in these studies (42). Given the previous time scale of macrophage phenotype transitions in response to biomaterials observed in our earlier studies (9), the time points of 1, 3 and 6 days were selected for analysis of macrophage phenotype on the bCaP coated disks. Primer

sequences can be found in Table 1. The cells were harvested for gene analysis using TRIzol reagent (Invitrogen Life Technologies, CA, USA). RNA was reverse transcribed into cDNA using EcoDry Premix (Oligo dT) (Cat# 639543, Clontech) and thermocycler (BIO-RAD Laboratories Inc., CA, USA) followed by Quantitative Polymerase chain reaction (qPCR) using iTaq™ universal SYBR® Green supermix kit (BIO-RAD Laboratories Inc., CA, USA) on a MyiQTM instrument. Values were normalized to GAPDH using $2^{-\Delta ct}$ method, where Δ*C*T is the result of subtracting [*C*T gene − *C*T GAPDH] of control or experimental group.

Kinetics of macrophage access to the factor below bCaP coating: LIVE® staining (Invitrogen Life Technologies, Grand Island, NY), as per the manufacturer's protocol, was used to evaluate THP-1 macrophage access over time to the cytotoxic AntiA adsorbed under the bCaP coating. Cells cultured on the disks were imaged at 100X magnification using an inverted microscope (TE300, Nikon) equipped with a camera (Diagnostic Instruments), and imaging software (Spot Insight, Nikon). THP-1 cell density was quantified as average percent fluorescent area via ImageJ software (U. S. National Institutes of Health, Bethesda, Maryland, US) as follows: the images were converted to grayscale; threshold to binary images and the percent area of LIVE stain were estimated using Image-J software (U. S. National Institutes of Health, Bethesda, Maryland, USA). Percent cell viability was calculated by comparing the average percent fluorescent area of the AntiA group to its AntiA-free control. ImageJ analysis was performed for 3 images per well with 3 wells per each experimental time point.

3.2.4 Statistical Analysis

Statistical analysis performed using unpaired t-tests for two groups or by one-way ANOVA ($P<0.05$) with Tukey post-test for 3 or more groups (using GraphPad Prism).

3.3. Results

3.3.1 Localized, temporally controlled drug delivery from bCaP coatings

To understand the timing of macrophage access to drug embedded below the bCaP barrier layer, human THP-1-derived macrophages were cultured on bCaP or bCaP-AntiA-coated disks and cell viability was quantified. While the macrophages initially proliferated in both groups, by day 3 the macrophages began to die on scaffolds coated with bCaP-AntiA, indicating that the cells accessed the cytotoxic drug by that time point (Figure 3.1). With regards to the dose of IFNγ adsorbed on the outer surface of the bCaP, ELISA testing revealed that 96% of the IFNγ placed on the bCaP bound to bCaP coating. The IFNγ concentration was not measurable in the 30 min rinse solution by ELISA. This further confirms the highly localized nature of delivery from a bCaP coating as reported earlier (27).

3.3.2 Response of macrophages to bCaP coatings

As a step towards understanding the effect of the bCaP coating itself without additional factors to modulate macrophage behavior, the response of macrophages to this material was compared to a control, non-tissue culture-treated polystyrene (PS). Culture of human THP1

monocyte-derived macrophages on the bCaP coating resulted in upregulation of all three M1 markers measured at 1 and 6 days of culture as compared to PS (Figure 3.2 A-C). The M2 markers were not affected by culture on bCaP compared to PS (Figure 3.2 D and E).

3.3.3 SIMV dose optimization

To determine the dose of SIMV delivered from bCaP that could influence M2 polarization, human THP1-derived macrophages were cultured on bCaP-coated disks containing 2 or 10 μg of SIMV in the presence of M1-polarizing stimuli, IFNγ and LPS, contained in culture medium for the first three days. Interestingly, increasing the dose of SIMV from 2 to 10 μg caused an increase in expression of the M1 marker *CCL1* at days 2 and 3 and in *CXCL10* at day 3. By day 4, however, SIMV caused the expression of all three M1 markers to decrease, concomitantly with an increase in expression of the M2 markers *CCL17* and *CD163* in a dose-responsive way (Figure 3.3 D and E).

3.3.4 Sequential delivery of IFNγ followed by SIMV

To determine if adsorbed IFNγ delivered from bCaP could promote early polarization to the M1 phenotype prior to SIMV-mediated M2 polarization, in the absence of inflammatory stimuli in the media, macrophages were cultured on bCaP coatings adsorbed with 0, 250 ng and 500 ng of IFNγ, with 10 μg SIMV embedded within the bCaP coating. Both doses of IFNγ polarized THP-1-derived macrophages to the M1 phenotype at the early time point (1 day), as measured by increased expression of *CCL1*, *CXCL10* and *CXCL11*, compared to the bCaP-SIMV

control (Figure 3.4 A-C). Upregulation of *CCL1* and *CXCL11* was also maintained on day 3. By day 6, the expression of all three M1 markers had returned to baseline levels of macrophages cultured on bCaP-SIMV without IFNγ. The expression of the M2 markers increased in all bCaP loaded with SIMV, but only at the day 6 time point (Figure 3.4 D and E). The shift from M1, stimulated by immediate IFNγ delivery from bCaP, to M2 phenotype, stimulated by delayed SIMV delivery from bCaP, confirmed the ability of bCaP to serve as barrier layer between the two factors delivered to macrophages with no overlap between the molecules to be delivered.

Finally, the optimal doses of IFNγ (250ng) and SIMV (10μg) were tested together and compared to the delivery of either molecule delivered alone from bCaP coating. The adsorption of IFNγ (without SIMV in the bCaP coatings) caused upregulation of M1 markers at both the early and late time points (Figure 3.5 A-C). However, upregulation of M1 markers was inhibited at later time points by the SIMV incorporated into the bCaP coating. Concurrently, at the later time points, there was upregulation of M2 markers by coatings containing SIMV with and without IFNγ adsorption (Figure 3.5 D, E), indicating that SIMV is both anti-inflammatory and M2-promoting.

3.3.5 Response of primary murine macrophages to the sequential delivery system

The ability of the sequential delivery system to polarize primary cells was tested in bone marrow derived macrophages from both aged (25 months) and adult C57/B16 male mice. As hypothesized, the sequential delivery of 250 ng IFNγ followed by 10 μg SIMV from bCaP resulted in elevation of M1 markers on day 1, as measured by the gene expression of Il1β, *Nos2* and *Cxcl11*, compared to cells cultured on bCaP control with no stimuli (Figure 6 A-C). The M2

markers *Ccl17* and *Arg1* were elevated on day 6 of culture compared to cells grown on bCaP (Figure 3.6 D and E).

Given reports of age-related alterations to macrophages, the effects of localized delivery SIMV by bCaP on M2 polarization of old macrophages were compared to the effects on macrophages from adult mice. In these studies, initial inflammatory conditions were induced by LPS and IFNγ included in the media for 3 days and not delivered by the bCaP. The expected initial inflammatory response arose from IFNγ and LPS in both young and aged macrophages as evidenced by an increase of M1 markers (*Il1β, Nos2* and *Cxcl1*). A successful shift to the M2 phenotype was seen on day 6 for both ages (Figure 3.7). Interestingly, there was a significant reduction in both M1 and M2 response of old macrophages to stimuli as compared to macrophages derived from the younger animals.

3.4. Discussion

Older individuals are at risk for increased falls, are more likely to suffer from fractures and have delayed bone healing due to an extended inflammatory response during fracture healing [6, 64, 290]. Inflammatory processes regulate skeletal cell activity through the release of cytokines and chemokines secreted by macrophages [158, 291, 292]. There is a need for therapeutic approaches that modulate impaired aged macrophage polarization to improve bone regeneration outcomes in older patients. A variety of strategies to activate M1 or M2 macrophage phenotypes have been pursued in the context of improving osteogenesis [154, 155, 263, 293, 294], but very few studies have been conducted in elderly animals that have impaired macrophage responses. Inhibition of inflammatory macrophages in elderly mice with fractures

was reported to prevent delayed healing of old mice [295]. That study administered macrophage modulating drugs to the mice to improve bone formation via systemic delivery for 10 days in their food. The novelty of the present study was to design a localized delivery system using factors known to positively influence osteoblast differentiation and to guide the transition of macrophages. Both the bCaP coating and SIMV contribute positively to new bone formation [164, 296-298]. This work paves the way for application of the bCaP delivery system to bone grafts which could be placed in open fractures or bone defects as a means to locally, in a site specific way, without systemic side effects, control host macrophage response and concurrently improve bone formation.

It is known that the aging process impairs the initiation of the M1 response and delays the M2 polarization in response to stimuli [121, 122, 270, 279, 299]; however, to our knowledge there are no studies that have evaluated the effects of locally delivered therapies from a biomaterial on aged macrophage modulation. In the present study we confirmed the ability of a bCaP biomaterial coating to polarize the impaired old mouse macrophages BMDM with sequential delivery of IFNγ followed by SIMV from bCaP in highly localized manner. Despite no measurable release of IFNγ or SIMV, there were measurable effects on the cells. It has been shown previously that the addition of a bCaP barrier layer to a poly-L-lysine/poly-L-glutamic acid polyelectrolyte multilayer coating effectively provided highly localized, cell mediated, sequential delivery of two biomolecules to osteoprogenitor cells [204], but it was unknown if bCaP alone could deliver two molecules and temporally guide macrophage polarization.

The physical and chemical properties of the biomaterial can influence macrophage modulation. For example, it has been reported that calcium and strontium ions on a nanostructure

titanium surface can increase M2 macrophage phenotype [300]. Another study reported that hydroxyapatite granules activate some M1, but more M2 activation of THP-1 cells [301]. In the present studies, the bCaP coating, which is carbonated hydroxyapatite in the form of a coating rather than in granules, was a potent M1 stimulator for THP-1 cells. An appropriate amount of inflammation and granulation tissue formation is a prerequisite for healthy and successful bone healing outcome, so the M1 stage is essential. Furthermore, given the ability of M1 macrophages to stimulate angiogenesis during tissue regeneration [264, 302], the enhanced M1 macrophage phenotype induced by the bCaP coating may contribute positively to tissue repair.

The underlying mechanism by which SIMV modulates macrophage phenotype has not been fully elucidated, but it is known that SIMV reduces pro-inflammatory cytokines that drive the M1 phenotype [177, 285-287]. Our results suggest that the dose of SIMV we tested promotes a hybrid M2 phenotype, characterized by both M2a and M2c markers (*CCL17* and *CD163*, respectively), which could be mediated through its increase in *IL10* [286, 287]. However, a slight increase in expression of two of the M1 markers was seen at the 10 μg dose of SIMV tested. It has been reported that SIMV caused swelling and inflammatory tissue reactions at milligram doses when implanted in rats [193, 194]. Further in vitro and in vivo dose response studies are needed to determine how to optimize the balance between inflammation and the resolution of inflammation in order to get a net gain during osteogenesis in older animals.

The phenotype of a macrophage changes over time to control bone healing events [39, 193, 194, 302-305]. The importance of the timing of macrophage modulation to osteogenesis was demonstrated in vitro by pipetting in IL-4 to M1-macrophages co-cultured with osteoprogenitors [293]. Only the delayed addition of IL-4 enhanced osteoblastic differentiation

as compared to its immediate administration. Appropriate temporal control over macrophage polarization is required to achieve the pro-anabolic contributions of macrophages to bone repair. The bCaP biomaterial system tested in the present studies provided a similarly timed, delayed modulation of macrophage polarization and thus may be an ideal design to promote osteogenesis. However, this study did have some limitations. First, we only evaluated gene expression of a handful of M1 and M2 markers, but not protein or functional level. Although gene expression has been shown in multiple studies to be a very thorough way to phenotype macrophages [306], it is not known if the M1 and M2 phenotypes promoted by the bCaP delivery system will translate to optimal biological activity and capable of inducing in vivo bone repair in old mice. These limitations notwithstanding, the results of the present study advance the design of immunomodulatory biomaterials that can modulate the behavior of aged macrophages.

3.5. Conclusions

The dysfunctional macrophage of the older person is a target for new approaches to improve bone formation and accelerate repair of bone injuries in the older person. These studies showed that a bioinspired apatite coating is an effective means of temporally separating delivery of an M1 macrophage-promoting stimulus from an M2 macrophage-promoting stimulus, resulting in effective M1-to-M2 phenotype transitions of THP-1 macrophages. The delivery of IFNγ followed by SIMV from bCaP was shown to successfully guide macrophage phenotype transitinos in a macrophage cell line from a young human, as well as primary macrophages derived from adult and old mice. These findings suggest that delivery of immunomodulatory

molecules from bCaP is a valuable strategy that should be pursued as a means of increasing bone formation in older patients who suffer from age-related impairments in macrophage function.

Table 1 PCR primer sequence		
Human peripheral blood THP-1: Housekeeping gene		
Gene	Forward Sequence	Reverse Sequence
GAPDH	AAGGTGAAGGTCGGAGTCAAC	GGGGTCATTGATGGCAACAATA
Human peripheral blood THP-1: M1 Markers		
Gene	Forward Sequence	Reverse Sequence
CCL1	GATGCTGAACAGTGACAAATC	TCAGGAACAGCCACCAGTG
CXCL11	GACGCTGTCTTTGCATAGGC	GGATTTAGGCATCGTTGTCCTTT
CXCL10	ACACTAGCCCCACGTTTTCT	GAGAGGTACTCCTTGAATGCCA
Human peripheral blood THP-1: M2 Markers		
Gene	Forward Sequence	Reverse Sequence
GAPDH	CAGTGCCAGCCTCGTCCCGTAGA	CTGCAAATGGCAGCCCTGGTGAC
CD163	TTTGTCAACTTGAGTCCCTTCAC	TCCCGCTACACTTGTTTTCAC
CCL17	CGGGACTACCTGGGACCTC	CCTCACTGTGGCTCTTCTTCG
CD206	AAGGCGGTGACCTCACAAG	AAAGTCCAATTCCTCGATGGTG
Mouse : Housekeeping gene		
Gene	Forward Sequence	Reverse Sequence
Gapdh	CAGTGCCAGCCTCGTCCCGTAGA	CTGCAAATGGCAGCCCTGGTGAC
Mouse: M1 Markers		
Gene	Forward Sequence	Reverse Sequence
Cxcl11	AGTAACGGCTGCGACAAAGT	GCACCTTTGTCGTTTATGAGC
Nos2	AAACCCCTTGTGCTGTTCTC	ATACTGTGGACGGGTCGATG
IL1β	TTCAGGCAGGCAGTATCACTC	GAAGGTCCACGGGAAAGACAC
Mouse: M2 Markers		
Gene	Forward Sequence	Reverse Sequence
Arg1	GCAGAGGTCCAGAAGAATGG	AGCATCCACCCAAATGACAC
Ccl17	TGCTTCTGGGGACTTTTCTG	CATCCCTGGAACACTCCACT

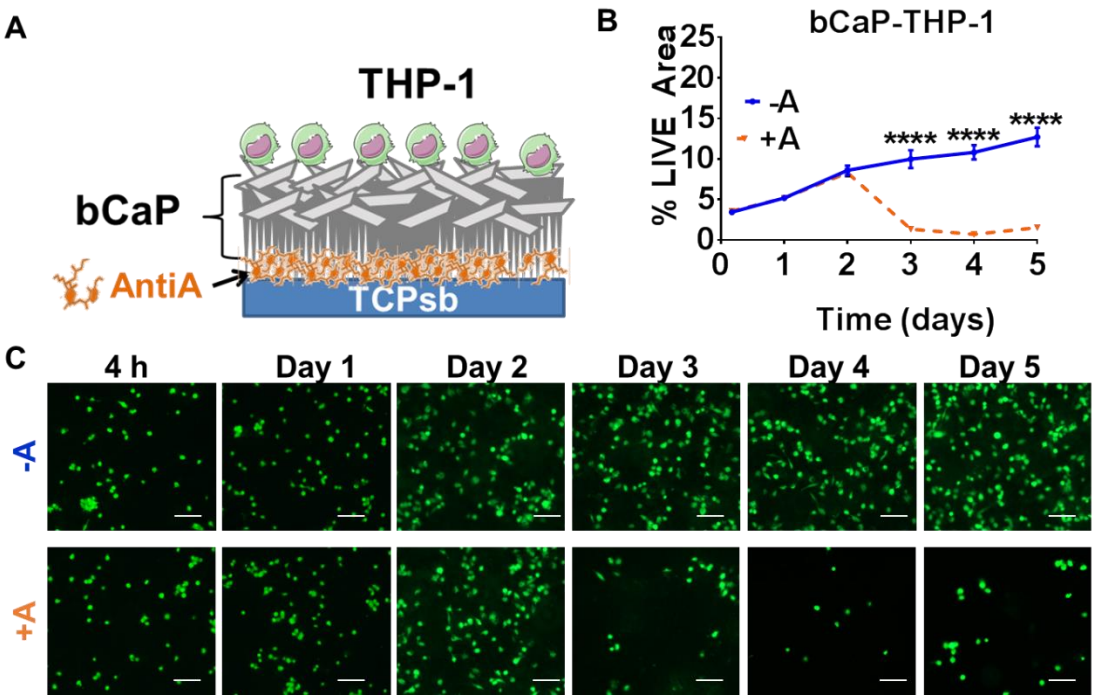

Figure 3.1: Evaluation of the kinetics of THP-1 macrophage access to the cytotoxic AntiA molecule below the biomimetic calcium phosphate (bCaP) barrier coating. (A) Schematic representation of the bCaP coating and AntiA location. (B) Quantified percent LIVE® stained area of THP-1 cells on bCaP coating (**** $P < 0.001$). (C) Fluorescent LIVE® stained images of cells cultured on bCaP alone (-A) as compared to cells cultured on bCaP-AntiA (+A) at over time in culture. Scale bar = 100 μm.

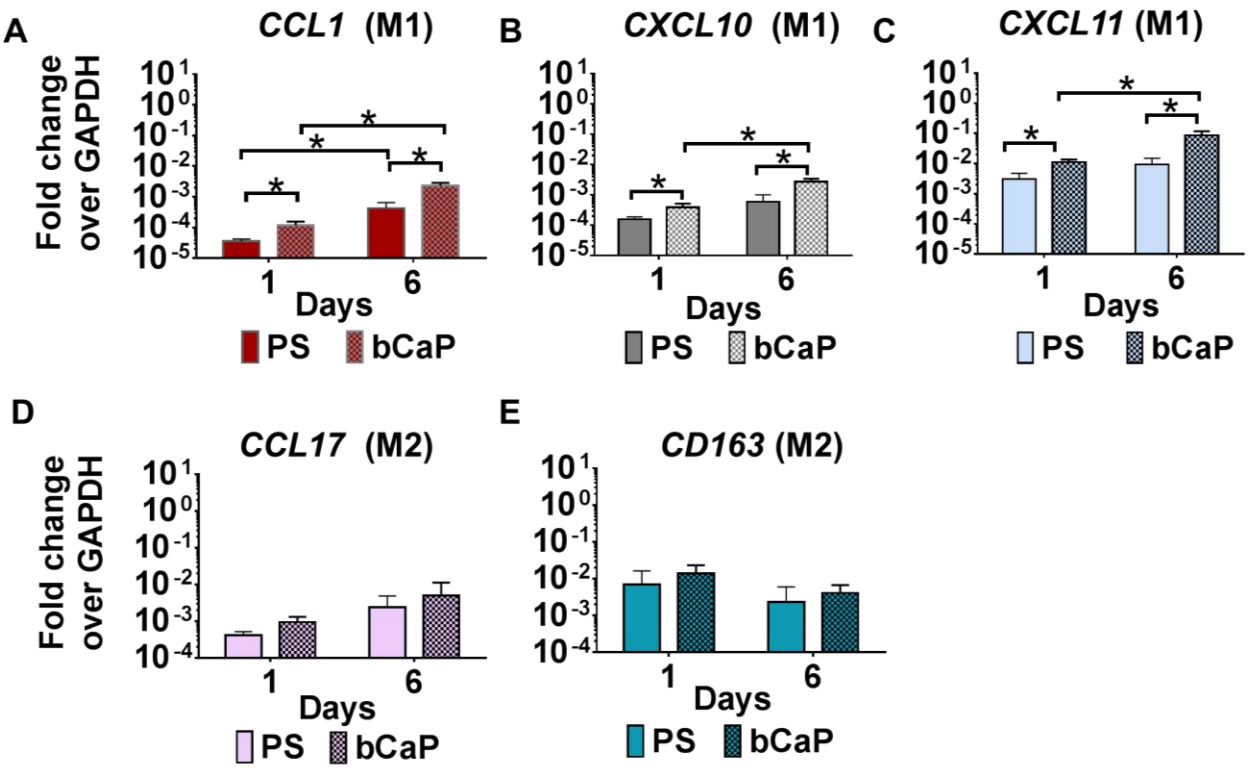

Figure 3.2: Gene expression of human THP-1 macrophages cultured on bCaP as compared to non-tissue culture-treated polystyrene (PS) on day 1 and day 6 of culture. (A-C) M1 macrophage markers. (D and E) M2 macrophage markers. qRT-PCR data presented as fold change over the housekeeping gene GAPDH. * $P < 0.05$.

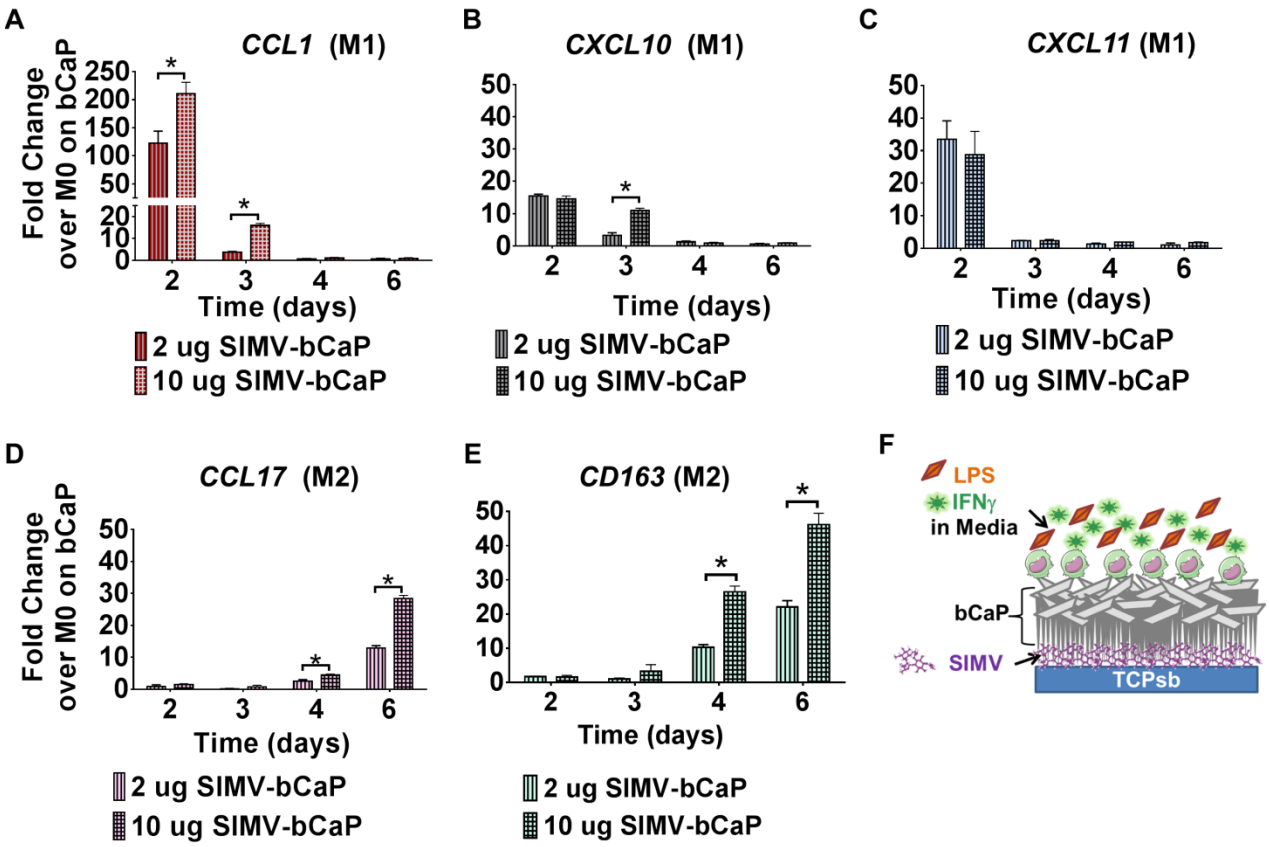

Figure 3.3: Simvastatin dose response study. Gene expression of human THP-1 macrophages cultured on bCaP with either 2 or 10 μg SIMV beneath the bCaP with LPS and IFNγ in the media for the first three days. (A-C) M1 macrophage markers and (D and E) M2 macrophage markers. (F) Schematic representation of the experimental configuration. qRT-PCR data presented as fold change over the housekeeping GAPDH and normalized to M0 macrophages cultured on bCaP without drug. * $P < 0.05$.

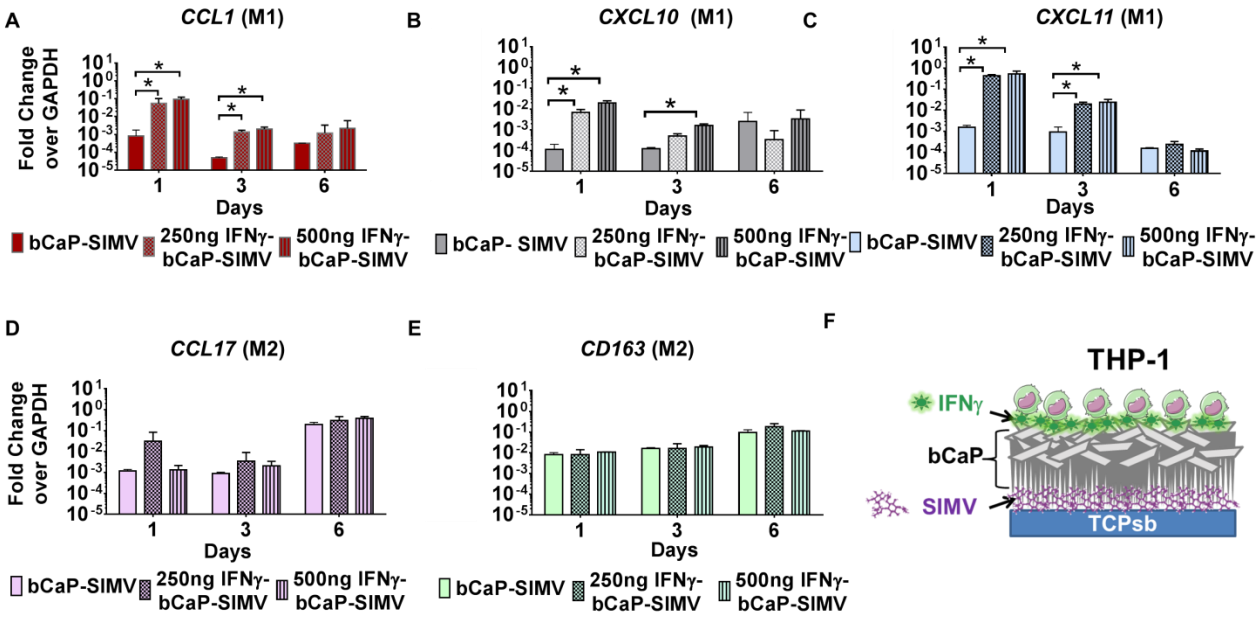

Figure 3.4: IFNγ dose response study in combination with 10 μg SIMV. Gene expression of human THP-1 macrophages cultured on bCaP with IFNγ on the exterior and SIMV below the bCaP barrier layer. (A- C) M1 macrophage markers. (D and E) M2 macrophage markers. Data presented as fold change over the housekeeping gene GAPDH. * $P < 0.05$.

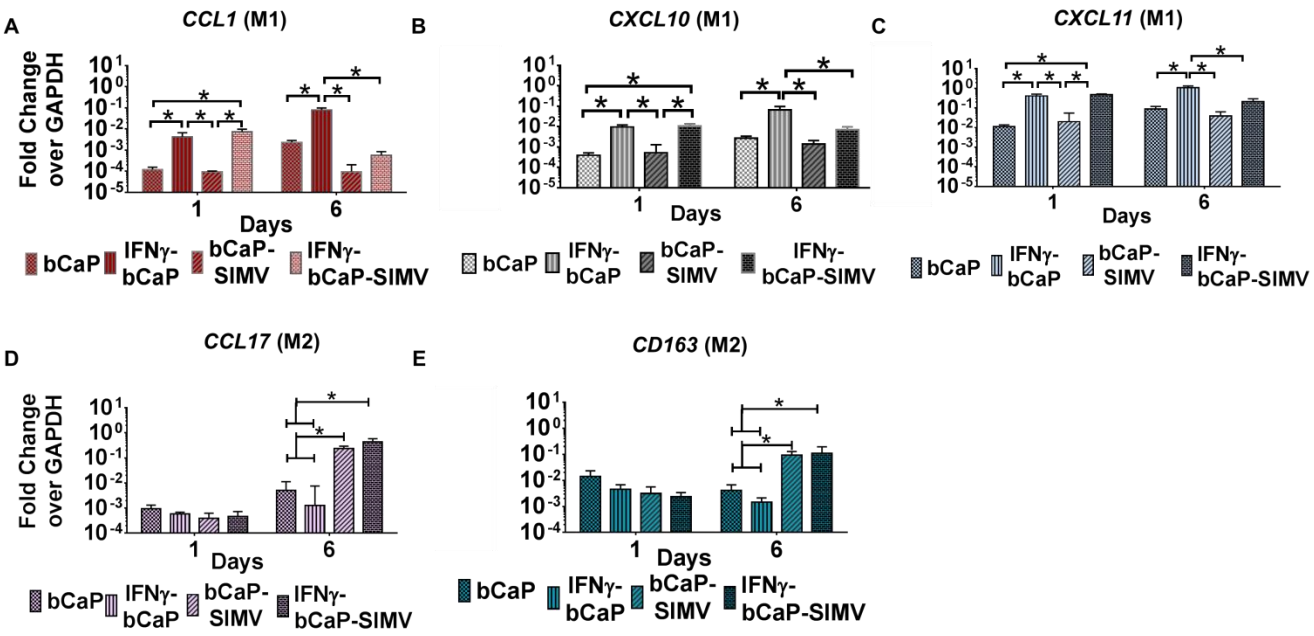

Figure 3.5: Gene expression for THP-1 cultured on bCaP surface with or without 250 ng IFNγ or 10 μg SIMV or both over 6 days. (A-C) M1 macrophage markers and (D and E) M2 macrophage markers. (F) Schematic representation of the sequential delivery system. * $P < 0.05$.

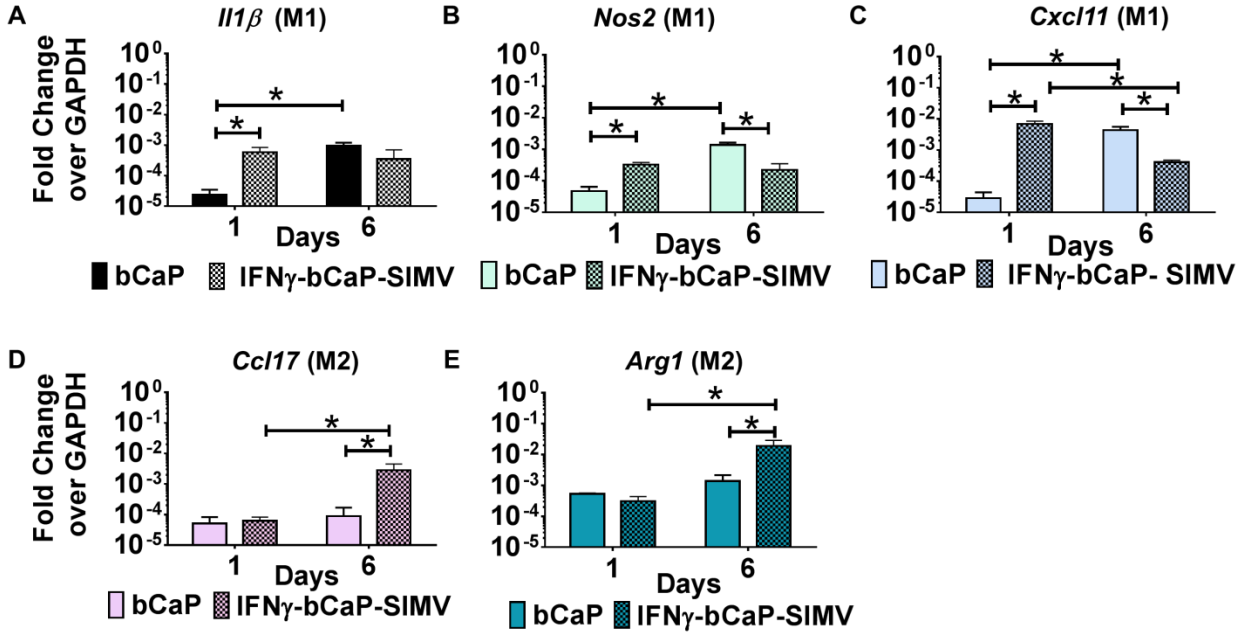

Figure 3.6: Gene expression of old murine bone marrow derived macrophages over time when cultured on bCaP with 250 ng IFNγ on the exterior and 10 μg SIMV below the bCaP barrier layer as compared to culture on the bCaP layer only. (A-C) M1 markers. (D and F) M2 markers. * $P < 0.05$.

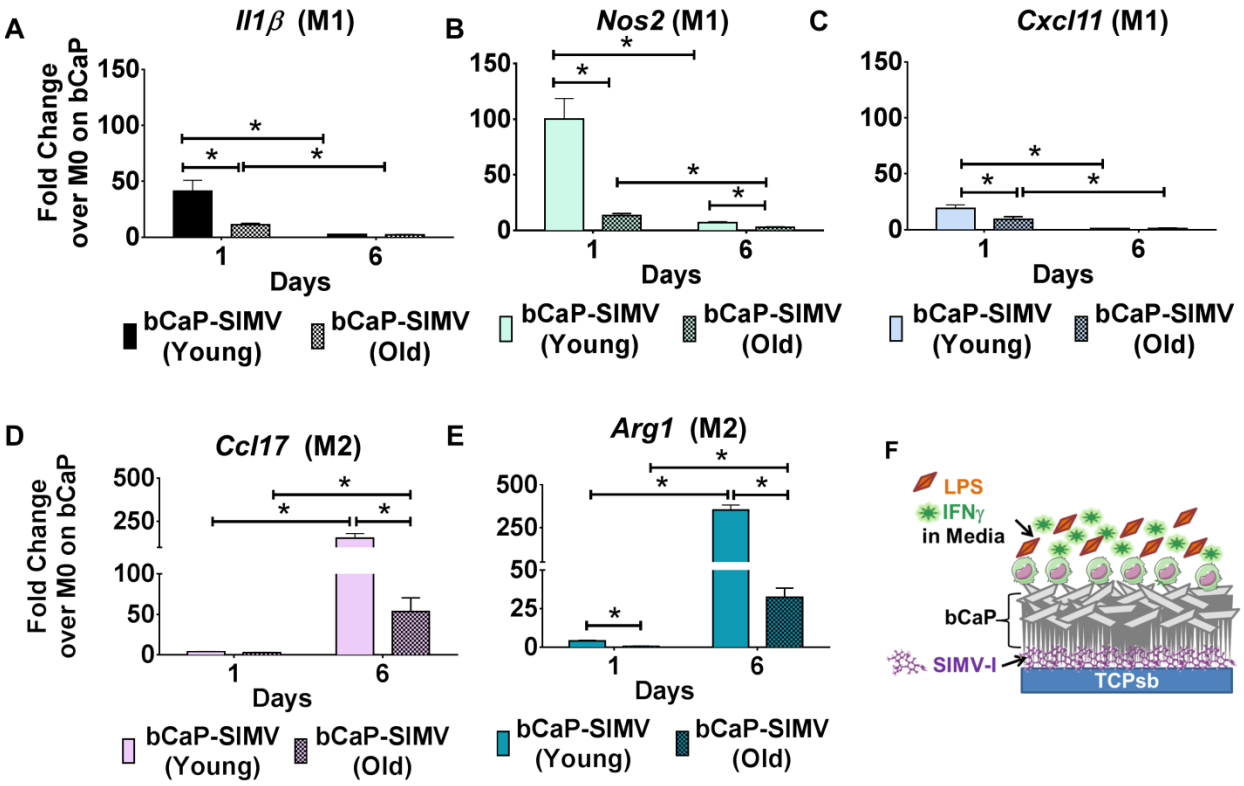

Figure 3.7: A comparison of the gene expression of primary bone marrow macrophages from young adult and old mice during culture on bCaP with 10 μg SIMV below the bCaP barrier layer. The M1 stimuli LPS and IFNγ were in the culture medium for the first 3 days. (A-C) M1 macrophage markers. (D, E) M2 macrophage markers. Data normalized to GAPDH and then expressed as fold change over M0 macrophages cultured on bCaP. * $P < 0.05$.

Chapter 4

Delayed Delivery of Simvastatin Increases Osteogenesis of Older human Osteoprogenitors

4.1 Introduction

Aging can cause a decline in regenerative potential of tissue and cellular functions in a variety of organs [307]. MSCs can differentiate under appropriate stimuli to osteoblasts, adipocytes, chondrocytes, and myocytes [308]. The regeneration potential of mesenchymal stem cells (MSCs) diminishes with advanced age and this contributes to changes in cellular functions. Several reports indicate that aging is accompanied reduction in number, proliferation, and osteogenic differentiation capacity [79, 85, 309, 310]. Therapeutic strategies that target altered cells of the older patient are needed to achieve youthful bone healing.

MSCs have an ability to mediate tissue repair, and their potency to do so is improved by the presence of inflammation at the site of injury [307]. To better understand the effect of inflammation on MSCs, several studies attempted to explore in vitro MSC-macrophage cross-talk [293, 311]. Macrophages were found to induce osteoblast differentiation and matrix mineralization of human MSCs while inhibiting unwanted adipogenesis [293, 311]. Similarly, M2 macrophages and their associated cytokines were shown to support the growth of hMSCs, while M1 macrophages and their associated cytokines inhibited the growth of hMSCs in vitro [40]. These data imply that providing a pro-reparative (M2) environment via localized delivery of therapeutic agent could be an effective strategy to maximize MSCs differentiation.

During senescent cells undergo irreversible growth arrest, but continue to be metabolically active and undergo characteristic changes in gene expression [132]. The senescent

cells can be examined by senescence-associated secretory phenotype (SASP) of senescent cells can be detected by senescence-associated β-galactosidase (SA-β-gal) activity and they are associated with the secretion of a variety of inflammatory cytokines and growth factors [312]. The highest senescent cell secreted factors are IL-4, IL-6, IL-8, IFNγ and β, Transforming Growth Factor Alpha (TGFα), and Monocyte Chemotactic Protein-1 (MCP1) [313-315]. These are factors associated with chronic systemic inflammation present known as inflammaging and immunosenescence [reviewed in [316, 317]]. For example, IL1β, TNFα and TNFβ are all linked to decreased MSC mineralization and increased bone resorption [318-320]. It has also been reported that the increased production of IL-6 by mouse, rat and human osteoblasts was associated with osteoporosis in postmenopausal women [321]. The potential effect of inflammatory cytokines on osteoprogenitor differentiation needs to be considered for optimal bone repair of older patients.

In the previous chapter we tested SIMV as an immunomodulator to modulate macrophage phenotype and shift them to the pro-reparative state. Beside SIMV's ability to serve as an anti-inflammatory agent [282, 283]; it stimulates bone morphological protein (BMP-2), increases recruitment and differentiation of osteoblasts precursors in dose-dependent manner, reduces osteoclast activity [322-329] and improves bone healing [188, 189]. In this chapter, the effect of delayed delivery of SIMV on cytokine expression and osteogenesis of older human osteoprogenitors was investigated. Based on SIMV properties, we hypothesized if pro-inflammatory cytokines negatively impact osteogenic differentiation, then delivery of anti-inflammatory SIMV, after the requisite pro-inflammatory phase, will modulate cytokines produced by osteoprogenitors and increase osteogenesis.

4.2 Materials and Methods

4.2.1 Delivery System

The bCaP coated disks were prepared using SBFx5 method, described in chapter 2. Prior to bCaP coatings, 10 μl of either 200 ug/ml or 1000 ug/ml (2 or 10 μg/disk) of SIMV in prodrug form was adsorbed onto the sandblasted plastic disks and allowed to completely dry to maximize binding. A stock solution was made by dissolving 10 mg of simvastatin compound (Sigma, PHR1438) in 1ml of 95% ethanol then diluted to the desired concentration with 95% ethanol. A fresh stock solution was made per each study. The bCaP coated disks were sterilized prior to cell culture by exposure to UV light for 10 min to each side.

4.2.2 Cell Culture on TCP

Human mesenchyme-derived progenitor cells (HMDPCs) were isolated from older human bone discarded during orthopedic surgery to treat arthritis in the hand. Bone chips were cut into small pieces and cultured in Alpha-MEM (#12561), 10 % FBS, L-glutamine (2 mM) and 1% Antibiotic/anti-mycotic. Cells began to migrate out of bone chips within 1 week in culture and reach confluence after 3-4 weeks. Previous studies showed that the flow cytometry markers of these MSC-like cells matched standard phenotype of MSCs obtained from bone marrow aspirates [111, 330]. Age-related changes observed in bone chip progenitor cells and fewer osteoprogenitors with altered receptors [309]. Patients on many medications are not selected for studies.

Cells used for Active β-hydroxy acid, SIMV-A dosing study: The β-hydroxy acid form of simvastatin (SIMV-A) was directly pipetted into osteoprogenitor cultures at 15,000 cell/cm^2 in 12-well tissue culture treated plate (Corning Inc., Corning, NY) at multiple time points. In the present SIMV-A studies, cells at passage 2 were detached from tissue culture dishes with 0.25% trypsin and 1 mM EDTA (Invitrogen, Cat. No. 25200-056) at 37°C. Cells were counted using an automated cell counter (Bio-Rad, TC20) with trypan blue staining to assess cell number and viability. Osteoprogenitors were seeded at 15 x 10^3 cells/cm^2 in 12-well tissue culture treated and proliferated to confluency in Alpha-MEM (#12561), 16.5 % FBS, L-glutamine (2 mM) and 1% Antibiotic/anti-mycotic. Medium was then switched to osteogenic medium on day 7 of culture. Osteogenic medium consisted of the same proliferation media ingredients plus dexamethasone (10nM), β-glycerophosphate (20mM) and Ascorbic acid-2 phosphate (50 uM). Osteogenic medium was replaced twice a week until day 21 or day 30.

β-hydroxy acid SIMV addition (timing and dose): Either 0.5 nM/ml or 10nM/ml SIMV-A or vehicle were directly pipetted into the culture wells started at either 4-hour, day 3 or day 7 and given twice a week until day 21 or day 30. Before addition to cultures, SIMV was converted from its lactone prodrug form to its active β-hydroxy acid open ring form (SIMV-A) following previously described method (37). Briefly, 21 mg of simvastatin compound (Sigma, PHR1438) was dissolved in 0.5 ml of 95% ethanol followed by the addition of 0.75 ml of l N NaOH. The solution was heated at 50 ˚C for 2 hours. Then the resulting solution was neutralized with l N HC1 to a pH of 7.2 and brought up to a volume of 5 ml with distilled water, and stored in multiple aliquots at -20°C until use. The final concentration was 10 mM. SIMV-A was diluted with culture medium and added to cell cultures. This study was repeated with cells obtained

from three female patients (66, 70 and 73 years old) with fresh β-hydroxy acid SIMV solution made per each study.

4.2.3 Cell Culture on bCaP

After SIMV adsorption followed by bCaP application, disks were UV sterilized and then placed into 12-well non-treated tissue culture plates (Corning Inc., Corning, NY) and incubated in α-MEM medium for 30-45 minutes prior to cell culture. Osteoprogenitors (derived from older donor age 62-78 female) were seeded at 3 x 10^4 cells/cm^2 in proliferation medium and then incubated at 37°C and 5% CO_2 . Osteogenic medium was then used on day 7. Culture medium was refreshed twice a week until day 30.

4.2.4 Cell Characterization

The percentages of senescent cells and Cytokines level: Bone chip progenitors derived from 78 years old donor were cultured in Alpha-MEM (#12561), 10 % FBS, L-glutamine (2 mM) and 1% Antibiotic/anti-mycotic. SBGA staining was performed on day 2 of culture using Senescence Cells Histochemical Staining Kit (Sigma, USA, Cat# CS0030) following manufacture's protocol. Total of eight images per well (3 wells total) were taken using an inverted microscope (TE300, Nikon) equipped with a camera (Diagnostic Instruments), and imaging software (Spot Insight, Nikon). The total number of cells and the blue-stained cells (senescent cells) were counted and the percentage of cells expressing SBGA staining was calculated manually over total number of cells.

Osteogenic differentiation on TCP: Mineralized nodules in osteogenic cultures were stained with the calcium dye xylenol orange (XO) (Sigma, St. Louis, MO) for a final 20 µM concentration. The plates were evaluated for the XO-stained nodules under a fluorescence microscope. Calcium content at day 21 or day 30 were also evaluated using (Eagle Diagnostic, Cat#2400-1) according to manufacturer's instructions. A panel of inflammatory (*IL1β, IL6, TNFα* and *IL10*) and osteogenic genes (*BSP*, *OCN*) was also evaluated.

Proliferation and osteogenic differentiation on bCaP: The proliferation of cells cultured on bCaP was evaluated with CellTiter-Blue® (Promega, Madison, WI, USA), fluorometric method for estimating the number of viable cells present on bCaP coated disks. A panel of inflammatory (*IL1β, IL6, TNFα* and *IL10*) and osteogenic genes (*COL1A1, BSP* and *OCN*) was also evaluated since mineral deposition cannot be conducted due to the cell culture on calcium rich bCaP.

Data Analysis: Quantitative PCR was conducted on a panel of inflammatory cytokines and osteogenic genes and normalized to *GAPDH* and baseline, 4hrs time point for cytokines and day 7 for osteogenic, using $2^{-\Delta\Delta t}$ method. Inflammatory cytokines experiments, all cytokines were analyzed after three days of SIMV-A dosing in all groups. To measure osteogenic genes, data were normalized over *GAPDH* and over day 7 time point.

All Quantitative PCR assays was performed by isolating total RNA from the cells using Total RNA was extracted from the dishes by using TRIzol reagent (Invitrogen Life Technologies, CA, USA) then three micrograms of RNA were reverse transcribed into cDNA using (Cat# 639543, Takara, Japan) and thermocycler (BIO-RAD Laboratories Inc., CA, USA) followed by quantitative PCR using iTaq™ universal SYBR® Green supermix kit (BIO-RAD

Laboratories Inc., CA, USA) on a MyiQTM instrument. Primer sequences can be found in table 4.1. In SIMV-A addition experiment, inflammatory genes were normalized to *GAPDH* and to non-treated cells before SIMV-A addition using $2^{-\Delta\Delta t}$ method, where $\Delta\Delta C$T is the result of subtracting [*C*T gene − *C*T *GAPDH*] (non-treated cells before SIMV-A addition) from [*C*T gene − *C*T *GAPDH*] (experimental group).

4.2.3 Statistical Analysis

Statistical analysis performed using t-tests if there are two groups or by one-way ANOVA ($P<0.05$) with Tukey post-test (t:test) for 3 or more multiple groups (using GraphPad Prism).

4.3 Results

4.3.1 Senescence Cell Percentage and Cytokines Level

To assess the cytokine background levels of older human osteoprogenitors as compared to younger osteoprogenitors, gene expression of cytokines of osteoprogenitors derived from older, 70 years, was compared to younger female, 44 years, on day 3 and day 10 of culture without any drugs. The older osteoprogenitors showed significant elevation in anti-inflammatory genes *IL1*β and *IL6* both day 3 and 10 of culture. However, *TNF*α gene expression was significantly increased in older donor at day 10 but not on day 3 of culture as compared to the younger donor. This study also showed significant reductions in pro-reparative gene *IL10* level of older osteoprogenitor as compared to younger donor (Figure 4.1 A).

To further assess bone chip cells molecular mechanisms underlying the cells ability to proliferate and undergo osteogenic differentiation; the percentage of senescence cells present in the culture of osteoprogenitors derived from 78 years old female was examined using SABG staining. The Senescence β-Galactosidase staining revealed that 80% of the cells obtained from the older donor are carrying senescence characteristics (Figure 4.1 B). The results from these studies motivated our laboratory to test SIMV, anti-senescence and anti-inflammatory agents, the effect on the cytokines production of older human osteoprogenitors in the following experiments.

4.3.2 SIMV β hydroxy acid Dose and Timing

Delayed dosing modulated cytokines: The overall goal of this study was to determine the timing of addition and optimal dose of SIMV-A to modulate cytokines and enhance osteogenesis. SIMV-A administered starting at 4 hours of culture caused an increase in anti-inflammatory markers *IL1β* and *IL6* associated with reductions in pro-reparative *IL10* level compared to control in all three patients tested on day 3 of culture (Figure 4.2A) and Appendix 1 Figures (1A, 2A, and 3 A). Administration of SIMV-A starting on day 3 of culture showed no changes in cytokines production measured on day 6 as compared to control (vehicle treated at day 3) (Figure 4.2B) and Appendix 1 Figures (1B, 2B, and 3B). SIMV-A administered with the osteogenic medium on day 7 of culture modulated cytokines production by reducing anti-inflammatory markers *IL1β, IL6* and *TNFα* and increased *IL10* by 4 folds as compared to control and to immediate dosing (Figure 4.2C) data of other patients tested can be found in Appendix 1 Figures (1C ,2C , and 3C).

Delayed dosing enhanced osteogenic differentiation over immediate dosing: To better assess the relation between cytokines productions and osteogeneses; dosing of SIMV-A starting at multiple time (4hr, day 3 or day 7) was tested to modulate osteogenic differentiation of older human osteoprogenitors. The early administration of SIMV-A starting at either 4hrs or day 3 of culture ,twice a week until day 30, caused suppression in cells ability to produce mineralized nodules as measured by XO staining (Figure 4.3 A and B). Low dose of SIMV-A, 0.5 nM, administered with osteogenic medium at day 7 , twice a week until day 30, resulted in more mineralization deposited by the cells significantly greater than vehicle and other groups tested in the study as seen by XO stained area (Figure 4.3 C). While administration of a higher dose of SIMV-A, 10nM, blocked cells ability to differentiate and mineralize. Increased Ca+ content, *BMP-2* expression and osteogenic genes, *BSP* and *OCN*, were also evidence with delayed addition of 0.5nM SIMV in cells from the three donors tested (Figure 4.4). Data of other patients tested can be found in Appendix 1 Figures (3, 4, 5, 6 and 7).

4.3.3 SIMV prodrug Delayed Delivery from bCaP

Delayed delivery from bCaP enhanced proliferation and pro-reparative cytokines osteogenic differentiation:

Proliferation: The objective of this study was to confirm that local delayed delivery of SIMV in prodrug form from bCaP delivery system could modulate cytokines produced by older human osteoprogenitors as well as their osteogenic response at later point. Either 2 μg or 10 μg was delayed delivered from bCaP coatings. SIMV delivered from bCaP resulted in significant improvement of cell proliferation in dose-dependent manner as compared to cells cultured on

bCaP w/o SIMV as seen by CellTiter-Blue® cell viability assay on day 7 of culture (Figure 4.5 A). Data of other patients tested can be found in Appendix 1 Figures (8A and 10A).

Cytokines productions: To examine the effect of SIMV prodrug delivered from bCaP coatings on cytokines productions; 2 μg or 10 μg of SIMV was delayed delivered from bCaP and gene expression of inflammatory cytokines were measured on day 7. Delivering either 2 μg or 10 μg of SIMV from bCaP resulted in significant reduction in early anti-inflammatory cytokines *IL1β*, *IL6* and *TNFα* of older human osteoprogenitors on day 7 of culture as compared to control cultured on drug-free bCaP coated disks in both 62 and 73 years old donors (Fig 4.5B) and appendix 1 (Figure 8 B and 10 B). However, one donor, 78YO, showed different response to 2 μg SIMV delivered from bCaP. An elevation in early inflammatory markers, cytokines *IL1β*, *IL6* and *TNFα*, was seen with 2 μg SIMV but not to 10 μg SIMV (appendix 1 Fig 10 B). Delivering SIMV in delayed manner from bCaP also resulted in elevation, up to 8 folds, of the essential pro-reparative marker *IL10* in osteoprogenitors derived from older human female age 62, 70 and 78 (Figure 4.5 B and appendix 1 Figure 8B and 10 B).

Osteogenesis of older human osteoprogenitors: To further test the effect of delayed delivery of SIMV from bCaP on osteogenic response of older human osteoprogenitors; 2 μg or 10μg, was delivered from under the bCaP coating and resulted in significant elevation of the osteogenic genes, *COL1A1*, *BSP* and *OCN* (Figure 4.6) compared to control. The higher dose of SIMV, 10 μg, resulted in further increases in both proliferation and osteogenic genes than the lower dose (2 μg) in two patients 62 and 78 years old (appendix 1, Figures 9,10 and 11) .

4.4 Discussion

Immunomodulation and tissue regeneration are closely related essential mechanisms in bone regeneration therapy. These biological features are both regulated in response to local environmental changes including the presence of senescence cells, growth factors, inflammatory cytokines, and other factors. Changes in the microenvironment during the normal aging process reduce osteoprogenitor activities [40, 311, 331]. Indeed, our studies showed that osteoprogenitors derived from older donors have elevated levels of anti-inflammatory markers with a reduction in pro-reparative markers. These cytokines are essential mediators that could direct macrophage polarization, osteogenic differentiation and osteoprogenitor behavior in vitro [332].

The multiple functions of SIMV, anti-inflammatory, anti-senescence and osteogenic mediator, made it an attractive molecule for treating compromised bone healing [333]. Previous studies have mainly focused on immediate administration of SIMV to cell cultures using high doses and cell lines [323-328, 334] or primary MSCs from young animals [335, 336] or young humans [337]. These studies have provided valuable information regarding the positive effect of SIMV on osteogenesis of cells from young animals or humans. However, we found only one study that tested osteogenic effects of SIMV on cells from older bones [322] and that study did not investigate anti-inflammatory effects. Therefore we investigated the combined effect of SIMV in terms of delivery timing and dose to increase osteogenic differentiation and reduce inflammatory cytokines of the older human osteoprogenitors. Our studies showed effectiveness of a lower dose and that a higher dose of SIMV, 10 nM, inhibited cell differentiation, which may be associated with the adverse effects that have been shown to result from high doses of

simvastatin [192, 322]. Our studies lead us to conclude that control over timing and dose of simvastatin is essential for positive effects on either MSC differentiation.

It is likely that the anabolic effect of simvastatin on older human osteoprogenitors is due to increasing BMP-2 expression [338]. BMP-2 binds to a specific receptor (receptor II) at the cell membrane and forms a complex that phosphates Smad protein [339]. The phosphorylated Smad complex translocates to the nucleus and regulates the transcriptional activity of the target genes [340]. BMP-2-induced osteogenesis is regulated by Runx2. A study was conducted with mouse MSCs and aimed to clarify the molecular mechanism of simvastatin-induced osteogenic differentiation [341]. That study concluded that SIMV induced osteogenic differentiation by activating the Ras homolog gene family, member A (RhoA) signaling pathway (primary cytoskeleton regulator) and increases cytoskeletal tension, as well as by enhancing cell rigidity which all play a crucial role in the osteogenic differentiation of MSCs.

The age-related alteration in MSC behavior and chronic inflammation associated with increased cytokine productions weakens the regenerative capacity of older MSCs. Therefore, it is likely that the successful regeneration of bone will require controlled, appropriately timed reduction of important inflammatory cytokines. Our findings support this and show that the early reduction of key pro-inflammatory cytokine genes, *IL1β*, *IL6* and *TNFα*, can have profound consequences for older progenitor cells and allowing them to differentiate and proliferate normally. Furthermore, we demonstrated that delayed delivery of simvastatin from bCaP coatings modulate inflammatory markers and promoted osteoblastic differentiation of older human. Previous studies have reported beneficial bone anabolic effects expected from lower and sustainable release of simvastatin. Various biomaterials, including poly(L-lactic acid) (PLA),

poly(lactic-co-glycolic acid) (PLGA), calcium sulfate, hyaluronic acid, gelatin and methylcellulose have been investigated for the local administration of simvastatin with slow-release [190, 342-346]. However, there are disadvantages to the use of hydrophobic carriers such as PLA or PLGA including increase inflammatory host-responses in the body and harmful byproduct from polymer degradation [347, 348].

The design of biomaterials with better biocompatibility for the sustained delivery of water-insoluble simvastatin remains a challenge. Therefore, multiple efforts have been made to use alternative to a polymer by the use of β-Tricalcium Phosphate with PCL-co-PEG copolymers to deliver SIMV [349]. Furthermore, the incorporation of SIMV in hydroxyapatite microspheres resulted in increased osteogenesis and angiogenesis in vitro [194, 350] and in vivo [351-353]. Similarly, the incorporation of SIMV with calcium phosphate coating or powder enhanced osteogenic potential after intramuscular and endosteal implantation in rabbits [354, 355]. However, these attempts were made by using calcium phosphate as a carrier for SIMV and resulted in immediate delivery rather than delayed delivery to maximize the beneficial effect of SIMV to improve bone repair. To our knowledge, this is the first report that examined the delayed delivery of simvastatin from bCaP on the proliferation and differentiation of older human MSCs.

Our results suggest that simvastatin is an osteoinductive drug that can increase osteogenic differentiation of MSCs and that delayed delivery from osteoconductive biomaterial coating may improve bone tissue regeneration. We proved that delayed delivery of simvastatin, in the prodrug form, by the bCaP coating increased in vitro pro-reparative *IL10*, proliferation and osteogenic differentiation of older human osteoprogenitors derived from bones of female patients ranging

between 62 to 78 years old. There was variation in gene expression between the patient samples tested. For example, for the 62 year old patient, the OS genes were elevated in both 2ug and further elevation with the 10 μg SIMV from bCaP. The osteogenic genes of the 78 year old sample were only elevated with 10 μg, but not with 2ug indicating a reduced sensitive to SIMV with age. These variations need to be confirmed with additional patient samples, but are beyond the scope of this study and remain for further investigation.

4.5 Conclusions

The goals of the studies were to: (a) determine if delayed active SIMV-A administration would modulate cytokines production and induce osteogenesis in human bone chip osteoprogenitors and (b) to determine if delayed inactive SIMV delivery from a novel biomaterial bCaP coating could modulate osteogenesis. A 0.5 nM solution dose added to the media with a 7 day delay from plating was found to decrease anti-inflammatory markers, increase pro-reparative *IL10* and increase osteogenesis more than vehicle and other groups tested in the study as seen by increased XO staining and osteogenic gene expression. Experiments with osteoprogenitors grown on SIMV embedded under bCaP resulted in successful modulation of cytokines and increased in osteogenic differentiation with delayed access to SIMV not seen without SIMV. This approach with delayed delivery of SIMV from novel biomaterial coatings has potential to enhance older patients bone regeneration with the ability to reduce unwanted extended inflammation time seen in older patients with bone injures.

Table 4.1 Human primer sequence		
Primer	**Forward**	**Reverse**
GAPDH	AAGGTGAAGGTCGGAGTCAAC	GGGGTCATTGATGGCAACAATA
IL1β	TTCGACACATGGGATAACGAGG	TTTTTGCTGTGAGTCCCGGAG
IL6	Thermo scientific Primer ID: Hs00174131	
IL10	GACTTTAAGGGTTACCTGGGTTG	TCACATGCGCCTTGATGTCTG
TNFα	AAGCACACTGGTTTCCACACT	TGGGTCCCTGCATATCCGTT
BMP-2	TTCGGCCTGAAACAGAGACC	CCTGAGTGCCTGCGATACAG
COL1A1	GAGGGCCAAGACGAAGACATC	CAGATCACGTCATCGCACAAC
BSP	GAACCTCGTGGGGACAATTAC	CATCATAGCCATCGTAGCCTTG
OCN	CATGAGAGCCCTCACA	AGAGCGACACCCTAGAC

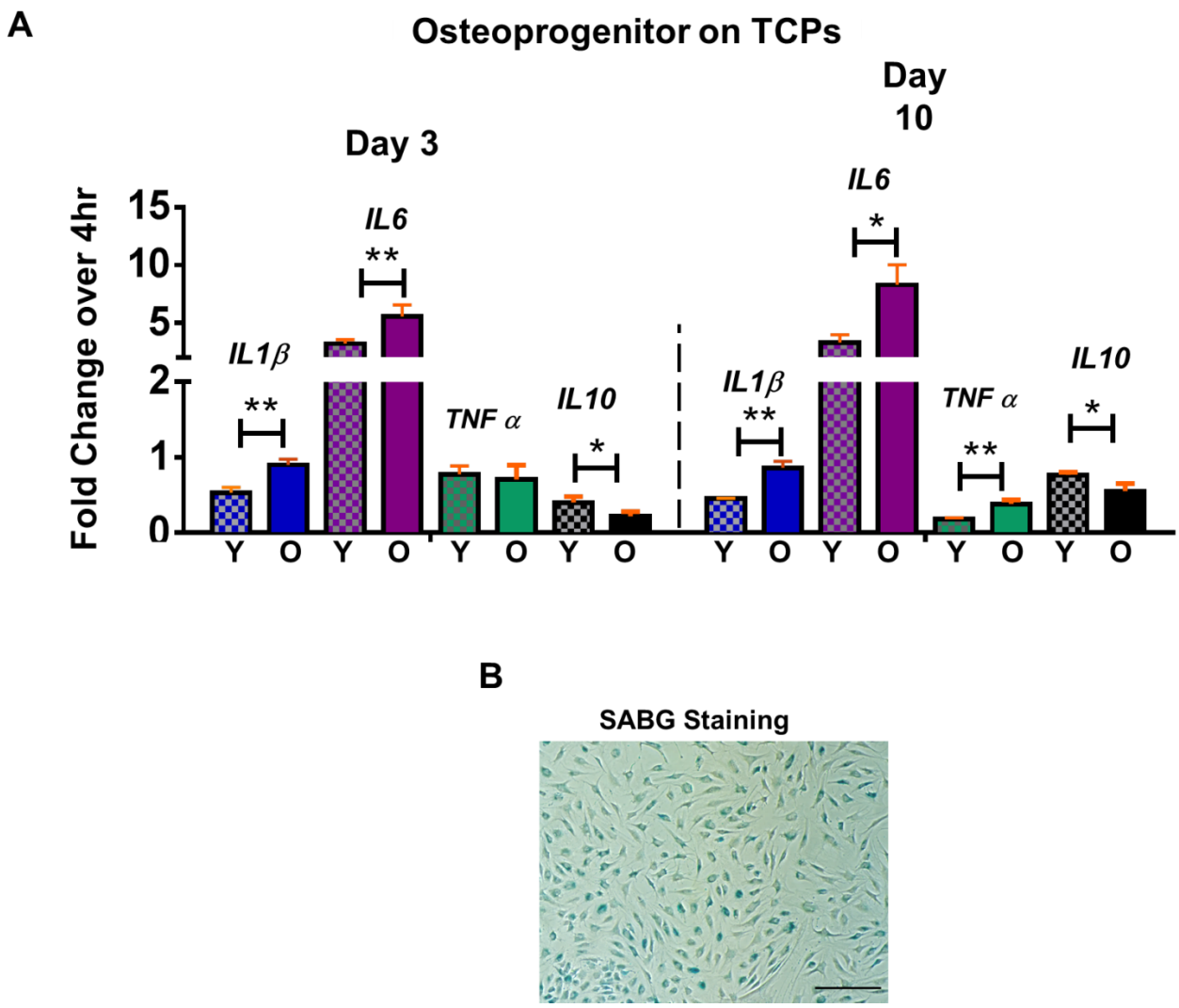

Figure 4.1: Age-related changes in osteoprogenitors (A) RT-qPCR cytokines gene expression. older human osteoprogenitors, 73 years old, as compared to younger cells, 44 years old. Data presented as fold-change over 4hrs baseline. Statistical analysis was performed using GraphPad software. t: test analysis of each gene of young vs old was performed and a $P < 0.05$ was considered significantly different. (B) β-Galactosidase (SABG) senescent staining of Osteoprogenitors obtained from 78 Years old female bone chip cells culture Scale bar=200um.

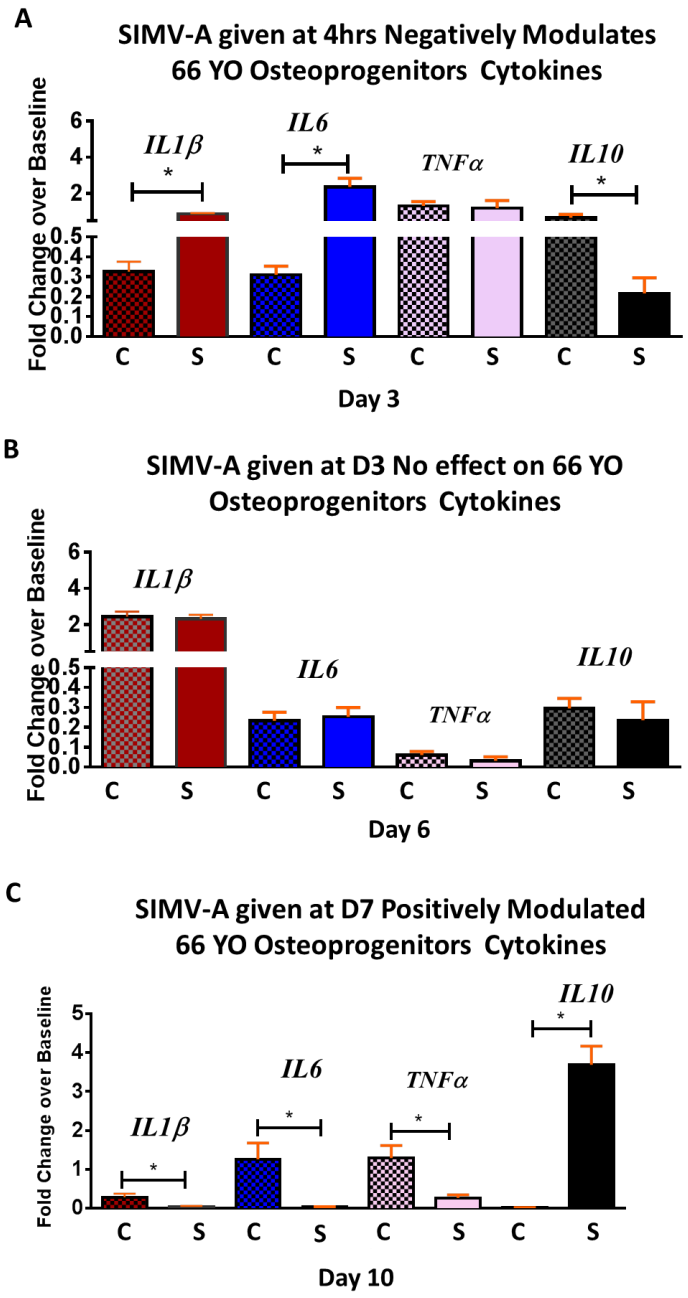

Figure 4.2: RT-qPCR cytokines gene expression of inflammatory cytokines of 66 years old human osteoprogenitors treated with SIMV-A. (A). Day 3 gene expression of inflammatory cytokines with SIMV-A given at 4hrs and continues twice a week until day 21. (B). Day 6 gene expression of inflammatory cytokines with SIMV-A given at day 3 continues twice a week until day 21. (C) Day 10 gene expression of inflammatory cytokines with SIMV-A given at day 7 continues twice a week until day 21. Data presented as fold-change compared to 4hrs baseline.

Statistical analysis was performed using GraphPad software. t: test analysis of each time point was performed and a $P < 0.05$ was considered significantly different.

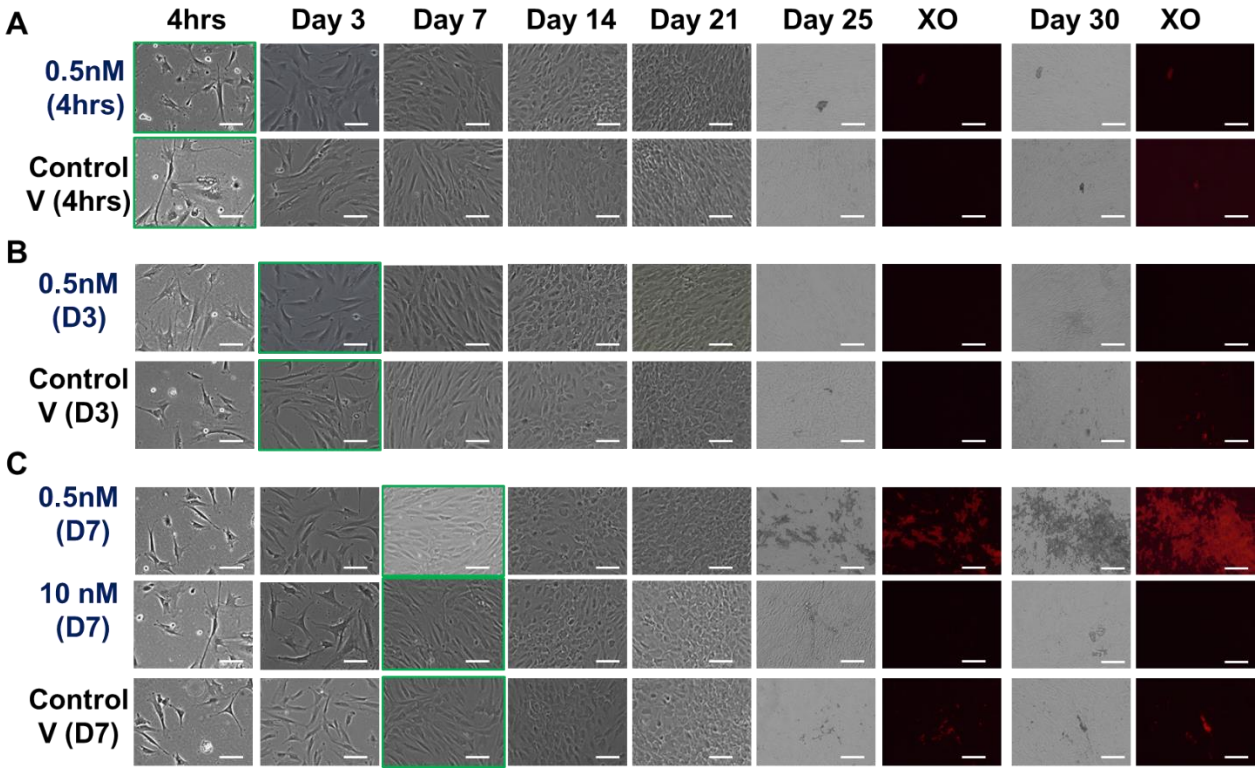

Figure 4.3: XO staining of human osteoprogenitor 66 years old , passage 2 seeded cells at 15,000 cells/cm^2, treated with SIMV-A at various timing. Green frame indicates the start time of SIMV-A treatment. A) 0.5nM of simvastatin was pipetted after 4hrs of culture and continued twice a week until day 30. B) 0.5nM of simvastatin was pipetted on day 3 of culture and continued twice a week until day 30. C) 0.5nM or 10 nM of simvastatin was pipetted with osteogenic medium on day 7 of culture and continued twice a week until day 30. Scale bar 100 um.

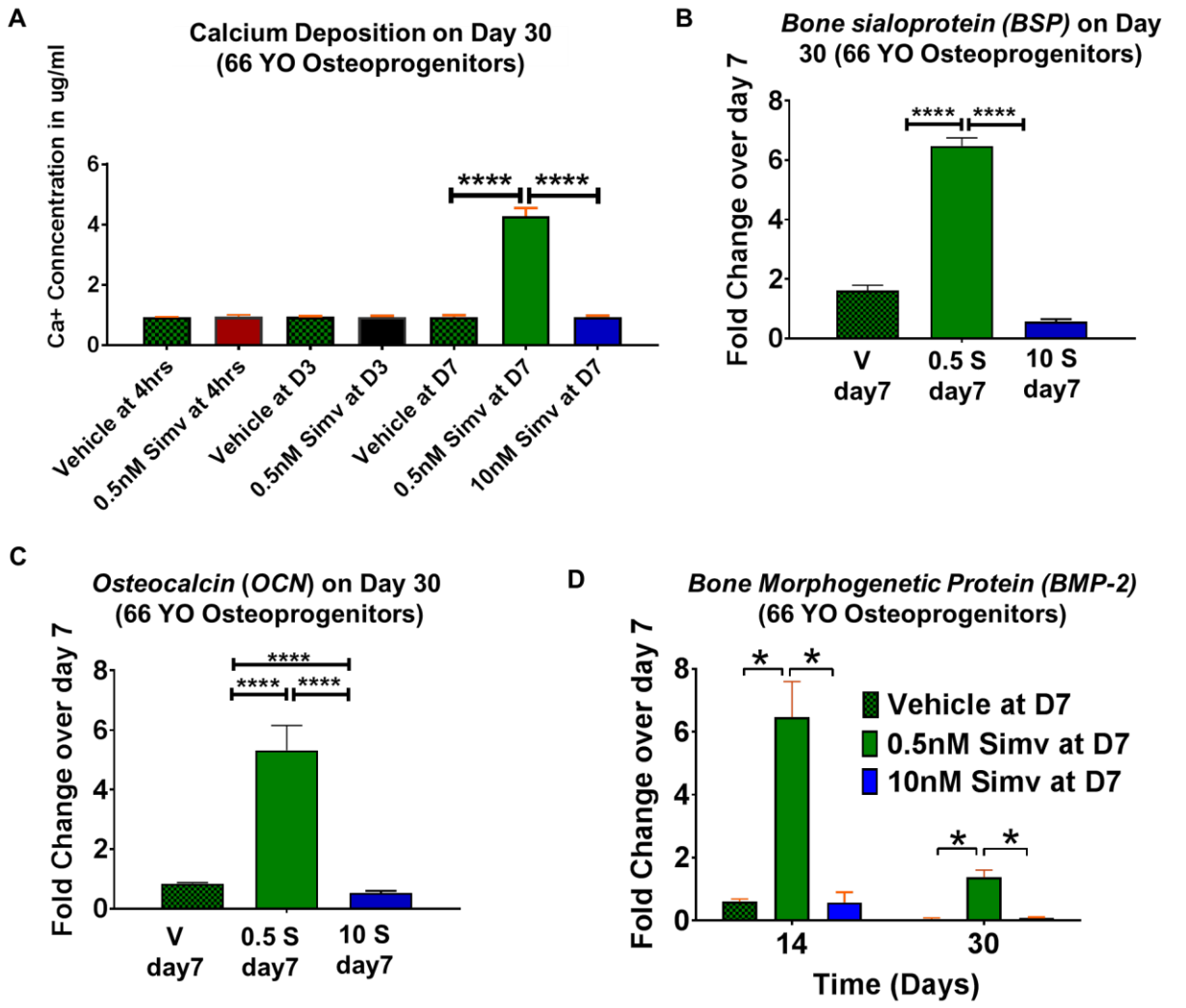

Figure 4.4: Calcium content and gene expression of human osteoprogenitor 66 years old treated with SIMV-A at various timing showing enhanced osteogenesis by delayed SIMV-A as measured by (A) Calcium content on day 30 of culture. (B, C, D) Osteogenic genes (*BSP*, *OCN* and *BMP-2*) with low dose ,0.5nM, given at day 7 as compared to higher dose given at the same time. Data presented as fold-change compared to day 7 baseline. Statistical analysis was performed using GraphPad software. Two way ANOVA multiple comparison analysis was performed and a $P < 0.05$ was considered significantly different (*$P < 0.05$, ****P= < 0.0001).

A

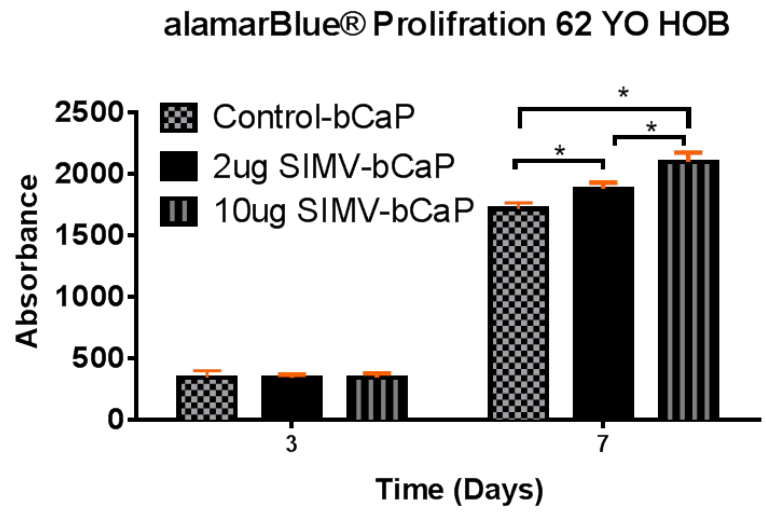

B

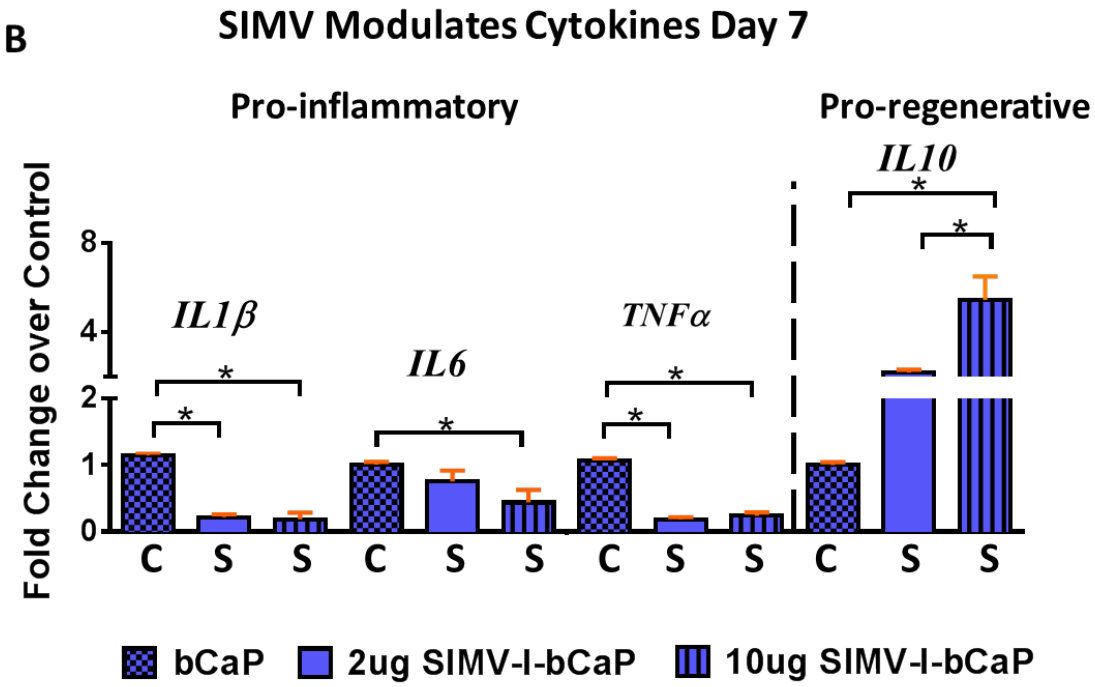

Figure 4.5: Human osteoprogenitor 62 years old seeded on bCaP coated disks (C) or (S) 2 μg or 10 μg SIMV-bCaP. (A) AlamarBlue cell proliferation assay (B) Gene expression anti-inflammatory markers (*IL1β*, *IL6* and *TNFα*) and pro-reparative *IL10*. Data presented as fold-change compared to control. Statistical analysis was performed using GraphPad software. Two

way ANOVA multiple comparison analysis of each gene was performed and a $P < 0.05$ was considered significantly different.

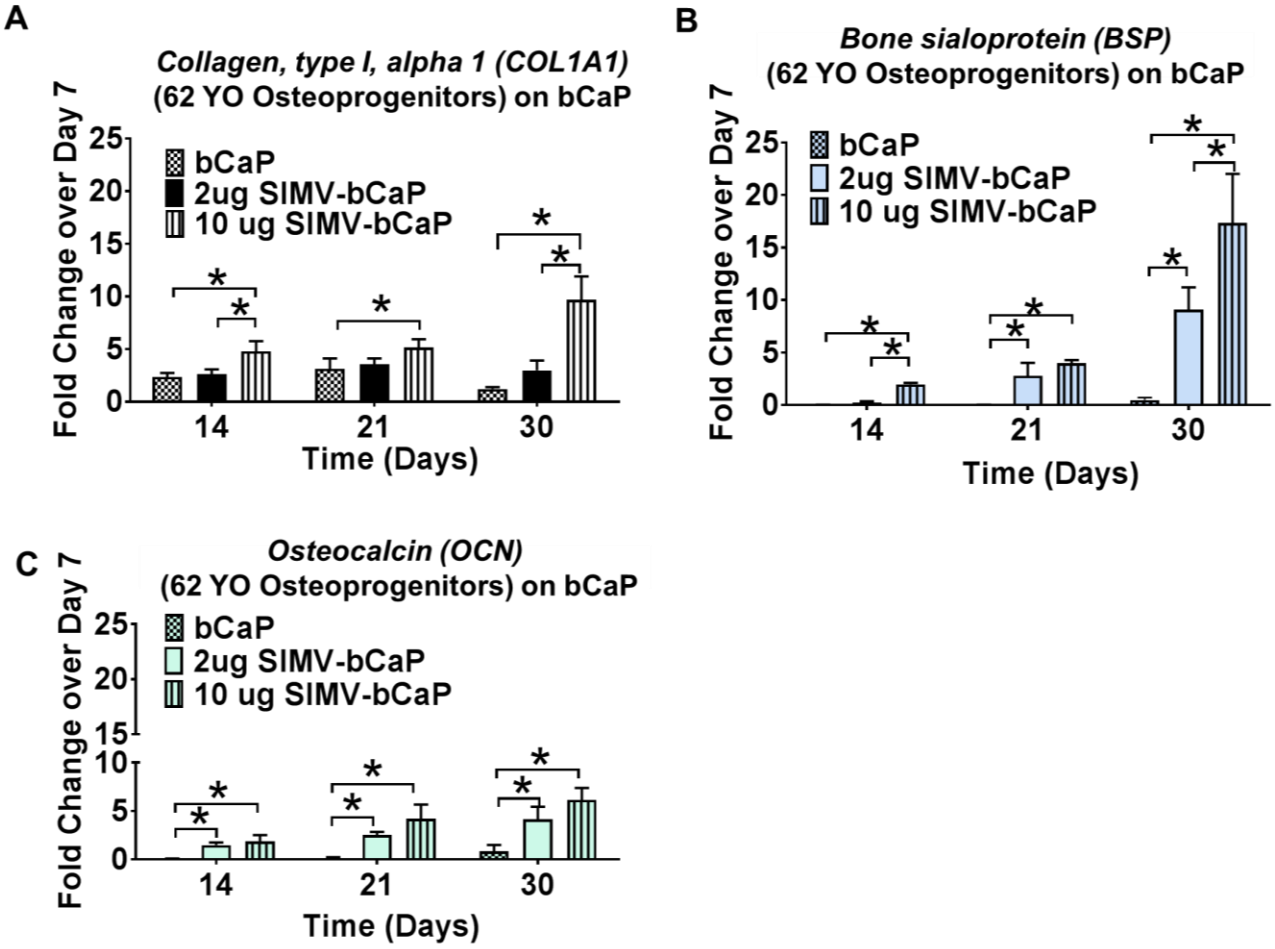

Figure 4.6: Osteogenic gene expression of Older human osteoprogenitor (62 YO) with delayed delivery of 2 μg or 10 μg SIMV from bCaP. (A) *COL1A1*. (B) *BSP* and (C) *OCN*. QPCR presented in fold change over day 7 (baseline) using 2-ΔΔCT. Statistical analysis was performed using GraphPad software. Unpaired t: test analysis of each time point was performed and a $P < 0.05$ was considered significantly different.

Chapter 5

Summary and Future Directions

5.1. Summary

The field of tissue engineering has developed rapidly over the past decade. There are numerous reports on various tissues grown in vitro including bone, cartilage, ligament, muscle and blood vessels. One of the key objectives of bone tissue engineering is the enhancement and guidance of osteogenic differentiation of stem cells within the implanted scaffold. Since macrophages have a major impact on the long term outcome of bone repair, ideal scaffolds should support and direct the activities of both cell types (osteoprogenitors and macrophages). Although many polymeric, ceramic, and composite scaffolds have been produced by a variety of methods, there is no delivery system that has been reported to be able to provide temporal control over two biomolecules to macrophages, as well as to osteoprogenitors. The primary goal of this research was thus to enhance bone healing by modulating macrophage phenotypes with the delivery of immunomodulatory agents from a biomimetic calcium phosphate delivery system. bCaP has many of the properties of an ideal bone tissue engineering scaffold including: supports osteoblast and MSC attachment, proliferation, and mineralization.

To achieve this goal, the modulation of macrophage phenotypes and osteogenic differentiation by therapeutic agents delivered from biomimetic calcium phosphate coatings was tested. In chapter 2, delayed delivery of cytotoxic agent, AntiA was tested using RAW 264.7 murine macrophage cell line. In this study, the biomimetic calcium phosphate coating created via a two-step incubation in simulated body fluid x5 successfully provided delayed delivery of the embedded factor to macrophages. SEM analysis revealed micro-openings generated by the macrophage on day 3 of culture as the mechanism the cells used to access the embedded factor.

Cells of the murine osteoblast-like cell line, MC3T3-E1, accessed the embedded factor on day 2 of culture without creating visible changes in the coating. From these studies, it was concluded that the bCaP coatings delivery system can provide time-specific delivery of the therapeutic agents embedded beneath the coating.

The fact that the timing of the delivery from bCaP varied depending on the cell type is a key characteristic of bCaP delivery system that must be considered when using it to enhance bone regeneration, as well as other regeneration applications. In chapter 3, the bCaP delivery system was used to sequentially deliver immunomodulatory agents, IFNγ followed by simvastatin, to macrophages. The novelty of this approach was the use of an FDA approved drug as a macrophage modulator, as well as an osteoinductive agent. The sequential delivery of IFNγ, an M1 stimuli, followed by simvastatin, an M2 stimuli; switched both the cell line and primary old macrophages from inflammatory phenotypes, or M1, to anti-inflammatory, M2, macrophage phenotypes. The studies used multiple cell types, a THP-1 cell line and old murine bone marrow derived macrophages, and this revealed differences between each cell type's responses to stimuli, as well as differences in young versus old macrophage response. For example, in the THP-1 cell line, gene expression of both M1 or M2 were higher than in primary cells. Furthermore, the expression of both M1 and M2 markers was reduced in bone marrow macrophages derived from old mice as compared to younger mice, indicating that aging can impair both M1 or M2 phenotype.

The delayed delivery of simvastatin from bCaP coatings was found to modulate cytokine production by older human osteoprogenitors and enhanced the presence of pro-reparative *IL10* gene expression. This approach also enhanced the gene expression of BMP-2, bone sialoprotein,

and osteocalcin production when cells cultured on simvastatin-bCaP surface over 21 or 30 days. Differences in cells derived from multiple patients were noticed emphasizing the importance of considering differences in response to therapies by each individual patient. The results from these studies indicate the importance of controlling the time of delivery from drug-delivery system to induce mineralization in cells delivered from older patients in vitro. These studies also provided valuable information about the increased production of cytokines in older cells compare to young and the effects of these cytokines on mineralization. In conclusion, the work presented in this dissertation indicates that this approach, delayed delivery of simvastatin, has potential to be used to heal elderly comprised bone via modulating macrophages response and may one day save these patients from potentially long-term hospital stays and repeated, painful orthopaedic and dental procedures.

5.2. Key Findings

On the basis of the results presented in this dissertation, there is significant evidence to support the hypotheses outlined in each aim. Namely, drug-delivery system characterization (Chapter 2) and macrophages modulation (Chapter 3) studies showed that bCaP can sequentially deliver two bio-active factors, such as FGF-2 and AntiA, or IFNγ and simvastatin, with 3 days delay in between the delivery to macrophages. (Chapter 2; Hypothesis 1) If bCaP serves as barrier layer to delay access to a cytotoxic compound, antimycin A, then macrophage or osteoprogenitors should show a delayed cell death rather than immediate cell death.

The use of the bCaP delivery system to deliver immunomodulatory agents to mouse and human macrophages (Chapter 3) revealed that simvastatin delivered in delayed manner could

switch macrophages from M1 to the M2 pro-reparative state. Chapter 3 Hypothesis: If bCaP sequentially delivers IFNγ and SIMV, then measurements of macrophage phenotypes should show a transition from M1 to M2 genes over time.

Moreover, the delayed delivery of simvastatin from our novel bCaP coating revealed the importance of controlling timing and dose of simvastatin to enhance osteogenesis of older human osteoprogenitors. Chapter 4 Hypothesis: If pro-inflammatory cytokines negatively impact osteogenic differentiation, then delivery of anti-inflammatory SIMV, after the requisite pro-inflammatory phase, will modulate cytokines produced by osteoprogenitors and increase osteogenesis.

To our knowledge, this is the first study that used bCaP coating to delayed deliver bio-molecular to macrophages. Previous studies used bCaP coating, alone or in combination with other materials, as a carrier to simvastatin which resulted in immediate long term sustain delivery of simvastatin to the defect area [194, 204, 352-355]. Other delivery system failed to provide sequential timely controlled delivery of macrophage modulating factors [155]. Our work with osteoprogenitors is the first report that demonstrates the value of a specific timing of simvastatin delivery to restore youthful osteogenesis and proliferation to older human osteoprogenitors. Previous studies used much higher doses of simvastatin to induce osteogenic differentiation of young cell or cell line [325-327] that could have unwanted side effects.

Our novel technology is innovative and is anticipated to shift current approaches towards an age-specific bioengineered bone graft to treat bone injuries in older patients. In fact, modulating macrophage phenotype transitions by time-controlled local delivery of an inexpensive, stable small molecule that modifies osteoprogenitors and senescent cell activity is novel, cost-effective direction to improve and accelerate bone regeneration in older patients.

Redirecting the use of an FDA approved drug as an immunomodulatory factor to enhance bone healing in older patients is a cost saving strategy because the safety profile of the drug is already known. Since simvastatin delivered from the bCaP coating system could modulate macrophage phenotypes, this approach can be used in other applications in immunology or tissue engineering that require to a delayed delivery of active biomolecules to modulate macrophages for better healing outcomes.

5.3. Future Directions

Although our approach described here has potential to be applied to create an age-specific successful bone graft substitute that can provide control over timing of delivery, there are still several issues that should be addressed. First, the complete degradation of the bCaP coating by macrophages in vitro or in vivo is unknown. A tissue engineered scaffold should ideally degrade at a rate complimentary to the rate of tissue ingrowth; however, macrophages created micro-opening in the bCaP coating described here on day 3 of culture at a rate depending on the cell number. A more comprehensive analysis needs to be performed to examine the degradation rate as a function of time, as well as cell number. Fourier-transform infrared spectroscopy (FTIR) imaging is one method to examine the coating as it degrades by macrophages. The infrared spectroscopy method can be used to map chemical properties of the coating and would be able to differentiate between the bCaP and the polystyrene disks material, revealed by the micro-openings over time to identify the extent of in vitro degradation at multiple time points.

The study of immunomodulatory effects of biomaterials on the macrophage combined with osteogenic effects is an expanding field. Future studies that investigate cell-cell crosstalk between macrophages and osteoprogenitors while being cultured on the bCaP are needed. Several studies have characterized the macrophage-osteoblast crosstalk on biomaterial substrates in vitro using a cell line or primary cells derived from young humans or animals [33, 293, 356-361]. More comprehensive investigations of the cross-talk between macrophage and osteoprogenitor derived from older human or animal are needed given the increased inflammation, inflammaging, and the slower immune response, immune-paralysis, in older individuals [316].

The time-controlled delivery of simvastatin described in our studies showed a promising anabolic effect on both macrophage polarization and osteoprogenitor differentiation. Beyond incorporation of stimulatory biomolecules, potential biomaterial-based implants that could selectively polarize macrophages on their own may prove beneficial. Several studies have shown the effect of the biomaterials surface structure and scaffold stiffness to promote M2 polarization [362-364]. Scaffold pore size was also shown to affect macrophage response. For example, a pore size of 34 μm reduced fibrous encapsulation while larger pore size (160 μm) caused more M1 infiltration compared with a smaller pore size [365]. A combination of two biomaterials with characteristics to promote M1 first and another biomaterial layered below with structure to stimulate M2 subtype could be a viable method to polarize macrophages. Continued research to identify cues from biomaterials that can positively interact with immune cells to polarize macrophage response following implantation is needed [366].

References

[1] Del Fattore A, Teti A, Rucci N. Bone cells and the mechanisms of bone remodelling. Front Biosci (Elite Ed). 2012;4:2302-21.
[2] Ikeda T, Nagai Y, Yamaguchi A, Yokose S, Yoshiki S. Age-related reduction in bone matrix protein mRNA expression in rat bone tissues: application of histomorphometry to in situ hybridization. Bone. 1995;16:17-23.
[3] Liang CT, Barnes J, Seedor JG, Quartuccio HA, Bolander M, Jeffrey JJ, et al. Impaired bone activity in aged rats: alterations at the cellular and molecular levels. Bone. 1992;13:435-41.
[4] Nishimoto SK, Chang CH, Gendler E, Stryker WF, Nimni ME. The effect of aging on bone formation in rats: biochemical and histological evidence for decreased bone formation capacity. Calcif Tissue Int. 1985;37:617-24.
[5] Skak SV, Jensen TT. Femoral shaft fracture in 265 children. Log-normal correlation with age of speed of healing. Acta Orthop Scand. 1988;59:704-7.
[6] Clark D, Nakamura M, Miclau T, Marcucio R. Effects of Aging on Fracture Healing. Curr Osteoporos Rep. 2017;15:601-8.
[7] Guillaumet-Adkins A, Yanez Y, Peris-Diaz MD, Calabria I, Palanca-Ballester C, Sandoval J. Epigenetics and Oxidative Stress in Aging. Oxid Med Cell Longev. 2017;2017:9175806.
[8] Colby SL, Ortman JM. Projections of the Size and Composition of the U.S. Population: 2014 to 2060. In: Bureau UC, editor. Washington, DC2014.
[9] Marsell R, Einhorn TA. The biology of fracture healing. Injury. 2011;42:551-5.
[10] Kolar P, Schmidt-Bleek K, Schell H, Gaber T, Toben D, Schmidmaier G, et al. The early fracture hematoma and its potential role in fracture healing. Tissue Eng Part B Rev. 2010;16:427-34.
[11] Einhorn TA, Gerstenfeld LC. Fracture healing: mechanisms and interventions. Nat Rev Rheumatol. 2015;11:45-54.
[12] Einhorn TA. The cell and molecular biology of fracture healing. Clin Orthop Relat Res. 1998:S7-21.
[13] Gerstenfeld LC, Cullinane DM, Barnes GL, Graves DT, Einhorn TA. Fracture healing as a post-natal developmental process: molecular, spatial, and temporal aspects of its regulation. J Cell Biochem. 2003;88:873-84.
[14] Iwaki A, Jingushi S, Oda Y, Izumi T, Shida JI, Tsuneyoshi M, et al. Localization and quantification of proliferating cells during rat fracture repair: detection of proliferating cell nuclear antigen by immunohistochemistry. J Bone Miner Res. 1997;12:96-102.
[15] Shapiro F. Bone development and its relation to fracture repair. The role of mesenchymal osteoblasts and surface osteoblasts. Eur Cell Mater. 2008;15:53-76.
[16] Barnes GL, Kostenuik PJ, Gerstenfeld LC, Einhorn TA. Growth factor regulation of fracture repair. J Bone Miner Res. 1999;14:1805-15.
[17] Thompson Z, Miclau T, Hu D, Helms JA. A model for intramembranous ossification during fracture healing. J Orthop Res. 2002;20:1091-8.
[18] Ornitz DM, Marie PJ. FGF signaling pathways in endochondral and intramembranous bone development and human genetic disease. Genes & development. 2002;16:1446-65.
[19] Martini F. Osseos Tissue and Bone Structure. 7 ed. San Franciso, CA: Pearson Education Inc.; 2006.

[20] Gilbert S. Osteogenesis: The Development of Bones. 6 ed. Sunderland, MA: Sinauer Associates; 2000.
[21] Alberts B JA, Lewis J, et al. Molecular Biology of the Cell. 4th edition. New York: Garland Science; 2002. Innate Immunity. Available from: https://www.ncbi.nlm.nih.gov/books/NBK26846.
[22] Gordon S, Martinez FO. Alternative activation of macrophages: mechanism and functions. Immunity. 2010;32:593-604.
[23] Shi C, Pamer EG. Monocyte recruitment during infection and inflammation. Nat Rev Immunol. 2011;11:762-74.
[24] Gordon S, Taylor PR. Monocyte and macrophage heterogeneity. Nat Rev Immunol. 2005;5:953-64.
[25] Celada A, Gray PW, Rinderknecht E, Schreiber RD. Evidence for a gamma-interferon receptor that regulates macrophage tumoricidal activity. J Exp Med. 1984;160:55-74.
[26] Spiller KL, Koh TJ. Macrophage-based therapeutic strategies in regenerative medicine. Adv Drug Deliv Rev. 2017;122:74-83.
[27] Lurier EB, Dalton D, Dampier W, Raman P, Nassiri S, Ferraro NM, et al. Transcriptome analysis of IL-10-stimulated (M2c) macrophages by next-generation sequencing. Immunobiology. 2017;222:847-56.
[28] Mosser DM, Edwards JP. Exploring the full spectrum of macrophage activation. Nat Rev Immunol. 2008;8:958-69.
[29] Murray PJ, Allen JE, Biswas SK, Fisher EA, Gilroy DW, Goerdt S, et al. Macrophage activation and polarization: nomenclature and experimental guidelines. Immunity. 2014;41:14-20.
[30] Spiller KL, Wrona EA, Romero-Torres S, Pallotta I, Graney PL, Witherel CE, et al. Differential gene expression in human, murine, and cell line-derived macrophages upon polarization. Exp Cell Res. 2016;347:1-13.
[31] Stein M, Keshav S, Harris N, Gordon S. Interleukin 4 potently enhances murine macrophage mannose receptor activity: a marker of alternative immunologic macrophage activation. J Exp Med. 1992;176:287-92.
[32] Jetten N, Verbruggen S, Gijbels MJ, Post MJ, De Winther MP, Donners MM. Anti-inflammatory M2, but not pro-inflammatory M1 macrophages promote angiogenesis in vivo. Angiogenesis. 2014;17:109-18.
[33] Gong L, Zhao Y, Zhang Y, Ruan Z. The Macrophage Polarization Regulates MSC Osteoblast Differentiation in vitro. Ann Clin Lab Sci. 2016;46:65-71.
[34] Lucas T, Waisman A, Ranjan R, Roes J, Krieg T, Muller W, et al. Differential roles of macrophages in diverse phases of skin repair. J Immunol. 2010;184:3964-77.
[35] Das A, Sinha M, Datta S, Abas M, Chaffee S, Sen CK, et al. Monocyte and macrophage plasticity in tissue repair and regeneration. Am J Pathol. 2015;185:2596-606.
[36] Chazaud B. Macrophages: supportive cells for tissue repair and regeneration. Immunobiology. 2014;219:172-8.
[37] Arron JR, Choi Y. Bone versus immune system. Nature. 2000;408:535-6.
[38] Anton K, Banerjee D, Glod J. Macrophage-associated mesenchymal stem cells assume an activated, migratory, pro-inflammatory phenotype with increased IL-6 and CXCL10 secretion. PLoS One. 2012;7:e35036.

[39] Kon T, Cho TJ, Aizawa T, Yamazaki M, Nooh N, Graves D, et al. Expression of osteoprotegerin, receptor activator of NF-kappaB ligand (osteoprotegerin ligand) and related proinflammatory cytokines during fracture healing. J Bone Miner Res. 2001;16:1004-14.
[40] Freytes DO, Kang JW, Marcos-Campos I, Vunjak-Novakovic G. Macrophages modulate the viability and growth of human mesenchymal stem cells. J Cell Biochem. 2013;114:220-9.
[41] Takahashi N, Mundy GR, Roodman GD. Recombinant human interferon-gamma inhibits formation of human osteoclast-like cells. J Immunol. 1986;137:3544-9.
[42] Takayanagi H, Ogasawara K, Hida S, Chiba T, Murata S, Sato K, et al. T-cell-mediated regulation of osteoclastogenesis by signalling cross-talk between RANKL and IFN-gamma. Nature. 2000;408:600-5.
[43] Boyle WJ, Simonet WS, Lacey DL. Osteoclast differentiation and activation. Nature. 2003;423:337-42.
[44] Burgess TL, Qian Y, Kaufman S, Ring BD, Van G, Capparelli C, et al. The ligand for osteoprotegerin (OPGL) directly activates mature osteoclasts. J Cell Biol. 1999;145:527-38.
[45] Nakagawa N, Kinosaki M, Yamaguchi K, Shima N, Yasuda H, Yano K, et al. RANK is the essential signaling receptor for osteoclast differentiation factor in osteoclastogenesis. Biochem Biophys Res Commun. 1998;253:395-400.
[46] Udagawa N, Takahashi N, Akatsu T, Tanaka H, Sasaki T, Nishihara T, et al. Origin of osteoclasts: mature monocytes and macrophages are capable of differentiating into osteoclasts under a suitable microenvironment prepared by bone marrow-derived stromal cells. Proc Natl Acad Sci U S A. 1990;87:7260-4.
[47] Yasuda H, Shima N, Nakagawa N, Mochizuki SI, Yano K, Fujise N, et al. Identity of osteoclastogenesis inhibitory factor (OCIF) and osteoprotegerin (OPG): a mechanism by which OPG/OCIF inhibits osteoclastogenesis in vitro. Endocrinology. 1998;139:1329-37.
[48] Yasuda H, Shima N, Nakagawa N, Yamaguchi K, Kinosaki M, Mochizuki S, et al. Osteoclast differentiation factor is a ligand for osteoprotegerin/osteoclastogenesis-inhibitory factor and is identical to TRANCE/RANKL. Proc Natl Acad Sci U S A. 1998;95:3597-602.
[49] Al-Rasheed A, Scheerens H, Rennick DM, Fletcher HM, Tatakis DN. Accelerated alveolar bone loss in mice lacking interleukin-10. J Dent Res. 2003;82:632-5.
[50] Xu LX, Kukita T, Kukita A, Otsuka T, Niho Y, Iijima T. Interleukin-10 selectively inhibits osteoclastogenesis by inhibiting differentiation of osteoclast progenitors into preosteoclast-like cells in rat bone marrow culture system. J Cell Physiol. 1995;165:624-9.
[51] Evans KE, Fox SW. Interleukin-10 inhibits osteoclastogenesis by reducing NFATc1 expression and preventing its translocation to the nucleus. BMC Cell Biol. 2007;8:4.
[52] Hong MH, Williams H, Jin CH, Pike JW. The inhibitory effect of interleukin-10 on mouse osteoclast formation involves novel tyrosine-phosphorylated proteins. J Bone Miner Res. 2000;15:911-8.
[53] Lovibond AC, Haque SJ, Chambers TJ, Fox SW. TGF-beta-induced SOCS3 expression augments TNF-alpha-induced osteoclast formation. Biochem Biophys Res Commun. 2003;309:762-7.
[54] Mohamed SG, Sugiyama E, Shinoda K, Taki H, Hounoki H, Abdel-Aziz HO, et al. Interleukin-10 inhibits RANKL-mediated expression of NFATc1 in part via suppression of c-Fos and c-Jun in RAW264.7 cells and mouse bone marrow cells. Bone. 2007;41:592-602.
[55] Shin HH, Lee JE, Lee EA, Kwon BS, Choi HS. Enhanced osteoclastogenesis in 4-1BB-deficient mice caused by reduced interleukin-10. J Bone Miner Res. 2006;21:1907-12.

[56] Liu D, Yao S, Wise GE. Effect of interleukin-10 on gene expression of osteoclastogenic regulatory molecules in the rat dental follicle. Eur J Oral Sci. 2006;114:42-9.
[57] Van Vlasselaer P, Borremans B, Van Den Heuvel R, Van Gorp U, de Waal Malefyt R. Interleukin-10 inhibits the osteogenic activity of mouse bone marrow. Blood. 1993;82:2361-70.
[58] Van Vlasselaer P, Borremans B, van Gorp U, Dasch JR, De Waal-Malefyt R. Interleukin 10 inhibits transforming growth factor-beta (TGF-beta) synthesis required for osteogenic commitment of mouse bone marrow cells. J Cell Biol. 1994;124:569-77.
[59] Dresner-Pollak R, Gelb N, Rachmilewitz D, Karmeli F, Weinreb M. Interleukin 10-deficient mice develop osteopenia, decreased bone formation, and mechanical fragility of long bones. Gastroenterology. 2004;127:792-801.
[60] Houri-Haddad Y, Soskolne WA, Halabi A, Shapira L. IL-10 gene transfer attenuates P. gingivalis-induced inflammation. J Dent Res. 2007;86:560-4.
[61] Lange J, Sapozhnikova A, Lu C, Hu D, Li X, Miclau T, 3rd, et al. Action of IL-1beta during fracture healing. J Orthop Res. 2010;28:778-84.
[62] Hughes FJ, Howells GL. Interleukin-6 inhibits bone formation in vitro. Bone Miner. 1993;21:21-8.
[63] Bastidas-Coral AP, Bakker AD, Zandieh-Doulabi B, Kleverlaan CJ, Bravenboer N, Forouzanfar T, et al. Cytokines TNF-alpha, IL-6, IL-17F, and IL-4 Differentially Affect Osteogenic Differentiation of Human Adipose Stem Cells. Stem Cells Int. 2016;2016:1318256.
[64] Gomberg BF, Gruen GS, Smith WR, Spott M. Outcomes in acute orthopaedic trauma: a review of 130,506 patients by age. Injury. 1999;30:431-7.
[65] Tomkinson A, Reeve J, Shaw RW, Noble BS. The death of osteocytes via apoptosis accompanies estrogen withdrawal in human bone. J Clin Endocrinol Metab. 1997;82:3128-35.
[66] Manolagas SC. Birth and death of bone cells: basic regulatory mechanisms and implications for the pathogenesis and treatment of osteoporosis. Endocr Rev. 2000;21:115-37.
[67] Busse B, Djonic D, Milovanovic P, Hahn M, Puschel K, Ritchie RO, et al. Decrease in the osteocyte lacunar density accompanied by hypermineralized lacunar occlusion reveals failure and delay of remodeling in aged human bone. Aging Cell. 2010;9:1065-75.
[68] Mullender MG, van der Meer DD, Huiskes R, Lips P. Osteocyte density changes in aging and osteoporosis. Bone. 1996;18:109-13.
[69] Manolagas SC. Steroids and osteoporosis: the quest for mechanisms. J Clin Invest. 2013;123:1919-21.
[70] Qiu S, Rao DS, Palnitkar S, Parfitt AM. Reduced iliac cancellous osteocyte density in patients with osteoporotic vertebral fracture. J Bone Miner Res. 2003;18:1657-63.
[71] Verborgt O, Gibson GJ, Schaffler MB. Loss of osteocyte integrity in association with microdamage and bone remodeling after fatigue in vivo. J Bone Miner Res. 2000;15:60-7.
[72] Elmardi AS, Katchburian MV, Katchburian E. Electron microscopy of developing calvaria reveals images that suggest that osteoclasts engulf and destroy osteocytes during bone resorption. Calcif Tissue Int. 1990;46:239-45.
[73] Yavropoulou MP, Yovos JG. The role of the Wnt signaling pathway in osteoblast commitment and differentiation. Hormones (Athens). 2007;6:279-94.
[74] Gu G, Mulari M, Peng Z, Hentunen TA, Vaananen HK. Death of osteocytes turns off the inhibition of osteoclasts and triggers local bone resorption. Biochem Biophys Res Commun. 2005;335:1095-101.

[75] Weinstein RS, Wan C, Liu Q, Wang Y, Almeida M, O'Brien CA, et al. Endogenous glucocorticoids decrease skeletal angiogenesis, vascularity, hydration, and strength in aged mice. Aging Cell. 2010;9:147-61.
[76] Komori T. Cell Death in Chondrocytes, Osteoblasts, and Osteocytes. Int J Mol Sci. 2016;17.
[77] Caplan AI, Hariri R. Body Management: Mesenchymal Stem Cells Control the Internal Regenerator. Stem Cells Transl Med. 2015;4:695-701.
[78] Stolzing A, Jones E, McGonagle D, Scutt A. Age-related changes in human bone marrow-derived mesenchymal stem cells: consequences for cell therapies. Mech Ageing Dev. 2008;129:163-73.
[79] Zhou S, Greenberger JS, Epperly MW, Goff JP, Adler C, Leboff MS, et al. Age-related intrinsic changes in human bone-marrow-derived mesenchymal stem cells and their differentiation to osteoblasts. Aging Cell. 2008;7:335-43.
[80] D'Ippolito G, Schiller PC, Ricordi C, Roos BA, Howard GA. Age-related osteogenic potential of mesenchymal stromal stem cells from human vertebral bone marrow. J Bone Miner Res. 1999;14:1115-22.
[81] Verma S, Rajaratnam JH, Denton J, Hoyland JA, Byers RJ. Adipocytic proportion of bone marrow is inversely related to bone formation in osteoporosis. J Clin Pathol. 2002;55:693-8.
[82] Duque G, Rivas D, Li W, Li A, Henderson JE, Ferland G, et al. Age-related bone loss in the LOU/c rat model of healthy ageing. Exp Gerontol. 2009;44:183-9.
[83] Yu JM, Wu X, Gimble JM, Guan X, Freitas MA, Bunnell BA. Age-related changes in mesenchymal stem cells derived from rhesus macaque bone marrow. Aging Cell. 2011;10:66-79.
[84] Asumda FZ, Chase PB. Age-related changes in rat bone-marrow mesenchymal stem cell plasticity. BMC Cell Biol. 2011;12:44.
[85] Coipeau P, Rosset P, Langonne A, Gaillard J, Delorme B, Rico A, et al. Impaired differentiation potential of human trabecular bone mesenchymal stromal cells from elderly patients. Cytotherapy. 2009;11:584-94.
[86] Rosen CJ, Bouxsein ML. Mechanisms of disease: is osteoporosis the obesity of bone? Nat Clin Pract Rheumatol. 2006;2:35-43.
[87] Meunier P, Aaron J, Edouard C, Vignon G. Osteoporosis and the replacement of cell populations of the marrow by adipose tissue. A quantitative study of 84 iliac bone biopsies. Clin Orthop Relat Res. 1971;80:147-54.
[88] Moerman EJ, Teng K, Lipschitz DA, Lecka-Czernik B. Aging activates adipogenic and suppresses osteogenic programs in mesenchymal marrow stroma/stem cells: the role of PPAR-gamma2 transcription factor and TGF-beta/BMP signaling pathways. Aging Cell. 2004;3:379-89.
[89] Peffers MJ, Collins J, Fang Y, Goljanek-Whysall K, Rushton M, Loughlin J, et al. Age-related changes in mesenchymal stem cells identified using a multi-omics approach. Eur Cell Mater. 2016;31:136-59.
[90] Wilson A, Shehadeh LA, Yu H, Webster KA. Age-related molecular genetic changes of murine bone marrow mesenchymal stem cells. BMC Genomics. 2010;11:229.
[91] Kuang W, Xu X, Lin J, Cao Y, Xu Y, Chen L, et al. Functional and Molecular Changes of MSCs in Aging. Curr Stem Cell Res Ther. 2015;10:384-91.
[92] Bellantuono I, Aldahmash A, Kassem M. Aging of marrow stromal (skeletal) stem cells and their contribution to age-related bone loss. Biochim Biophys Acta. 2009;1792:364-70.

[93] Sui BD, Hu CH, Zheng CX, Jin Y. Microenvironmental Views on Mesenchymal Stem Cell Differentiation in Aging. J Dent Res. 2016;95:1333-40.
[94] Barnes GL, Kostenuik PJ, Gerstenfeld LC, Einhorn TA. Growth Factor Regulation of Fracture Repair. Journal of Bone and Mineral Research. 1999;14:1805-15.
[95] Deckers MM, van Bezooijen RL, van der Horst G, Hoogendam J, van Der Bent C, Papapoulos SE, et al. Bone morphogenetic proteins stimulate angiogenesis through osteoblast-derived vascular endothelial growth factor A. Endocrinology. 2002;143:1545-53.
[96] Groeneveld EH, Burger EH. Bone morphogenetic proteins in human bone regeneration. Eur J Endocrinol. 2000;142:9-21.
[97] Beederman M, Lamplot JD, Nan G, Wang J, Liu X, Yin L, et al. BMP signaling in mesenchymal stem cell differentiation and bone formation. J Biomed Sci Eng. 2013;6:32-52.
[98] Fleet JC, Cashman K, Cox K, Rosen V. The effects of aging on the bone inductive activity of recombinant human bone morphogenetic protein-2. Endocrinology. 1996;137:4605-10.
[99] Meyer RA, Jr., Meyer MH, Tenholder M, Wondracek S, Wasserman R, Garges P. Gene expression in older rats with delayed union of femoral fractures. J Bone Joint Surg Am. 2003;85-A:1243-54.
[100] Floege J, Eng E, Young BA, Alpers CE, Barrett TB, Bowen-Pope DF, et al. Infusion of platelet-derived growth factor or basic fibroblast growth factor induces selective glomerular mesangial cell proliferation and matrix accumulation in rats. J Clin Invest. 1993;92:2952-62.
[101] Heldin CH, Westermark B. Mechanism of action and in vivo role of platelet-derived growth factor. Physiol Rev. 1999;79:1283-316.
[102] Andrew JG, Hoyland JA, Freemont AJ, Marsh DR. Platelet-derived growth factor expression in normally healing human fractures. Bone. 1995;16:455-60.
[103] Hollinger JO, Hart CE, Hirsch SN, Lynch S, Friedlaender GE. Recombinant human platelet-derived growth factor: biology and clinical applications. J Bone Joint Surg Am. 2008;90 Suppl 1:48-54.
[104] Caplan AI, Correa D. PDGF in bone formation and regeneration: new insights into a novel mechanism involving MSCs. J Orthop Res. 2011;29:1795-803.
[105] Ashcroft GS, Horan MA, Ferguson MW. The effects of ageing on wound healing: immunolocalisation of growth factors and their receptors in a murine incisional model. J Anat. 1997;190 (Pt 3):351-65.
[106] Globus RK, Plouet J, Gospodarowicz D. Cultured bovine bone cells synthesize basic fibroblast growth factor and store it in their extracellular matrix. Endocrinology. 1989;124:1539-47.
[107] Gospodarowicz D. Fibroblast growth factor. Chemical structure and biologic function. Clin Orthop Relat Res. 1990:231-48.
[108] Hauschka PV, Mavrakos AE, Iafrati MD, Doleman SE, Klagsbrun M. Growth factors in bone matrix. Isolation of multiple types by affinity chromatography on heparin-Sepharose. J Biol Chem. 1986;261:12665-74.
[109] Montero A, Okada Y, Tomita M, Ito M, Tsurukami H, Nakamura T, et al. Disruption of the fibroblast growth factor-2 gene results in decreased bone mass and bone formation. J Clin Invest. 2000;105:1085-93.
[110] Aronson J. Modulation of distraction osteogenesis in the aged rat by fibroblast growth factor. Clin Orthop Relat Res. 2004:264-83.

[111] Hurley MM, Gronowicz G, Zhu L, Kuhn LT, Rodner C, Xiao L. Age-Related Changes in FGF-2, Fibroblast Growth Factor Receptors and beta-Catenin Expression in Human Mesenchyme-Derived Progenitor Cells. J Cell Biochem. 2016;117:721-9.
[112] Liu JP, Baker J, Perkins AS, Robertson EJ, Efstratiadis A. Mice carrying null mutations of the genes encoding insulin-like growth factor I (Igf-1) and type 1 IGF receptor (Igf1r). Cell. 1993;75:59-72.
[113] Nicolas V, Prewett A, Bettica P, Mohan S, Finkelman RD, Baylink DJ, et al. Age-related decreases in insulin-like growth factor-I and transforming growth factor-beta in femoral cortical bone from both men and women: implications for bone loss with aging. J Clin Endocrinol Metab. 1994;78:1011-6.
[114] Boonen S, Lesaffre E, Dequeker J, Aerssens J, Nijs J, Pelemans W, et al. Relationship between baseline insulin-like growth factor-I (IGF-I) and femoral bone density in women aged over 70 years: potential implications for the prevention of age-related bone loss. J Am Geriatr Soc. 1996;44:1301-6.
[115] Langlois JA, Rosen CJ, Visser M, Hannan MT, Harris T, Wilson PW, et al. Association between insulin-like growth factor I and bone mineral density in older women and men: the Framingham Heart Study. J Clin Endocrinol Metab. 1998;83:4257-62.
[116] Sroga GE, Wu PC, Vashishth D. Insulin-like growth factor 1, glycation and bone fragility: implications for fracture resistance of bone. PLoS One. 2015;10:e0117046.
[117] Franceschi C, Bonafe M, Valensin S, Olivieri F, De Luca M, Ottaviani E, et al. Inflamm-aging. An evolutionary perspective on immunosenescence. Ann N Y Acad Sci. 2000;908:244-54.
[118] Cavaillon JM. Cytokines and macrophages. Biomed Pharmacother. 1994;48:445-53.
[119] Champagne CM, Takebe J, Offenbacher S, Cooper LF. Macrophage cell lines produce osteoinductive signals that include bone morphogenetic protein-2. Bone. 2002;30:26-31.
[120] Gibon E, Lu L, Goodman SB. Aging, inflammation, stem cells, and bone healing. Stem Cell Res Ther. 2016;7:44.
[121] Barrett JP, Costello DA, O'Sullivan J, Cowley TR, Lynch MA. Bone marrow-derived macrophages from aged rats are more responsive to inflammatory stimuli. J Neuroinflammation. 2015;12:67.
[122] Gibon E, Loi F, Cordova LA, Pajarinen J, Lin T, Lu L, et al. Aging Affects Bone Marrow Macrophage Polarization: Relevance to Bone Healing. Regen Eng Transl Med. 2016;2:98-104.
[123] Hotokezaka H, Sakai E, Ohara N, Hotokezaka Y, Gonzales C, Matsuo K, et al. Molecular analysis of RANKL-independent cell fusion of osteoclast-like cells induced by TNF-alpha, lipopolysaccharide, or peptidoglycan. J Cell Biochem. 2007;101:122-34.
[124] Vester H, Huber-Lang MS, Kida Q, Scola A, van Griensven M, Gebhard F, et al. The immune response after fracture trauma is different in old compared to young patients. Immun Ageing. 2014;11:20.
[125] Sebastian C, Herrero C, Serra M, Lloberas J, Blasco MA, Celada A. Telomere shortening and oxidative stress in aged macrophages results in impaired STAT5a phosphorylation. J Immunol. 2009;183:2356-64.
[126] Schlundt C, El Khassawna T, Serra A, Dienelt A, Wendler S, Schell H, et al. Macrophages in bone fracture healing: Their essential role in endochondral ossification. Bone. 2015.

[127] Cauley JA, Danielson ME, Boudreau RM, Forrest KY, Zmuda JM, Pahor M, et al. Inflammatory markers and incident fracture risk in older men and women: the Health Aging and Body Composition Study. J Bone Miner Res. 2007;22:1088-95.
[128] Grey A, Mitnick MA, Masiukiewicz U, Sun BH, Rudikoff S, Jilka RL, et al. A role for interleukin-6 in parathyroid hormone-induced bone resorption in vivo. Endocrinology. 1999;140:4683-90.
[129] Lau AN, Adachi JD. Geriatric Rheumatology: A Comprehensive Approach: Springer Science+Business Media; 2011.
[130] Landgraeber S, Jager M, Jacobs JJ, Hallab NJ. The pathology of orthopedic implant failure is mediated by innate immune system cytokines. Mediators Inflamm. 2014;2014:185150.
[131] Bruunsgaard H. Effects of tumor necrosis factor-alpha and interleukin-6 in elderly populations. Eur Cytokine Netw. 2002;13:389-91.
[132] Hayflick L, Moorhead PS. The serial cultivation of human diploid cell strains. Exp Cell Res. 1961;25:585-621.
[133] Collado M, Blasco MA, Serrano M. Cellular senescence in cancer and aging. Cell. 2007;130:223-33.
[134] Geissmann F, Manz MG, Jung S, Sieweke MH, Merad M, Ley K. Development of monocytes, macrophages, and dendritic cells. Science. 2010;327:656-61.
[135] Boccardi V, Paolisso G. Telomerase activation: a potential key modulator for human healthspan and longevity. Ageing Res Rev. 2014;15:1-5.
[136] Baker DJ, Wijshake T, Tchkonia T, LeBrasseur NK, Childs BG, van de Sluis B, et al. Clearance of p16Ink4a-positive senescent cells delays ageing-associated disorders. Nature. 2011;479:232-6.
[137] Farr JN, Fraser DG, Wang H, Jaehn K, Ogrodnik MB, Weivoda MM, et al. Identification of Senescent Cells in the Bone Microenvironment. J Bone Miner Res. 2016;31:1920-9.
[138] Haugstetter AM, Loddenkemper C, Lenze D, Grone J, Standfuss C, Petersen I, et al. Cellular senescence predicts treatment outcome in metastasised colorectal cancer. Br J Cancer. 2010;103:505-9.
[139] Provinciali M, Cardelli M, Marchegiani F, Pierpaoli E. Impact of cellular senescence in aging and cancer. Curr Pharm Des. 2013;19:1699-709.
[140] Coppe JP, Patil CK, Rodier F, Sun Y, Munoz DP, Goldstein J, et al. Senescence-associated secretory phenotypes reveal cell-nonautonomous functions of oncogenic RAS and the p53 tumor suppressor. PLoS Biol. 2008;6:2853-68.
[141] Conboy IM, Conboy MJ, Wagers AJ, Girma ER, Weissman IL, Rando TA. Rejuvenation of aged progenitor cells by exposure to a young systemic environment. Nature. 2005;433:760-4.
[142] Baht GS, Silkstone D, Vi L, Nadesan P, Amani Y, Whetstone H, et al. Exposure to a youthful circulaton rejuvenates bone repair through modulation of beta-catenin. Nat Commun. 2015;6:7131.
[143] Bektas A, Schurman SH, Sen R, Ferrucci L. Human T cell immunosenescence and inflammation in aging. J Leukoc Biol. 2017;102:977-88.
[144] Shaw AC, Joshi S, Greenwood H, Panda A, Lord JM. Aging of the innate immune system. Curr Opin Immunol. 2010;22:507-13.
[145] Linehan E, Dombrowski Y, Snoddy R, Fallon PG, Kissenpfennig A, Fitzgerald DC. Aging impairs peritoneal but not bone marrow-derived macrophage phagocytosis. Aging Cell. 2014;13:699-708.

[146] Chelvarajan RL, Collins SM, Van Willigen JM, Bondada S. The unresponsiveness of aged mice to polysaccharide antigens is a result of a defect in macrophage function. J Leukoc Biol. 2005;77:503-12.
[147] Oishi Y, Manabe I. Macrophages in age-related chronic inflammatory diseases. NPJ Aging Mech Dis. 2016;2:16018.
[148] Gomez CR, Hirano S, Cutro BT, Birjandi S, Baila H, Nomellini V, et al. Advanced age exacerbates the pulmonary inflammatory response after lipopolysaccharide exposure. Crit Care Med. 2007;35:246-51.
[149] Yang HC, Rossini M, Ma LJ, Zuo Y, Ma J, Fogo AB. Cells derived from young bone marrow alleviate renal aging. J Am Soc Nephrol. 2011;22:2028-36.
[150] Shaik-Dasthagirisaheb YB, Kantarci A, Gibson FC, 3rd. Immune response of macrophages from young and aged mice to the oral pathogenic bacterium Porphyromonas gingivalis. Immun Ageing. 2010;7:15.
[151] Burns EA, Goodwin JS. Immunodeficiency of aging. Drugs Aging. 1997;11:374-97.
[152] Mokarram N, Merchant A, Mukhatyar V, Patel G, Bellamkonda RV. Effect of modulating macrophage phenotype on peripheral nerve repair. Biomaterials. 2012;33:8793-801.
[153] Reeves AR, Spiller KL, Freytes DO, Vunjak-Novakovic G, Kaplan DL. Controlled release of cytokines using silk-biomaterials for macrophage polarization. Biomaterials. 2015;73:272-83.
[154] Pajarinen J, Tamaki Y, Antonios JK, Lin TH, Sato T, Yao Z, et al. Modulation of mouse macrophage polarization in vitro using IL-4 delivery by osmotic pumps. J Biomed Mater Res A. 2015;103:1339-45.
[155] Spiller KL, Nassiri S, Witherel CE, Anfang RR, Ng J, Nakazawa KR, et al. Sequential delivery of immunomodulatory cytokines to facilitate the M1-to-M2 transition of macrophages and enhance vascularization of bone scaffolds. Biomaterials. 2015;37:194-207.
[156] Keeler GD, Durdik JM, Stenken JA. Localized delivery of dexamethasone-21-phosphate via microdialysis implants in rat induces M(GC) macrophage polarization and alters CCL2 concentrations. Acta Biomater. 2015;12:11-20.
[157] Pers JO, Saraux A, Pierre R, Youinou P. Anti-TNF-alpha immunotherapy is associated with increased gingival inflammation without clinical attachment loss in subjects with rheumatoid arthritis. J Periodontol. 2008;79:1645-51.
[158] Glass GE, Chan JK, Freidin A, Feldmann M, Horwood NJ, Nanchahal J. TNF-alpha promotes fracture repair by augmenting the recruitment and differentiation of muscle-derived stromal cells. Proc Natl Acad Sci U S A. 2011;108:1585-90.
[159] Li H, Hong S, Qian J, Zheng Y, Yang J, Yi Q. Cross talk between the bone and immune systems: osteoclasts function as antigen-presenting cells and activate CD4+ and CD8+ T cells. Blood. 2010;116:210-7.
[160] Dziak R. Osteoimmunology: cross-talk between bone and immune cells. Immunol Invest. 2013;42:657-60.
[161] Carbone LD, Tylavsky FA, Cauley JA, Harris TB, Lang TF, Bauer DC, et al. Association between bone mineral density and the use of nonsteroidal anti-inflammatory drugs and aspirin: impact of cyclooxygenase selectivity. J Bone Miner Res. 2003;18:1795-802.
[162] Puzas JE, O'Keefe RJ, Schwarz EM, Zhang X. Pharmacologic modulators of fracture healing: the role of cyclooxygenase inhibition. J Musculoskelet Neuronal Interact. 2003;3:308-12; discussion 20-1.

[163] Helin-Salmivaara A, Korhonen MJ, Lehenkari P, Junnila SY, Neuvonen PJ, Ruokoniemi P, et al. Statins and hip fracture prevention--a population based cohort study in women. PLoS One. 2012;7:e48095.
[164] Montagnani A, Gonnelli S, Cepollaro C, Pacini S, Campagna MS, Franci MB, et al. Effect of simvastatin treatment on bone mineral density and bone turnover in hypercholesterolemic postmenopausal women: a 1-year longitudinal study. Bone. 2003;32:427-33.
[165] Konstantinidis I, Papageorgiou SN, Kyrgidis A, Tzellos TG, Kouvelas D. Effect of non-steroidal anti-inflammatory drugs on bone turnover: an evidence-based review. Rev Recent Clin Trials. 2013;8:48-60.
[166] Garcia MJ, Reinoso RF, Sanchez Navarro A, Prous JR. Clinical pharmacokinetics of statins. Methods Find Exp Clin Pharmacol. 2003;25:457-81.
[167] Stancu C, Sima A. Statins: mechanism of action and effects. J Cell Mol Med. 2001;5:378-87.
[168] Blumenthal RS. Statins: effective antiatherosclerotic therapy. Am Heart J. 2000;139:577-83.
[169] Terblanche M, Almog Y, Rosenson RS, Smith TS, Hackam DG. Statins and sepsis: multiple modifications at multiple levels. Lancet Infect Dis. 2007;7:358-68.
[170] Waldman A, Kritharides L. The pleiotropic effects of HMG-CoA reductase inhibitors: their role in osteoporosis and dementia. Drugs. 2003;63:139-52.
[171] Montecucco F, Burger F, Pelli G, Poku NK, Berlier C, Steffens S, et al. Statins inhibit C-reactive protein-induced chemokine secretion, ICAM-1 upregulation and chemotaxis in adherent human monocytes. Rheumatology (Oxford). 2009;48:233-42.
[172] Nishibori M, Takahashi HK, Mori S. The regulation of ICAM-1 and LFA-1 interaction by autacoids and statins: a novel strategy for controlling inflammation and immune responses. J Pharmacol Sci. 2003;92:7-12.
[173] Jougasaki M, Ichiki T, Takenoshita Y, Setoguchi M. Statins suppress interleukin-6-induced monocyte chemo-attractant protein-1 by inhibiting Janus kinase/signal transducers and activators of transcription pathways in human vascular endothelial cells. Br J Pharmacol. 2010;159:1294-303.
[174] Singh P, Kohr D, Kaps M, Blaes F. Influence of statins on MHC class I expression. Ann N Y Acad Sci. 2009;1173:746-51.
[175] Akasaki Y, Matsuda S, Nakayama K, Fukagawa S, Miura H, Iwamoto Y. Mevastatin reduces cartilage degradation in rabbit experimental osteoarthritis through inhibition of synovial inflammation. Osteoarthritis Cartilage. 2009;17:235-43.
[176] van der Most PJ, Dolga AM, Nijholt IM, Luiten PG, Eisel UL. Statins: mechanisms of neuroprotection. Prog Neurobiol. 2009;88:64-75.
[177] Kagami S, Kanari H, Suto A, Fujiwara M, Ikeda K, Hirose K, et al. HMG-CoA reductase inhibitor simvastatin inhibits proinflammatory cytokine production from murine mast cells. Int Arch Allergy Immunol. 2008;146 Suppl 1:61-6.
[178] Basraon SK, Costantine MM, Saade G, Menon R. The Effect of Simvastatin on Infection-Induced Inflammatory Response of Human Fetal Membranes. Am J Reprod Immunol. 2015;74:54-61.
[179] Jung JY, Woo SM, Kim WJ, Lee BN, Nor JE, Min KS, et al. Simvastatin inhibits the expression of inflammatory cytokines and cell adhesion molecules induced by LPS in human dental pulp cells. Int Endod J. 2017;50:377-86.

[180] Liu M, Yu Y, Jiang H, Zhang L, Zhang PP, Yu P, et al. Simvastatin suppresses vascular inflammation and atherosclerosis in ApoE(-/-) mice by downregulating the HMGB1-RAGE axis. Acta Pharmacol Sin. 2013;34:830-6.
[181] Zhang X, Jin J, Peng X, Ramgolam VS, Markovic-Plese S. Simvastatin inhibits IL-17 secretion by targeting multiple IL-17-regulatory cytokines and by inhibiting the expression of IL-17 transcription factor RORC in CD4+ lymphocytes. J Immunol. 2008;180:6988-96.
[182] Wang PS, Solomon DH, Mogun H, Avorn J. HMG-CoA reductase inhibitors and the risk of hip fractures in elderly patients. JAMA. 2000;283:3211-6.
[183] Hatzigeorgiou C, Jackson JL. Hydroxymethylglutaryl-coenzyme A reductase inhibitors and osteoporosis: a meta-analysis. Osteoporos Int. 2005;16:990-8.
[184] Lupattelli G, Scarponi AM, Vaudo G, Siepi D, Roscini AR, Gemelli F, et al. Simvastatin increases bone mineral density in hypercholesterolemic postmenopausal women. Metabolism. 2004;53:744-8.
[185] Aleksandar Dimic, Dimitrije Jankovic, Irena Jankovic, Todorka Savic, Nevena Karanovic. The effects of one-year simvastatin therapy on women's bone mineral density. Cent Eur J Med. 2010;5(5) • 2010 • 588-592.
[186] https://www.rxlist.com/zocor-side-effects-drug-center.htm.
[187] Piskin E, Isoglu IA, Bolgen N, Vargel I, Griffiths S, Cavusoglu T, et al. In vivo performance of simvastatin-loaded electrospun spiral-wound polycaprolactone scaffolds in reconstruction of cranial bone defects in the rat model. J Biomed Mater Res A. 2009;90:1137-51.
[188] Jeon JH, Piepgrass WT, Lin YL, Thomas MV, Puleo DA. Localized intermittent delivery of simvastatin hydroxyacid stimulates bone formation in rats. J Periodontol. 2008;79:1457-64.
[189] Zhao S, Wen F, He F, Liu L, Yang G. In vitro and in vivo evaluation of the osteogenic ability of implant surfaces with a local delivery of simvastatin. Int J Oral Maxillofac Implants. 2014;29:211-20.
[190] Qi Y, Zhao T, Yan W, Xu K, Shi Z, Wang J. Mesenchymal stem cell sheet transplantation combined with locally released simvastatin enhances bone formation in a rat tibia osteotomy model. Cytotherapy. 2013;15:44-56.
[191] Skoglund B, Aspenberg P. Locally applied Simvastatin improves fracture healing in mice. BMC Musculoskelet Disord. 2007;8:98.
[192] Nyan M, Sato D, Kihara H, Machida T, Ohya K, Kasugai S. Effects of the combination with alpha-tricalcium phosphate and simvastatin on bone regeneration. Clin Oral Implants Res. 2009;20:280-7.
[193] Stein D, Lee Y, Schmid MJ, Killpack B, Genrich MA, Narayana N, et al. Local simvastatin effects on mandibular bone growth and inflammation. J Periodontol. 2005;76:1861-70.
[194] Ito T, Takemasa M, Makino K, Otsuka M. Preparation of calcium phosphate nanocapsules including simvastatin/deoxycholic acid assembly, and their therapeutic effect in osteoporosis model mice. J Pharm Pharmacol. 2013;65:494-502.
[195] Peter B, Pioletti DP, Laib S, Bujoli B, Pilet P, Janvier P, et al. Calcium phosphate drug delivery system: influence of local zoledronate release on bone implant osteointegration. Bone. 2005;36:52-60.
[196] Haghbin-Nazarpak M, Moztarzadeh F, Solati-Hashjin M, Tahriri M, Khoshroo K. Injectable and bioresorbable calcium phosphate delivery system with gentamicin sulphate for treatment of bone diseases: in vitro study. Advances in Applied Ceramics. 2011;110:482-9.

[197] Verron E, Khairoun I, Guicheux J, Bouler JM. Calcium phosphate biomaterials as bone drug delivery systems: a review. Drug Discov Today. 2010;15:547-52.
[198] Liechty WB, Kryscio DR, Slaughter BV, Peppas NA. Polymers for drug delivery systems. Annu Rev Chem Biomol Eng. 2010;1:149-73.
[199] Lee K, Silva EA, Mooney DJ. Growth factor delivery-based tissue engineering: general approaches and a review of recent developments. J R Soc Interface. 2011;8:153-70.
[200] Sundararaj SC, Thomas MV, Peyyala R, Dziubla TD, Puleo DA. Design of a multiple drug delivery system directed at periodontitis. Biomaterials. 2013;34:8835-42.
[201] Kuhn LT, Ou G, Charles L, Hurley MM, Rodner CM, Gronowicz G. Fibroblast growth factor-2 and bone morphogenetic protein-2 have a synergistic stimulatory effect on bone formation in cell cultures from elderly mouse and human bone. J Gerontol A Biol Sci Med Sci. 2013;68:1170-80.
[202] Lim SM, Oh SH, Lee HH, Yuk SH, Im GI, Lee JH. Dual growth factor-releasing nanoparticle/hydrogel system for cartilage tissue engineering. J Mater Sci Mater Med. 2010;21:2593-600.
[203] Jiang B, Zhang G, Brey EM. Dual delivery of chlorhexidine and platelet-derived growth factor-BB for enhanced wound healing and infection control. Acta Biomater. 2013;9:4976-84.
[204] Jacobs EE, Gronowicz G, Hurley MM, Kuhn LT. Biomimetic calcium phosphate/polyelectrolyte multilayer coatings for sequential delivery of multiple biological factors. J Biomed Mater Res A. 2017;105:1500-9.
[205] Gronowicz G, Jacobs E, Peng T, Zhu L, Hurley M, Kuhn LT. (*) Calvarial Bone Regeneration Is Enhanced by Sequential Delivery of FGF-2 and BMP-2 from Layer-by-Layer Coatings with a Biomimetic Calcium Phosphate Barrier Layer. Tissue Eng Part A. 2017;23:1490-501.
[206] Chang PC, Chong LY, Dovban AS, Lim LP, Lim JC, Kuo MY, et al. Sequential platelet-derived growth factor-simvastatin release promotes dentoalveolar regeneration. Tissue Eng Part A. 2014;20:356-64.
[207] Park JB. Combined effects of simvastatin and fibroblast growth factor-2 on the proliferation and differentiation of preosteoblasts. Biomed Rep. 2013;1:812-4.
[208] Jeon JH, Puleo DA. Alternating release of different bioactive molecules from a complexation polymer system. Biomaterials. 2008;29:3591-8.
[209] Gerstenfeld LC, Einhorn TA. COX inhibitors and their effects on bone healing. Expert Opin Drug Saf. 2004;3:131-6.
[210] Gomes FI, Aragao MG, de Paulo Teixeira Pinto V, Gondim DV, Barroso FC, Silva AA, et al. Effects of nonsteroidal anti-inflammatory drugs on osseointegration: a review. J Oral Implantol. 2015;41:219-30.
[211] Reikeras O, Shegarfi H, Wang JE, Utvag SE. Lipopolysaccharide impairs fracture healing: an experimental study in rats. Acta Orthop. 2005;76:749-53.
[212] Reikeras O, Wang JE, Foster SJ, Utvag SE. Staphylococcus aureus peptidoglycan impairs fracture healing: an experimental study in rats. J Orthop Res. 2007;25:262-6.
[213] Jetten N, Roumans N, Gijbels MJ, Romano A, Post MJ, de Winther MP, et al. Wound administration of M2-polarized macrophages does not improve murine cutaneous healing responses. PLoS One. 2014;9:e102994.
[214] Saki N, Abroun S, Salari F, Rahim F, Shahjahani M, Javad MA. Molecular Aspects of Bone Resorption in beta-Thalassemia Major. Cell J. 2015;17:193-200.

[215] Schmidt-Bleek K, Petersen A, Dienelt A, Schwarz C, Duda GN. Initiation and early control of tissue regeneration - bone healing as a model system for tissue regeneration. Expert Opin Biol Ther. 2014;14:247-59.
[216] Lorenzo J, Horowitz M, Choi Y. Osteoimmunology: interactions of the bone and immune system. Endocr Rev. 2008;29:403-40.
[217] Takayanagi H. Osteoimmunology: shared mechanisms and crosstalk between the immune and bone systems. Nat Rev Immunol. 2007;7:292-304.
[218] Alexander KA, Chang MK, Maylin ER, Kohler T, Muller R, Wu AC, et al. Osteal macrophages promote in vivo intramembranous bone healing in a mouse tibial injury model. J Bone Miner Res. 2011;26:1517-32.
[219] Schlundt C, El Khassawna T, Serra A, Dienelt A, Wendler S, Schell H, et al. Macrophages in bone fracture healing: Their essential role in endochondral ossification. Bone. 2018;106:78-89.
[220] Claes L, Recknagel S, Ignatius A. Fracture healing under healthy and inflammatory conditions. Nat Rev Rheumatol. 2012;8:133-43.
[221] Bayer EA, Fedorchak MV, Little SR. The Influence of Platelet-Derived Growth Factor and Bone Morphogenetic Protein Presentation on Tubule Organization by Human Umbilical Vascular Endothelial Cells and Human Mesenchymal Stem Cells in Coculture. Tissue Eng Part A. 2016;22:1296-304.
[222] Wang Y, Cooke MJ, Sachewsky N, Morshead CM, Shoichet MS. Bioengineered sequential growth factor delivery stimulates brain tissue regeneration after stroke. J Control Release. 2013;172:1-11.
[223] Jo JY, Jeong SI, Shin YM, Kang SS, Kim SE, Jeong CM, et al. Sequential delivery of BMP-2 and BMP-7 for bone regeneration using a heparinized collagen membrane. Int J Oral Maxillofac Surg. 2015;44:921-8.
[224] Yilgor P, Hasirci N, Hasirci V. Sequential BMP-2/BMP-7 delivery from polyester nanocapsules. J Biomed Mater Res A. 2010;93:528-36.
[225] Yilgor P, Sousa RA, Reis RL, Hasirci N, Hasirci V. Effect of scaffold architecture and BMP-2/BMP-7 delivery on in vitro bone regeneration. J Mater Sci Mater Med. 2010;21:2999-3008.
[226] Yilgor P, Tuzlakoglu K, Reis RL, Hasirci N, Hasirci V. Incorporation of a sequential BMP-2/BMP-7 delivery system into chitosan-based scaffolds for bone tissue engineering. Biomaterials. 2009;30:3551-9.
[227] Basmanav FB, Kose GT, Hasirci V. Sequential growth factor delivery from complexed microspheres for bone tissue engineering. Biomaterials. 2008;29:4195-204.
[228] Kim S, Kang Y, Krueger CA, Sen M, Holcomb JB, Chen D, et al. Sequential delivery of BMP-2 and IGF-1 using a chitosan gel with gelatin microspheres enhances early osteoblastic differentiation. Acta Biomater. 2012;8:1768-77.
[229] Strobel C, Bormann N, Kadow-Romacker A, Schmidmaier G, Wildemann B. Sequential release kinetics of two (gentamicin and BMP-2) or three (gentamicin, IGF-I and BMP-2) substances from a one-component polymeric coating on implants. J Control Release. 2011;156:37-45.
[230] Raiche AT, Puleo DA. In vitro effects of combined and sequential delivery of two bone growth factors. Biomaterials. 2004;25:677-85.

[231] Perez RA, Kim JH, Buitrago JO, Wall IB, Kim HW. Novel therapeutic core-shell hydrogel scaffolds with sequential delivery of cobalt and bone morphogenetic protein-2 for synergistic bone regeneration. Acta Biomater. 2015;23:295-308.
[232] Lee HJ, Koh WG. Hydrogel micropattern-incorporated fibrous scaffolds capable of sequential growth factor delivery for enhanced osteogenesis of hMSCs. ACS Appl Mater Interfaces. 2014;6:9338-48.
[233] Lee AL, Wang Y, Cheng HY, Pervaiz S, Yang YY. The co-delivery of paclitaxel and Herceptin using cationic micellar nanoparticles. Biomaterials. 2009;30:919-27.
[234] Kokubo T, Ito S, Huang ZT, Hayashi T, Sakka S, Kitsugi T, et al. Ca,P-rich layer formed on high-strength bioactive glass-ceramic A-W. J Biomed Mater Res. 1990;24:331-43.
[235] Barrere F, Layrolle P, van Blitterswijk CA, de Groot K. Biomimetic calcium phosphate coatings on Ti6AI4V: a crystal growth study of octacalcium phosphate and inhibition by Mg2+ and HCO3. Bone. 1999;25:107S-11S.
[236] Liu Y, Layrolle P, de Bruijn J, van Blitterswijk C, de Groot K. Biomimetic coprecipitation of calcium phosphate and bovine serum albumin on titanium alloy. J Biomed Mater Res. 2001;57:327-35.
[237] Lin HY, Liu Y, Wismeijer D, Crielaard W, Deng DM. Effects of oral implant surface roughness on bacterial biofilm formation and treatment efficacy. Int J Oral Maxillofac Implants. 2013;28:1226-31.
[238] Barrere F, Layrolle P, Van Blitterswijk CA, De Groot K. Biomimetic coatings on titanium: a crystal growth study of octacalcium phosphate. J Mater Sci Mater Med. 2001;12:529-34.
[239] Barrere F, van Blitterswijk CA, de Groot K, Layrolle P. Influence of ionic strength and carbonate on the Ca-P coating formation from SBFx5 solution. Biomaterials. 2002;23:1921-30.
[240] Wu G, Hunziker EB, Zheng Y, Wismeijer D, Liu Y. Functionalization of deproteinized bovine bone with a coating-incorporated depot of BMP-2 renders the material efficiently osteoinductive and suppresses foreign-body reactivity. Bone. 2011;49:1323-30.
[241] Wu G, Liu Y, Iizuka T, Hunziker EB. The effect of a slow mode of BMP-2 delivery on the inflammatory response provoked by bone-defect-filling polymeric scaffolds. Biomaterials. 2010;31:7485-93.
[242] Liu T, Wu G, Wismeijer D, Gu Z, Liu Y. Deproteinized bovine bone functionalized with the slow delivery of BMP-2 for the repair of critical-sized bone defects in sheep. Bone. 2013;56:110-8.
[243] Liu T, Wu G, Zheng Y, Wismeijer D, Everts V, Liu Y. Cell-mediated BMP-2 release from a novel dual-drug delivery system promotes bone formation. Clin Oral Implants Res. 2014;25:1412-21.
[244] Stigter M, de Groot K, Layrolle P. Incorporation of tobramycin into biomimetic hydroxyapatite coating on titanium. Biomaterials. 2002;23:4143-53.
[245] Wu G, Liu Y, Iizuka T, Hunziker EB. Biomimetic coating of organic polymers with a protein-functionalized layer of calcium phosphate: the surface properties of the carrier influence neither the coating characteristics nor the incorporation mechanism or release kinetics of the protein. Tissue Eng Part C Methods. 2010;16:1255-65.
[246] Liu Y, de Groot K, Hunziker EB. Osteoinductive implants: the mise-en-scene for drug-bearing biomimetic coatings. Ann Biomed Eng. 2004;32:398-406.
[247] Liu Y, Hunziker EB, Layrolle P, De Bruijn JD, De Groot K. Bone morphogenetic protein 2 incorporated into biomimetic coatings retains its biological activity. Tissue Eng. 2004;10:101-8.

[248] Liu Y, Hunziker EB, Randall NX, de Groot K, Layrolle P. Proteins incorporated into biomimetically prepared calcium phosphate coatings modulate their mechanical strength and dissolution rate. Biomaterials. 2003;24:65-70.
[249] Liu Y, Huse RO, de Groot K, Buser D, Hunziker EB. Delivery mode and efficacy of BMP-2 in association with implants. J Dent Res. 2007;86:84-9.
[250] Yu X, Qu H, Knecht DA, Wei M. Incorporation of bovine serum albumin into biomimetic coatings on titanium with high loading efficacy and its release behavior. J Mater Sci Mater Med. 2009;20:287-94.
[251] Yu X, Wang L, Jiang X, Rowe D, Wei M. Biomimetic CaP coating incorporated with parathyroid hormone improves the osseointegration of titanium implant. J Mater Sci Mater Med. 2012;23:2177-86.
[252] Yu X, Wei M. Preparation and evaluation of parathyroid hormone incorporated CaP coating via a biomimetic method. J Biomed Mater Res B Appl Biomater. 2011;97:345-54.
[253] Goldberg AJ, Liu Y, Advincula MC, Gronowicz G, Habibovic P, Kuhn LT. Fabrication and characterization of hydroxyapatite-coated polystyrene disks for use in osteoprogenitor cell culture. J Biomater Sci Polym Ed. 2010;21:1371-87.
[254] Barrere F, van BC, de GK, Layrolle P. Nucleation of biomimetic Ca-P coatings on ti6A14V from a SBF x 5 solution: influence of magnesium. Biomaterials. 2002;23:2211-20.
[255] Habibovic PB FvB, C.A.; de Groot, K.; Layrolle, P. . Biomimetic Hydroxyapatite Coating on Metal Implants. . Journal of American Ceramic Society 2002;85:517- 22.
[256] Fischer D, Li Y, Ahlemeyer B, Krieglstein J, Kissel T. In vitro cytotoxicity testing of polycations: influence of polymer structure on cell viability and hemolysis. Biomaterials. 2003;24:1121-31.
[257] Arnold LJ, Jr., Dagan A, Gutheil J, Kaplan NO. Antineoplastic activity of poly(L-lysine) with some ascites tumor cells. Proc Natl Acad Sci U S A. 1979;76:3246-50.
[258] Amgad Hanna, Daniel L. Thompson, Daniel J. Hellenbrand, Jae-Sung Lee, Casey J. Madura, Meredith G. Wesley, et al. Sustained release of neurotrophin-3 via calcium phosphate-coated sutures promotes axonal regeneration after spinal cord injury. Journal of Neuroscience Research. 2016; 94.
[259] Jae Sung Lee aYL, b Geoffrey S. Baer,c Mark D. Markelb and William L. Murphy. Controllable protein delivery from coated surgical sutures. Journal of Materials Chemistry. 2010;20, 8894-8903.
[260] Leenaporn Jongpaiboonkit TF-F, and William L. Murphy Coated Polymer Microspheres for ControlledProtein Binding and Release. Adv Mater 2009; 21, 1960–1963.
[261] Leuschner F, Dutta P, Gorbatov R, Novobrantseva TI, Donahoe JS, Courties G, et al. Therapeutic siRNA silencing in inflammatory monocytes in mice. Nat Biotechnol. 2011;29:1005-10.
[262] Godwin JW, Pinto AR, Rosenthal NA. Macrophages are required for adult salamander limb regeneration. Proc Natl Acad Sci U S A. 2013;110:9415-20.
[263] Brown BN, Londono R, Tottey S, Zhang L, Kukla KA, Wolf MT, et al. Macrophage phenotype as a predictor of constructive remodeling following the implantation of biologically derived surgical mesh materials. Acta Biomater. 2012;8:978-87.
[264] Spiller KL, Anfang RR, Spiller KJ, Ng J, Nakazawa KR, Daulton JW, et al. The role of macrophage phenotype in vascularization of tissue engineering scaffolds. Biomaterials. 2014;35:4477-88.

[265] Richert L, Schneider A, Vautier D, Vodouhe C, Jessel N, Payan E, et al. Imaging cell interactions with native and crosslinked polyelectrolyte multilayers. Cell Biochem Biophys. 2006;44:273-85.
[266] Igeta K, Kuwamura Y, Horiuchi N, Nozaki K, Shiraishi D, Aizawa M, et al. Morphological and functional changes in RAW264 macrophage-like cells in response to a hydrated layer of carbonate-substituted hydroxyapatite. J Biomed Mater Res A. 2017;105:1063-70.
[267] Mirza R, Koh TJ. Dysregulation of monocyte/macrophage phenotype in wounds of diabetic mice. Cytokine. 2011;56:256-64.
[268] Kigerl KA, Gensel JC, Ankeny DP, Alexander JK, Donnelly DJ, Popovich PG. Identification of two distinct macrophage subsets with divergent effects causing either neurotoxicity or regeneration in the injured mouse spinal cord. J Neurosci. 2009;29:13435-44.
[269] Graney PL, Lurier EB, Spiller KL. Biomaterials and Bioactive Factor Delivery Systems for the Control of Macrophage Activation in Regenerative Medicine. ACS Biomaterials Science & Engineering. 2017.
[270] Mahbub S, Deburghgraeve CR, Kovacs EJ. Advanced age impairs macrophage polarization. J Interferon Cytokine Res. 2012;32:18-26.
[271] Swift ME, Burns AL, Gray KL, DiPietro LA. Age-related alterations in the inflammatory response to dermal injury. J Invest Dermatol. 2001;117:1027-35.
[272] Boehmer ED, Goral J, Faunce DE, Kovacs EJ. Age-dependent decrease in Toll-like receptor 4-mediated proinflammatory cytokine production and mitogen-activated protein kinase expression. J Leukoc Biol. 2004;75:342-9.
[273] Renshaw M, Rockwell J, Engleman C, Gewirtz A, Katz J, Sambhara S. Cutting edge: impaired Toll-like receptor expression and function in aging. J Immunol. 2002;169:4697-701.
[274] Hachim D, Wang N, Lopresti ST, Stahl EC, Umeda YU, Rege RD, et al. Effects of aging upon the host response to implants. J Biomed Mater Res A. 2017;105:1281-92.
[275] van Duin D, Mohanty S, Thomas V, Ginter S, Montgomery RR, Fikrig E, et al. Age-associated defect in human TLR-1/2 function. J Immunol. 2007;178:970-5.
[276] Yoon P, Keylock KT, Hartman ME, Freund GG, Woods JA. Macrophage hypo-responsiveness to interferon-gamma in aged mice is associated with impaired signaling through Jak-STAT. Mech Ageing Dev. 2004;125:137-43.
[277] Lumeng CN, Liu J, Geletka L, Delaney C, Delproposto J, Desai A, et al. Aging is associated with an increase in T cells and inflammatory macrophages in visceral adipose tissue. J Immunol. 2011;187:6208-16.
[278] Takayama T, Hirano-Kawamoto A, Yamamoto M, Murakami G, Katori Y, Kitamura K, et al. Macrophage infiltration into thyroid follicles: an immunohistochemical study using donated elderly cadavers. Okajimas Folia Anat Jpn. 2016;93:73-80.
[279] Stahl EC, Brown BN. Pro-Inflammatory Monocyte Derived Macrophages Accumulate in Uninjured Aged Murine Livers. The FASEB Journal. 2017;31:328.9-.9.
[280] Xing Z, Lu C, Hu D, Miclau T, 3rd, Marcucio RS. Rejuvenation of the inflammatory system stimulates fracture repair in aged mice. J Orthop Res. 2010;28:1000-6.
[281] Danon D, Kowatch MA, Roth GS. Promotion of wound repair in old mice by local injection of macrophages. Proc Natl Acad Sci U S A. 1989;86:2018-20.

[282] Tuomisto TT, Lumivuori H, Kansanen E, Hakkinen SK, Turunen MP, van Thienen JV, et al. Simvastatin has an anti-inflammatory effect on macrophages via upregulation of an atheroprotective transcription factor, Kruppel-like factor 2. Cardiovasc Res. 2008;78:175-84.
[283] Sakoda K, Yamamoto M, Negishi Y, Liao JK, Node K, Izumi Y. Simvastatin decreases IL-6 and IL-8 production in epithelial cells. J Dent Res. 2006;85:520-3.
[284] Dombrecht EJ, Van Offel JF, Bridts CH, Ebo DG, Seynhaeve V, Schuerwegh AJ, et al. Influence of simvastatin on the production of pro-inflammatory cytokines and nitric oxide by activated human chondrocytes. Clin Exp Rheumatol. 2007;25:534-9.
[285] Rezaie-Majd A, Maca T, Bucek RA, Valent P, Muller MR, Husslein P, et al. Simvastatin reduces expression of cytokines interleukin-6, interleukin-8, and monocyte chemoattractant protein-1 in circulating monocytes from hypercholesterolemic patients. Arterioscler Thromb Vasc Biol. 2002;22:1194-9.
[286] Cicek Ari V, Ilarslan YD, Erman B, Sarkarati B, Tezcan I, Karabulut E, et al. Statins and IL-1beta, IL-10, and MPO Levels in Gingival Crevicular Fluid: Preliminary Results. Inflammation. 2016;39:1547-57.
[287] Mouchrek Junior JCE, Macedo CG, Abdalla HB, Saba AK, Teixeira LN, Mouchrek A, et al. Simvastatin modulates gingival cytokine and MMP production in a rat model of ligature-induced periodontitis. Clin Cosmet Investig Dent. 2017;9:33-8.
[288] Li QZ, Sun J, Han JJ, Qian ZJ. [Anti-inflammation of simvastatin by polarization of murine macrophages from M1 phenotype to M2 phenotype]. Zhonghua Yi Xue Za Zhi. 2013;93:2071-4.
[289] Nadon NL. Exploiting the rodent model for studies on the pharmacology of lifespan extension. Aging Cell. 2006;5:9-15.
[290] Manolagas SC, Parfitt AM. What old means to bone. Trends Endocrinol Metab. 2010;21:369-74.
[291] Gerstenfeld LC, Cho TJ, Kon T, Aizawa T, Cruceta J, Graves BD, et al. Impaired intramembranous bone formation during bone repair in the absence of tumor necrosis factor-alpha signaling. Cells Tissues Organs. 2001;169:285-94.
[292] Ito H. Chemokines in mesenchymal stem cell therapy for bone repair: a novel concept of recruiting mesenchymal stem cells and the possible cell sources. Mod Rheumatol. 2011;21:113-21.
[293] Loi F, Cordova LA, Zhang R, Pajarinen J, Lin TH, Goodman SB, et al. The effects of immunomodulation by macrophage subsets on osteogenesis in vitro. Stem Cell Res Ther. 2016;7:15.
[294] Li T, Peng M, Yang Z, Zhou X, Deng Y, Jiang C, et al. 3D-printed IFN-gamma-loading calcium silicate-beta-tricalcium phosphate scaffold sequentially activates M1 and M2 polarization of macrophages to promote vascularization of tissue engineering bone. Acta Biomater. 2018.
[295] Slade Shantz JA, Yu YY, Andres W, Miclau T, 3rd, Marcucio R. Modulation of macrophage activity during fracture repair has differential effects in young adult and elderly mice. J Orthop Trauma. 2014;28 Suppl 1:S10-4.
[296] Wang L, Zhang B, Bao C, Habibovic P, Hu J, Zhang X. Ectopic osteoid and bone formation by three calcium-phosphate ceramics in rats, rabbits and dogs. PLoS One. 2014;9:e107044.

[297] Daculsi G. FBH, Miramond T. The Essential Role of Calcium Phosphate Bioceramics in Bone Regeneration. In: Ben-Nissan B. (eds) Advances in Calcium Phosphate Biomaterials. Springer Series in Biomaterials Science and Engineering, vol 2. Springer, Berlin, Heidelberg. 2014.
[298] Edwards CJ, Hart DJ, Spector TD. Oral statins and increased bone-mineral density in postmenopausal women. Lancet. 2000;355:2218-9.
[299] Brown BN, Haschak MJ, Lopresti ST, Stahl EC. Effects of age-related shifts in cellular function and local microenvironment upon the innate immune response to implants. Semin Immunol. 2017;29:24-32.
[300] Lee CH, Kim YJ, Jang JH, Park JW. Modulating macrophage polarization with divalent cations in nanostructured titanium implant surfaces. Nanotechnology. 2016;27:085101.
[301] Fernandes KR, Zhang Y, Magri AMP, Renno ACM, van den Beucken J. Biomaterial Property Effects on Platelets and Macrophages: An in Vitro Study. ACS Biomater Sci Eng. 2017;3:3318-27.
[302] Willenborg S, Lucas T, van Loo G, Knipper JA, Krieg T, Haase I, et al. CCR2 recruits an inflammatory macrophage subpopulation critical for angiogenesis in tissue repair. Blood. 2012;120:613-25.
[303] Arora M, Chen L, Paglia M, Gallagher I, Allen JE, Vyas YM, et al. Simvastatin promotes Th2-type responses through the induction of the chitinase family member Ym1 in dendritic cells. Proc Natl Acad Sci U S A. 2006;103:7777-82.
[304] Andrew JG, Andrew SM, Freemont AJ, Marsh DR. Inflammatory cells in normal human fracture healing. Acta Orthop Scand. 1994;65:462-6.
[305] Xing Z, Lu C, Hu D, Yu YY, Wang X, Colnot C, et al. Multiple roles for CCR2 during fracture healing. Dis Model Mech. 2010;3:451-8.
[306] Xue J, Schmidt SV, Sander J, Draffehn A, Krebs W, Quester I, et al. Transcriptome-based network analysis reveals a spectrum model of human macrophage activation. Immunity. 2014;40:274-88.
[307] Rando TA. Stem cells, ageing and the quest for immortality. Nature. 2006;441:1080-6.
[308] Aubin JE. Regulation of osteoblast formation and function. Rev Endocr Metab Disord. 2001;2:81-94.
[309] Zhang H, Lewis CG, Aronow MS, Gronowicz GA. The effects of patient age on human osteoblasts' response to Ti-6Al-4V implants in vitro. J Orthop Res. 2004;22:30-8.
[310] Wan Y, Zhuo N, Li Y, Zhao W, Jiang D. Autophagy promotes osteogenic differentiation of human bone marrow mesenchymal stem cell derived from osteoporotic vertebrae. Biochem Biophys Res Commun. 2017;488:46-52.
[311] Guihard P, Danger Y, Brounais B, David E, Brion R, Delecrin J, et al. Induction of osteogenesis in mesenchymal stem cells by activated monocytes/macrophages depends on oncostatin M signaling. Stem Cells. 2012;30:762-72.
[312] Rodier F, Munoz DP, Teachenor R, Chu V, Le O, Bhaumik D, et al. DNA-SCARS: distinct nuclear structures that sustain damage-induced senescence growth arrest and inflammatory cytokine secretion. J Cell Sci. 2011;124:68-81.
[313] Sepulveda JC, Tome M, Fernandez ME, Delgado M, Campisi J, Bernad A, et al. Cell senescence abrogates the therapeutic potential of human mesenchymal stem cells in the lethal endotoxemia model. Stem Cells. 2014;32:1865-77.

[314] Wagner W, Horn P, Castoldi M, Diehlmann A, Bork S, Saffrich R, et al. Replicative senescence of mesenchymal stem cells: a continuous and organized process. PLoS One. 2008;3:e2213.
[315] Geissler S, Textor M, Kuhnisch J, Konnig D, Klein O, Ode A, et al. Functional comparison of chronological and in vitro aging: differential role of the cytoskeleton and mitochondria in mesenchymal stromal cells. PLoS One. 2012;7:e52700.
[316] Fulop T, Dupuis G, Baehl S, Le Page A, Bourgade K, Frost E, et al. From inflamm-aging to immune-paralysis: a slippery slope during aging for immune-adaptation. Biogerontology. 2016;17:147-57.
[317] Fulop T, Larbi A, Dupuis G, Le Page A, Frost EH, Cohen AA, et al. Immunosenescence and Inflamm-Aging As Two Sides of the Same Coin: Friends or Foes? Front Immunol. 2017;8:1960.
[318] Lacey DC, Simmons PJ, Graves SE, Hamilton JA. Proinflammatory cytokines inhibit osteogenic differentiation from stem cells: implications for bone repair during inflammation. Osteoarthritis Cartilage. 2009;17:735-42.
[319] Gowen M, Wood DD, Ihrie EJ, McGuire MK, Russell RG. An interleukin 1 like factor stimulates bone resorption in vitro. Nature. 1983;306:378-80.
[320] Bertolini DR, Nedwin GE, Bringman TS, Smith DD, Mundy GR. Stimulation of bone resorption and inhibition of bone formation in vitro by human tumour necrosis factors. Nature. 1986;319:516-8.
[321] Girasole G, Jilka RL, Passeri G, Boswell S, Boder G, Williams DC, et al. 17 beta-estradiol inhibits interleukin-6 production by bone marrow-derived stromal cells and osteoblasts in vitro: a potential mechanism for the antiosteoporotic effect of estrogens. J Clin Invest. 1992;89:883-91.
[322] Liu M, Wang K, Tang T, Dai K, Zhu Z. The effect of simvastatin on the differentiation of marrow stromal cells from aging rats. Pharmazie. 2009;64:43-8.
[323] Yazawa H, Zimmermann B, Asami Y, Bernimoulin JP. Simvastatin promotes cell metabolism, proliferation, and osteoblastic differentiation in human periodontal ligament cells. J Periodontol. 2005;76:295-302.
[324] Chen PY, Sun JS, Tsuang YH, Chen MH, Weng PW, Lin FH. Simvastatin promotes osteoblast viability and differentiation via Ras/Smad/Erk/BMP-2 signaling pathway. Nutr Res. 2010;30:191-9.
[325] Maeda T, Kawane T, Horiuchi N. Statins augment vascular endothelial growth factor expression in osteoblastic cells via inhibition of protein prenylation. Endocrinology. 2003;144:681-92.
[326] Maeda T, Matsunuma A, Kurahashi I, Yanagawa T, Yoshida H, Horiuchi N. Induction of osteoblast differentiation indices by statins in MC3T3-E1 cells. J Cell Biochem. 2004;92:458-71.
[327] Maeda T, Matsunuma A, Kawane T, Horiuchi N. Simvastatin promotes osteoblast differentiation and mineralization in MC3T3-E1 cells. Biochem Biophys Res Commun. 2001;280:874-7.
[328] Sugiyama M, Kodama T, Konishi K, Abe K, Asami S, Oikawa S. Compactin and simvastatin, but not pravastatin, induce bone morphogenetic protein-2 in human osteosarcoma cells. Biochem Biophys Res Commun. 2000;271:688-92.
[329] Yamashita M, Otsuka F, Mukai T, Yamanaka R, Otani H, Matsumoto Y, et al. Simvastatin inhibits osteoclast differentiation induced by bone morphogenetic protein-2 and RANKL through regulating MAPK, AKT and Src signaling. Regul Pept. 2010;162:99-108.

[330] Robey PG, Termine JD. Human bone cells in vitro. Calcif Tissue Int. 1985;37:453-60.
[331] Yew TL, Chiu FY, Tsai CC, Chen HL, Lee WP, Chen YJ, et al. Knockdown of p21(Cip1/Waf1) enhances proliferation, the expression of stemness markers, and osteogenic potential in human mesenchymal stem cells. Aging Cell. 2011;10:349-61.
[332] Evans CE, Jones S. Soluble factors secreted by macrophage-like cells in vitro cause osteoprogenitor cell detachment. Calcif Tissue Int. 1998;63:496-504.
[333] Assmus B, Urbich C, Aicher A, Hofmann WK, Haendeler J, Rossig L, et al. HMG-CoA reductase inhibitors reduce senescence and increase proliferation of endothelial progenitor cells via regulation of cell cycle regulatory genes. Circ Res. 2003;92:1049-55.
[334] Lecka-Czernik B, Gubrij I, Moerman EJ, Kajkenova O, Lipschitz DA, Manolagas SC, et al. Inhibition of Osf2/Cbfa1 expression and terminal osteoblast differentiation by PPARgamma2. J Cell Biochem. 1999;74:357-71.
[335] Mundy G, Garrett R, Harris S, Chan J, Chen D, Rossini G, et al. Stimulation of bone formation in vitro and in rodents by statins. Science. 1999;286:1946-9.
[336] Song C, Guo Z, Ma Q, Chen Z, Liu Z, Jia H, et al. Simvastatin induces osteoblastic differentiation and inhibits adipocytic differentiation in mouse bone marrow stromal cells. Biochem Biophys Res Commun. 2003;308:458-62.
[337] Ohnaka K, Shimoda S, Nawata H, Shimokawa H, Kaibuchi K, Iwamoto Y, et al. Pitavastatin enhanced BMP-2 and osteocalcin expression by inhibition of Rho-associated kinase in human osteoblasts. Biochem Biophys Res Commun. 2001;287:337-42.
[338] Ghosh-Choudhury N, Mandal CC, Choudhury GG. Statin-induced Ras activation integrates the phosphatidylinositol 3-kinase signal to Akt and MAPK for bone morphogenetic protein-2 expression in osteoblast differentiation. J Biol Chem. 2007;282:4983-93.
[339] Ehrlich M, Gutman O, Knaus P, Henis YI. Oligomeric interactions of TGF-beta and BMP receptors. FEBS Lett. 2012;586:1885-96.
[340] Gonzalez-Sastre A, Molina MD, Salo E. Inhibitory Smads and bone morphogenetic protein (BMP) modulate anterior photoreceptor cell number during planarian eye regeneration. Int J Dev Biol. 2012;56:155-63.
[341] Tai IC, Wang YH, Chen CH, Chuang SC, Chang JK, Ho ML. Simvastatin enhances Rho/actin/cell rigidity pathway contributing to mesenchymal stem cells' osteogenic differentiation. Int J Nanomedicine. 2015;10:5881-94.
[342] Thylin MR, McConnell JC, Schmid MJ, Reckling RR, Ojha J, Bhattacharyya I, et al. Effects of simvastatin gels on murine calvarial bone. J Periodontol. 2002;73:1141-8.
[343] Naito Y, Terukina T, Galli S, Kozai Y, Vandeweghe S, Tagami T, et al. The effect of simvastatin-loaded polymeric microspheres in a critical size bone defect in the rabbit calvaria. Int J Pharm. 2014;461:157-62.
[344] Bae MS, Yang DH, Lee JB, Heo DN, Kwon YD, Youn IC, et al. Photo-cured hyaluronic acid-based hydrogels containing simvastatin as a bone tissue regeneration scaffold. Biomaterials. 2011;32:8161-71.
[345] Huang X, Huang Z, Li W. Highly efficient release of simvastatin from simvastatin-loaded calcium sulphate scaffolds enhances segmental bone regeneration in rabbits. Mol Med Rep. 2014;9:2152-8.
[346] Fukui T, Ii M, Shoji T, Matsumoto T, Mifune Y, Kawakami Y, et al. Therapeutic effect of local administration of low-dose simvastatin-conjugated gelatin hydrogel for fracture healing. J Bone Miner Res. 2012;27:1118-31.

[347] Liu X, Holzwarth JM, Ma PX. Functionalized synthetic biodegradable polymer scaffolds for tissue engineering. Macromol Biosci. 2012;12:911-9.
[348] Tanigo T, Takaoka R, Tabata Y. Sustained release of water-insoluble simvastatin from biodegradable hydrogel augments bone regeneration. J Control Release. 2010;143:201-6.
[349] Canal C, Khurana, K., Gallinetti, S., Bhatt, S., Pulpytel, J., Arefi-Khonsari, F., & Ginebra, M. -. Design of calcium phosphate scaffolds with controlled simvastatin release by plasma polymerization. Polymer (United Kingdom), . 92, 170-178 101016/jpolymer201603069. 2016.
[350] Santana WM, Sousa DN, Ferreira VM, Duarte WR. Simvastatin and biphasic calcium phosphate affects bone formation in critical-sized rat calvarial defects. Acta Cir Bras. 2016;31:300-7.
[351] Yu WL, Sun TW, Qi C, Zhao HK, Ding ZY, Zhang ZW, et al. Enhanced osteogenesis and angiogenesis by mesoporous hydroxyapatite microspheres-derived simvastatin sustained release system for superior bone regeneration. Sci Rep. 2017;7:44129.
[352] Liu Y, Zhang X, Liu Y, Jin X, Fan C, Ye H, et al. Bi-functionalization of a calcium phosphate-coated titanium surface with slow-release simvastatin and metronidazole to provide antibacterial activities and pro-osteodifferentiation capabilities. PLoS One. 2014;9:e97741.
[353] Zhang X, Jiang W, Liu Y, Zhang P, Wang L, Li W, et al. Human adipose-derived stem cells and simvastatin-functionalized biomimetic calcium phosphate to construct a novel tissue-engineered bone. Biochem Biophys Res Commun. 2018;495:1264-70.
[354] Yin H, Li YG, Si M, Li JM. Simvastatin-loaded macroporous calcium phosphate cement: preparation, in vitro characterization, and evaluation of in vivo performance. J Biomed Mater Res A. 2012;100:2991-3000.
[355] Montazerolghaem M, Engqvist H, Karlsson Ott M. Sustained release of simvastatin from premixed injectable calcium phosphate cement. J Biomed Mater Res A. 2014;102:340-7.
[356] Joensuu K, Uusitalo L, Alm JJ, Aro HT, Hentunen TA, Heino TJ. Enhanced osteoblastic differentiation and bone formation in co-culture of human bone marrow mesenchymal stromal cells and peripheral blood mononuclear cells with exogenous VEGF. Orthop Traumatol Surg Res. 2015;101:381-6.
[357] Salati S, Lisignoli G, Manferdini C, Pennucci V, Zini R, Bianchi E, et al. Co-culture of hematopoietic stem/progenitor cells with human osteblasts favours mono/macrophage differentiation at the expense of the erythroid lineage. PLoS One. 2013;8:e53496.
[358] Naskar D, Nayak S, Dey T, Kundu SC. Non-mulberry silk fibroin influence osteogenesis and osteoblast-macrophage cross talk on titanium based surface. Sci Rep. 2014;4:4745.
[359] Tu MG, Chen YW, Shie MY. Macrophage-mediated osteogenesis activation in co-culture with osteoblast on calcium silicate cement. J Mater Sci Mater Med. 2015;26:276.
[360] Schroder HC, Wang XH, Wiens M, Diehl-Seifert B, Kropf K, Schlossmacher U, et al. Silicate modulates the cross-talk between osteoblasts (SaOS-2) and osteoclasts (RAW 264.7 cells): inhibition of osteoclast growth and differentiation. J Cell Biochem. 2012;113:3197-206.
[361] Chen Z, Yuen J, Crawford R, Chang J, Wu C, Xiao Y. The effect of osteoimmunomodulation on the osteogenic effects of cobalt incorporated beta-tricalcium phosphate. Biomaterials. 2015;61:126-38.
[362] McWhorter FY, Wang T, Nguyen P, Chung T, Liu WF. Modulation of macrophage phenotype by cell shape. Proc Natl Acad Sci U S A. 2013;110:17253-8.

[363] Chen S, Jones JA, Xu Y, Low HY, Anderson JM, Leong KW. Characterization of topographical effects on macrophage behavior in a foreign body response model. Biomaterials. 2010;31:3479-91.
[364] Murphy CM, Matsiko A, Haugh MG, Gleeson JP, O'Brien FJ. Mesenchymal stem cell fate is regulated by the composition and mechanical properties of collagen-glycosaminoglycan scaffolds. J Mech Behav Biomed Mater. 2012;11:53-62.
[365] Sussman EM, Halpin MC, Muster J, Moon RT, Ratner BD. Porous implants modulate healing and induce shifts in local macrophage polarization in the foreign body reaction. Ann Biomed Eng. 2014;42:1508-16.
[366] Patel NR, Bole M, Chen C, Hardin CC, Kho AT, Mih J, et al. Cell elasticity determines macrophage function. PLoS One. 2012;7:e41024.

Appendix 1: Older Human Osteoprogenitors Data

This appendix represents the in vitro assessment of:

A- Cytokine production by human osteoprogenitors derived from older patients treated with β-hydroxy acid form of SIMV at either 4 hrs , day 3 or day 7.

B- Mineralized nodules by human osteoprogenitors derived from older patients treated with β-hydroxy acid addition of SIMV at either 4 hrs , day 3 or day 7.

C- Osteogenic genes of human osteoprogenitors derived from older patients with β-hydroxy acid addition of SIMV starting on day 7.

D- Cytokine production and proliferation response of human osteoprogenitors derived from older patients treated with SIMV delayed delivered from bCaP.

E- Osteogenic genes of human osteoprogenitors derived from older patients treated with SIMV delayed delivered from bCaP.

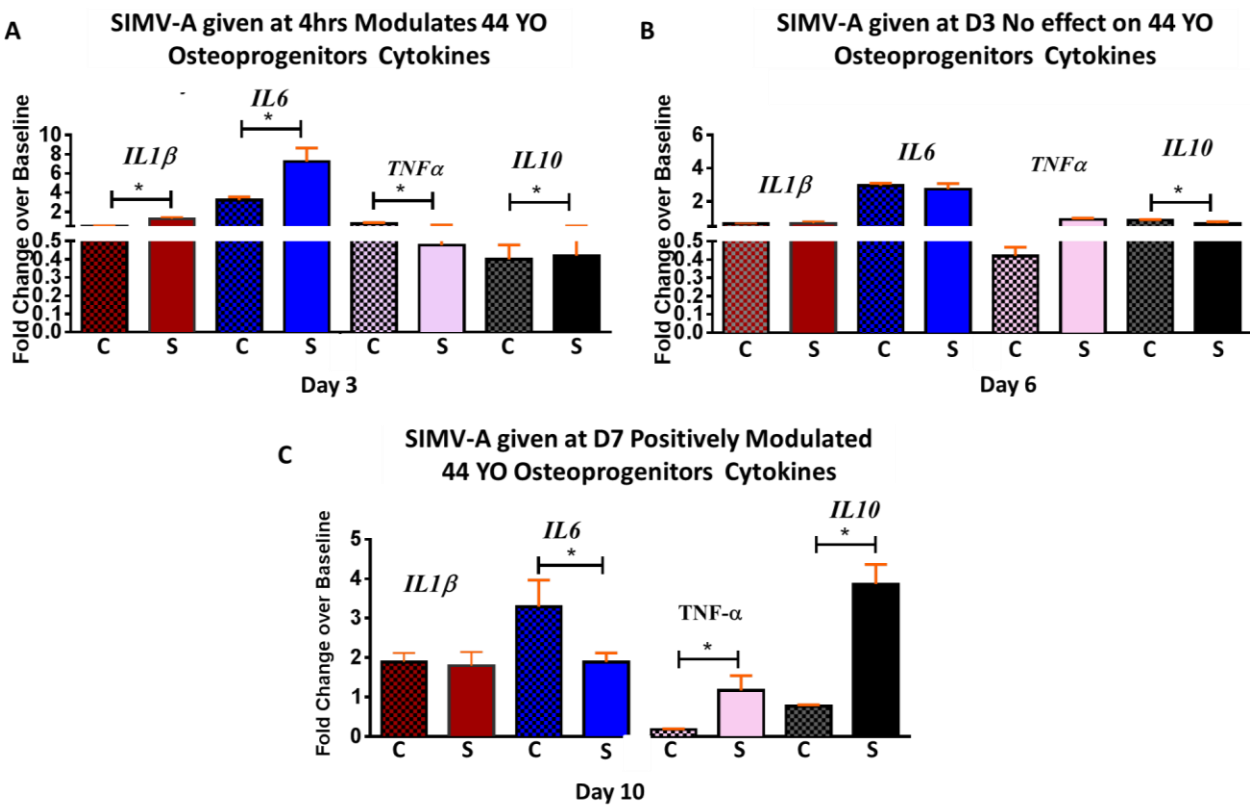

Appendix 1-Figure 1: RT-qPCR gene expression of inflammatory cytokines of human osteoprogenitors from a 44 year old female treated with SIMV-A. (A). Day 3 gene expression of inflammatory cytokines with SIMV-A given at 4hrs showing increased in (*IL1β* and *IL6* but not *TNFα*) and reduced pro-reparative *IL10* as compared to vehicle-treated control. Data presented as fold-change compared to 4hrs baseline. (B). Day 6 gene expression of inflammatory cytokines with SIMV-A given at day 3 showing no change in cytokines production as compared to vehicle-treated control. Data presented as fold-change compared to day 3 baseline. And (C). Day 10 gene expression of inflammatory cytokines with SIMV-A given at day 7 showing reduction in (*IL1β* and *IL6* but not *TNFα*) with increased in pro-reparative *IL10* as compared to vehicle-treated control. Data presented as fold-change compared to day 7 baseline. Statistical analysis was performed using GraphPad software. t: test analysis of each time point was performed and a $P < 0.05$ was considered significantly different.

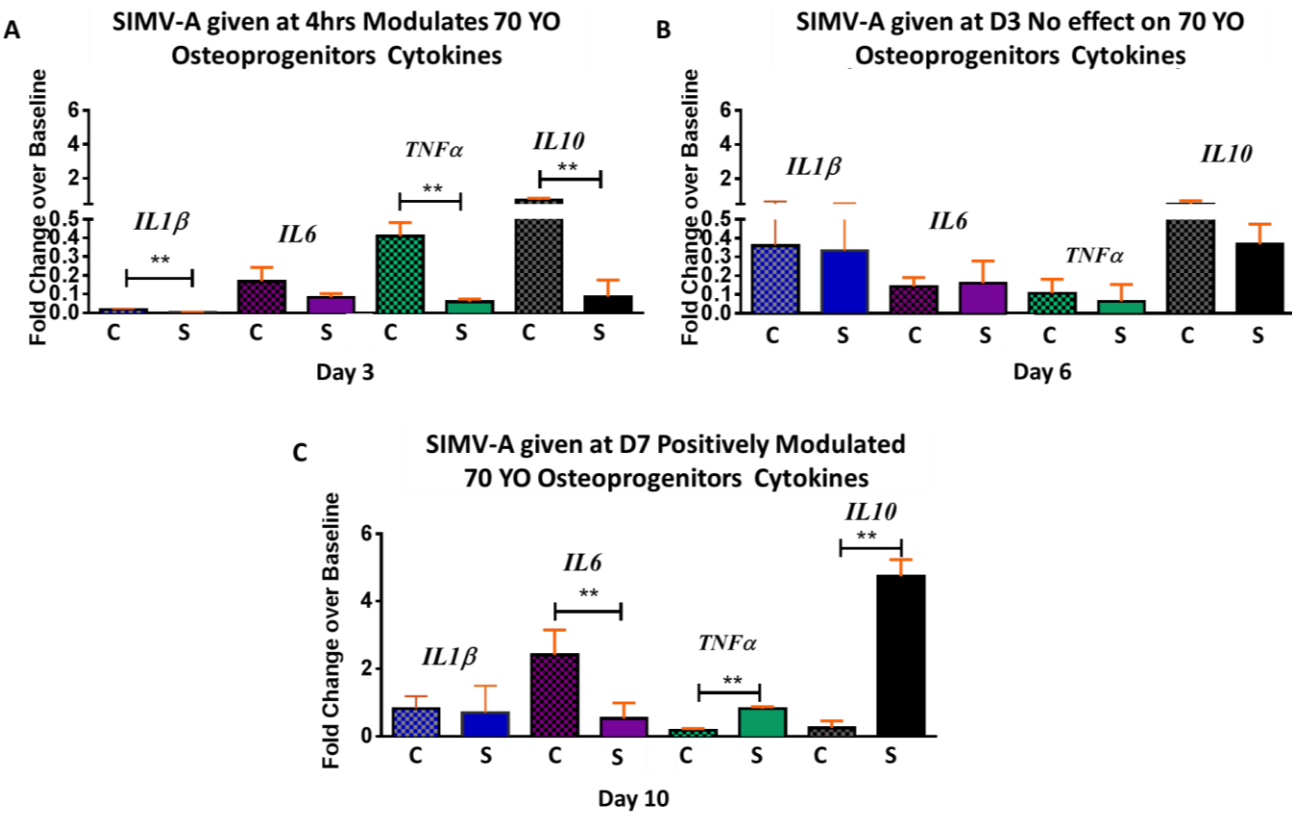

Appendix 1-Figure 2 : Delayed dosing of SIMV-A enhanced pro-reparative cytokines. RT-qPCR gene expression of inflammatory cytokines of human osteoprogenitors from a 70 year old female treated with SIMV-A. (A). Day 3 gene expression of inflammatory cytokines with SIMV-A given at 4hrs showing increased in (*IL1β*, *IL6* and *TNFα*) and reduced pro-reparative *IL10* as compared to vehicle-treated control. Data presented as fold-change compared to 4hrs baseline. (B). Day 6 gene expression of inflammatory cytokines with SIMV-A given at day 3 showing no change in cytokines production as compared to vehicle-treated control. Data presented as fold-change compared to day 3 baseline. And (C). Day 10 gene expression of inflammatory cytokines with SIMV-A given at day 7 showing reduction in (*IL1β* and *IL6* but not *TNFα*) with increased in pro-reparative *IL10* as compared to vehicle-treated control. Data presented as fold-change compared to day 7 baseline. Statistical analysis was performed using GraphPad software. t: test analysis of each time point was performed and a $P < 0.05$ was considered significantly different.

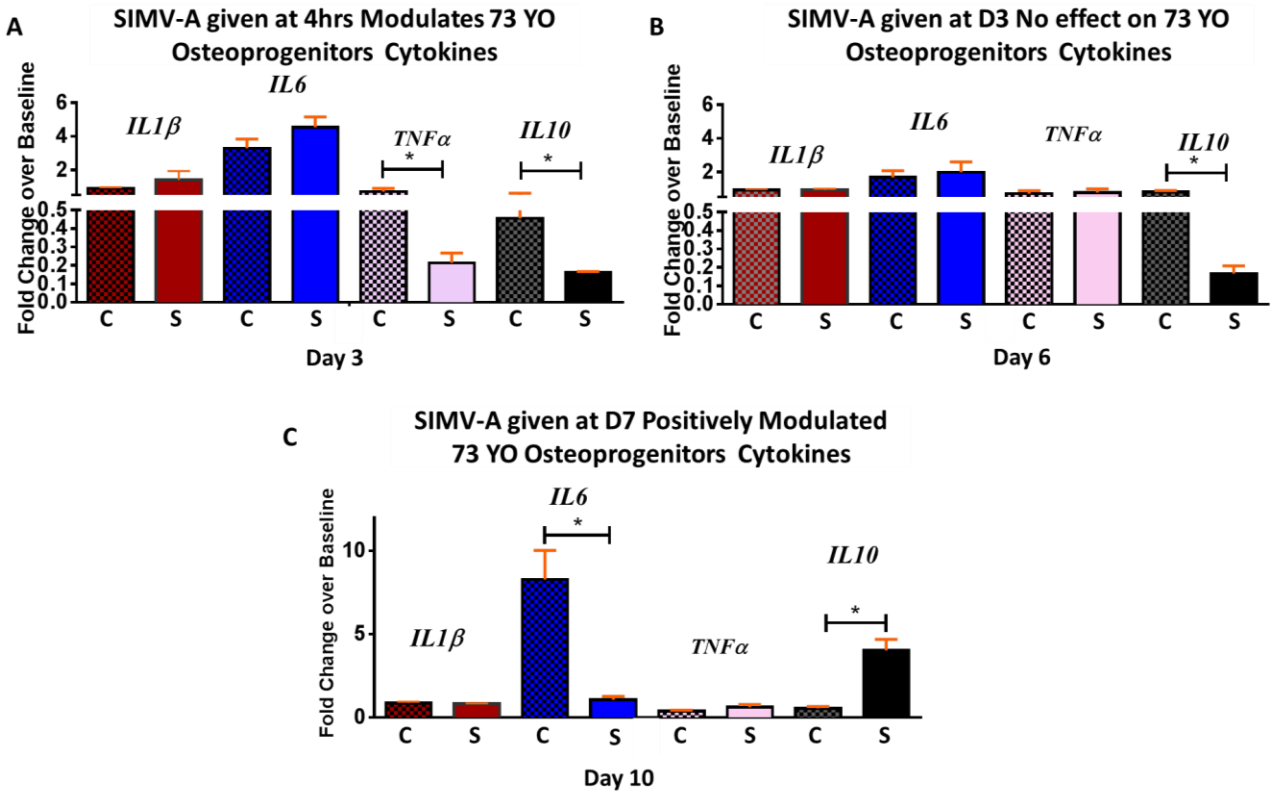

Appendix 1-Figure 3: Delayed dosing of SIMV-A enhanced pro-reparative cytokines. RT-qPCR gene expression of inflammatory cytokines of human osteoprogenitors from a 73 year old female treated with SIMV-A. (A). Day 3 gene expression of inflammatory cytokines with SIMV-A given at 4hrs showing increased in (*IL1β* and *IL6*, but not *TNFα*) and reduced pro-reparative *IL10* as compared to vehicle-treated control. Data presented as fold-change compared to 4hrs baseline. (B). Day 6 gene expression of inflammatory cytokines with SIMV-A given at day 3 showing no change in cytokines production as compared to vehicle-treated control. Data presented as fold-change compared to day 3 baseline. And (C). Day 10 gene expression of inflammatory cytokines with SIMV-A given at day 7 showing reduction in (*IL1β* and *IL6* but not *TNFα*) with increased in pro-reparative *IL10* as compared to vehicle-treated control. Data presented as fold-change compared to day 7 baseline. Statistical analysis was performed using GraphPad software. t: test analysis of each time point was performed and a $P < 0.05$ was considered significantly different.

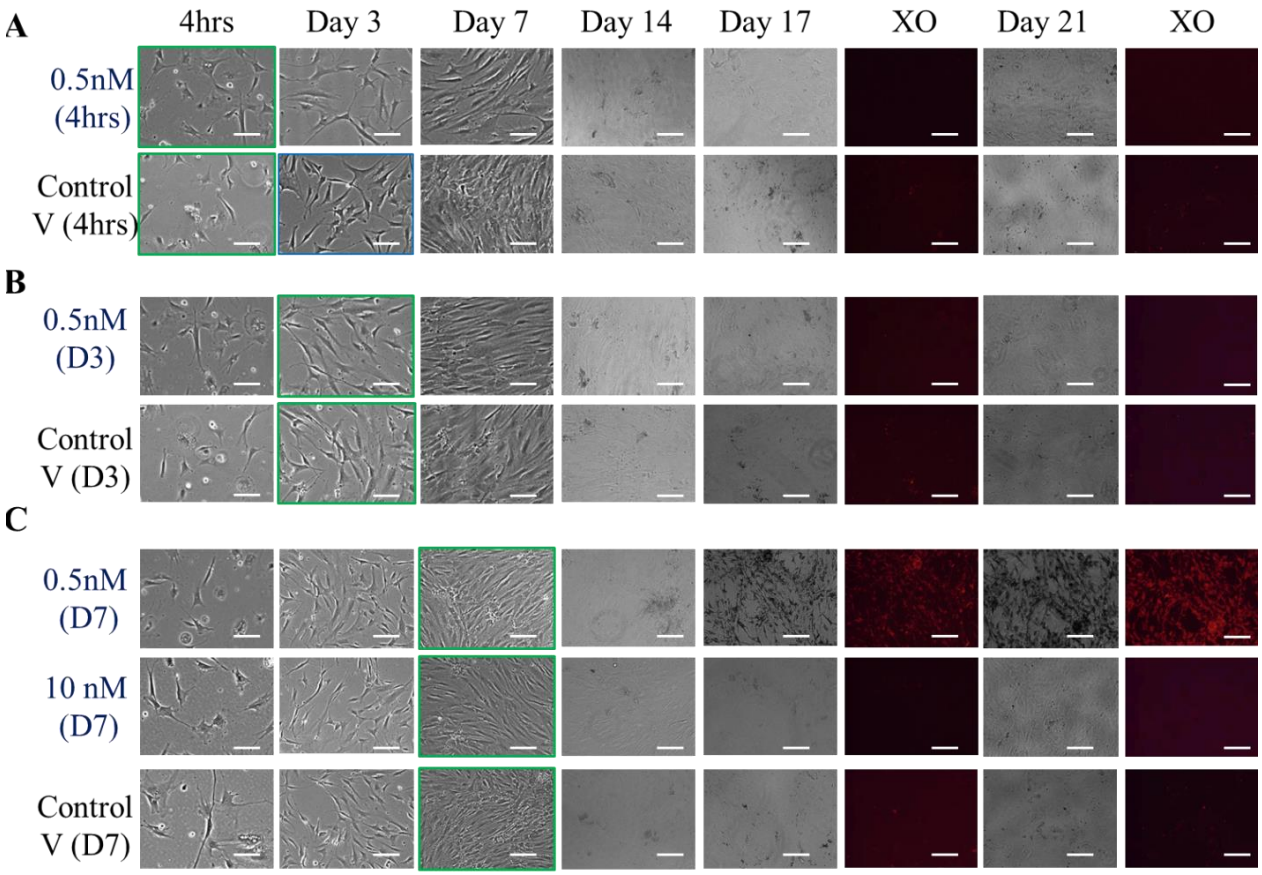

Appendix 1-Figure 4: Human osteoprogenitors from a 70 year old female, passage 2, cells seeded at 15,000 cells/cm^2, treated with SIMV-A, initiated at various times. Green frames indicate the start time of SIMV-A treatment. A) 0.5nM of simvastatin was pipetted after 4hrs of culture and continued twice a week until day 30. B) 0.5nM of simvastatin was pipetted on day 3 of culture and continued twice a week until day 30. C) 0.5nM or 10 nM of simvastatin was pipetted with osteogenic medium on day 7 of culture and continued twice a week until day 30. Osteogenesis of older human osteoprogenitors is increased by delayed 0.5 nM SIMV-A as measured by XO calcium staining. Scale bar 100 um.

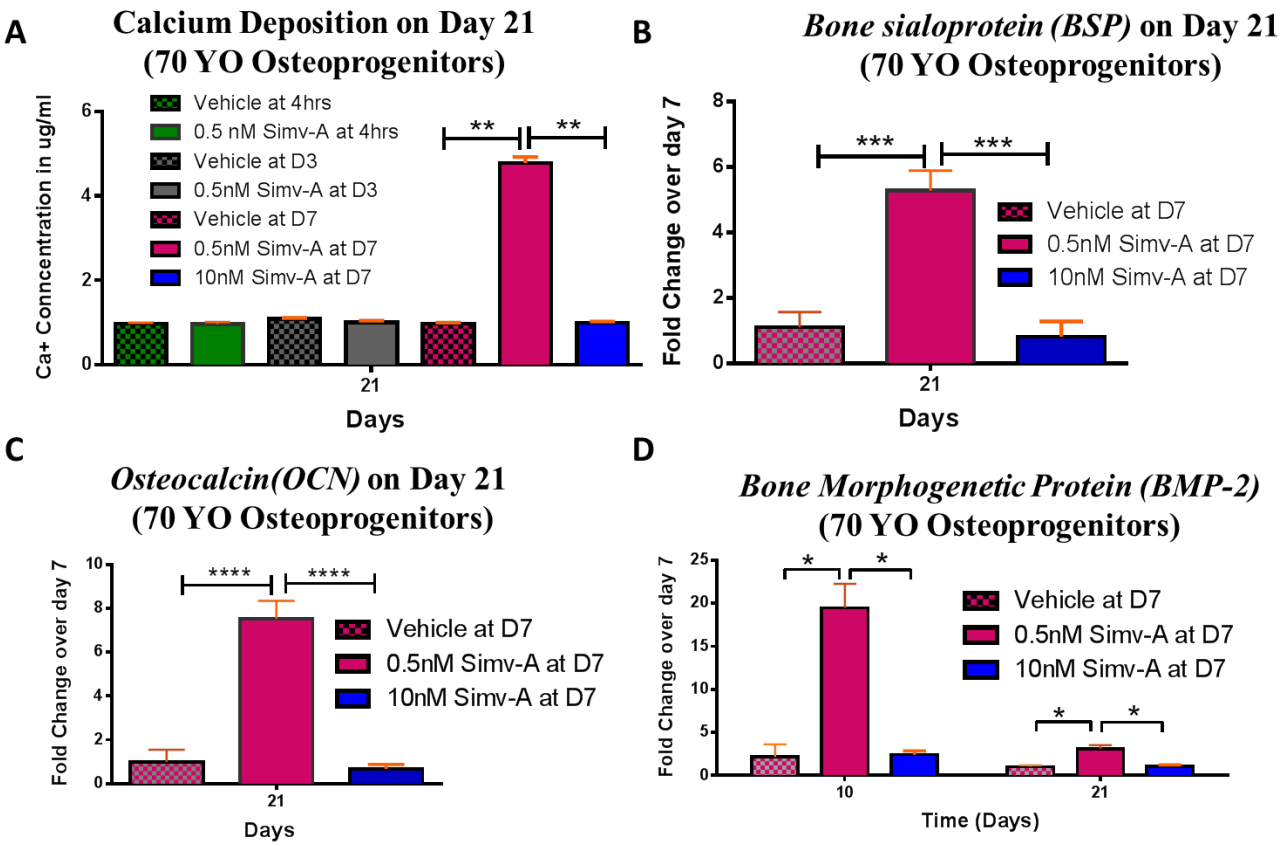

Appendix 1-Figure 5: Human osteoprogenitor 70 years old , passage 2 seeded cells on TCP at 15,000 cells/cm2, treated with SIMV-A at various timing showing enhanced osteogenesis by delayed SIMV-A as measured by (A) Calcium content on day 21 of culture. (B, C, D) elevated osteogenic genes (*BSP*, *OCN* and *BMP-2*) was observed with the addition of 0.5nM at day 7 of culture similar to previous patients. Data presented as fold-change compared to day 7 baseline. Statistical analysis was performed using GraphPad software. Two way ANOVA multiple comparison analysis of each gene was performed and a $P< 0.05$ was considered significantly different. (*P=0.0142, **P= 0.0028 , ****$P< 0.0001$)

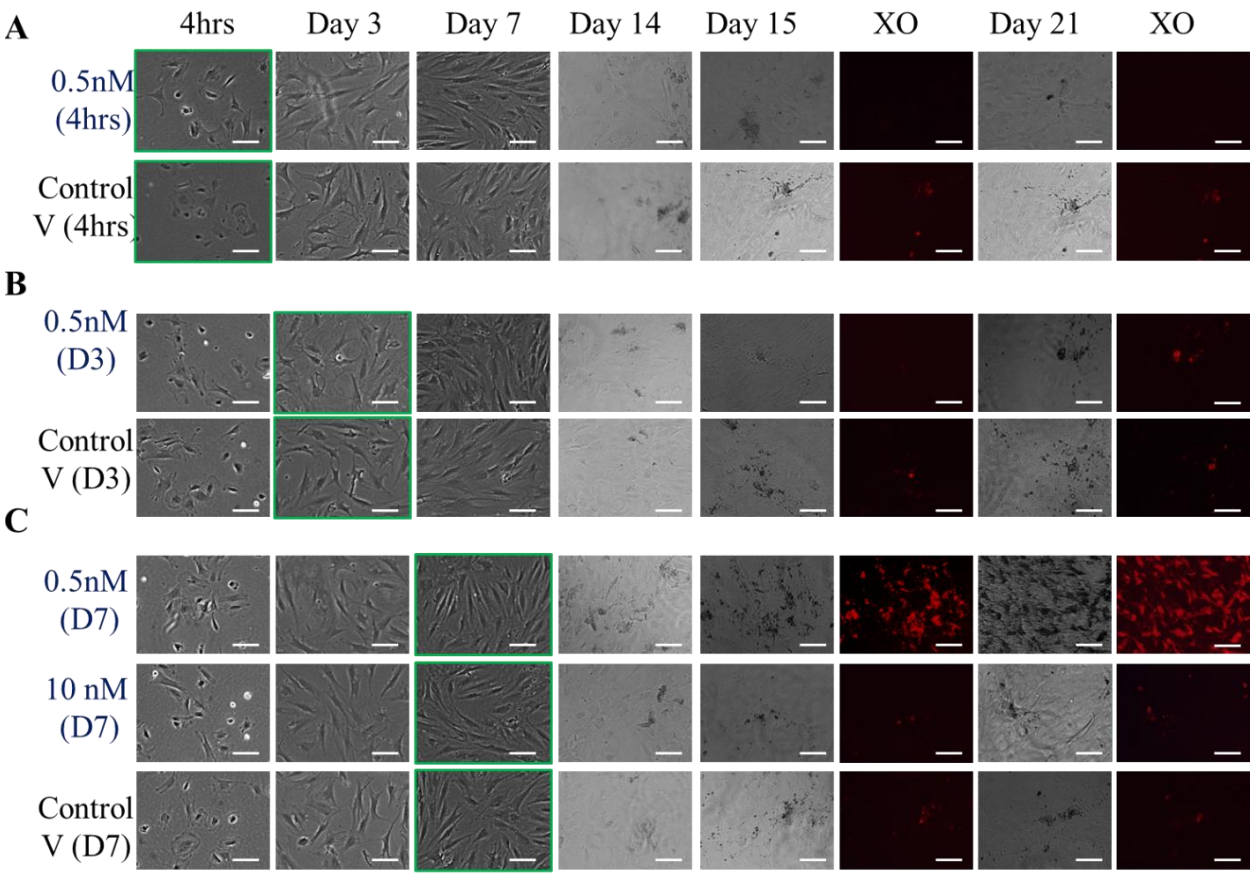

Appendix 1-Figure 6: Human osteoprogenitor 73 years old , passage 2 seeded cells on TCP at 15,000 cells/cm2, treated with SIMV-A at various timing. Green frame indicate the start time of SIMV-A treatment. A) 0.5nM of simvastatin was pipetted after 4hrs of culture and continued twice a week until day 30. B) 0.5nM of simvastatin was pipetted on day 3 of culture and continued twice a week until day 21. C) 0.5nM or 10 nM of simvastatin was pipetted with osteogenic medium on day 7 of culture and continued twice a week until day 21. Osteogenesis of older human osteoprogenitors is increased by delayed 0.5 nM SIMV-A as measured by XO calcium staining. Scale bar 100 um.

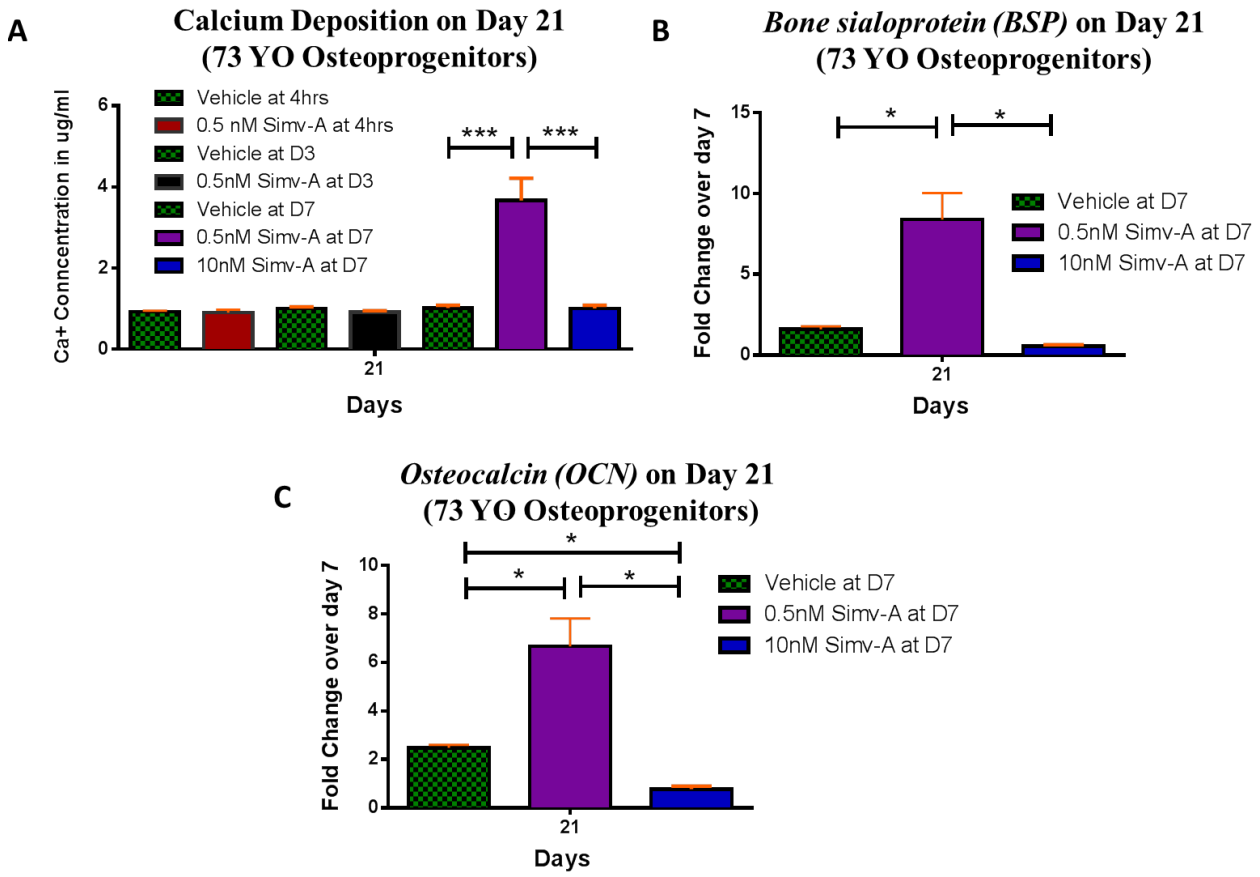

Appendix 1-Figure 7: Human osteoprogenitor 73 years old , passage 2 seeded cells at 15,000 cells/cm2 on TCP, SIMV-A added at various timing showing enhanced osteogenesis by delayed SIMV-A as measured by (A) Calcium content on day 21 of culture. (B, C) elevated osteogenic genes (*BSP*, *OCN* and *BMP-2*) with 0.5nM given at day 7. Data presented as fold-change compared to day 7 baseline. Statistical analysis was performed using GraphPad software. Two way ANOVA multiple comparison analysis of each gene was performed and a $P < 0.05$ was considered significantly different. (*P= 0.0128 , ***P= 0.0003)

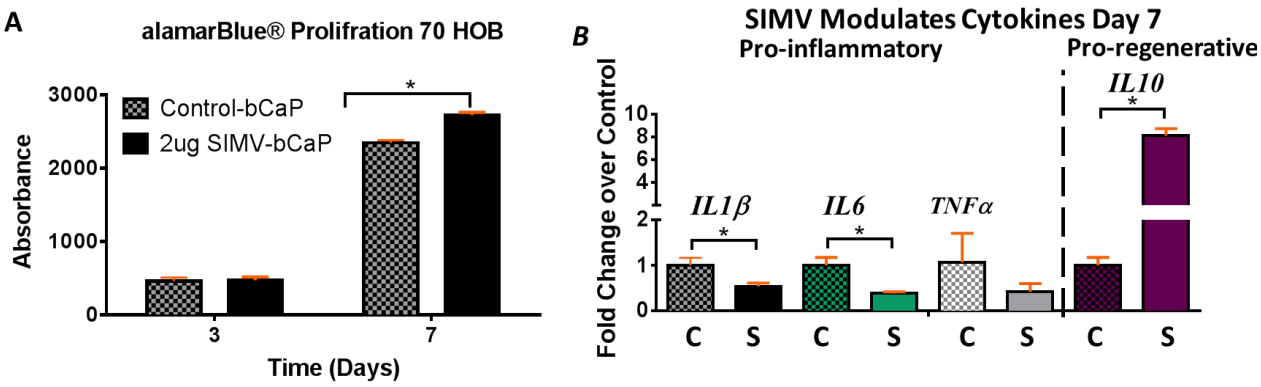

Appendix 1-Figure 8: Human osteoprogenitor 70 years old , passage 2 seeded cells at 30,000 cells/cm2 on C: bCaP coated disks or S: 2 μg SIMV-bCaP. (A) Enhanced proliferation in a dose dependent manner when cultured on 2 μg SIMV-bCaP coated disks as compared to control (bCaP only). (B) Decreased in anti-inflammatory markers (IL1b and *IL6*) with elevation in pro-reparative *IL10* on day 7 when cultured on 2 μg SIMV-bCaP. Data presented as fold-change compared to control. Statistical analysis was performed using GraphPad software. t:test comparison analysis of each gene was performed and a $P < 0.05$ was considered significantly different.

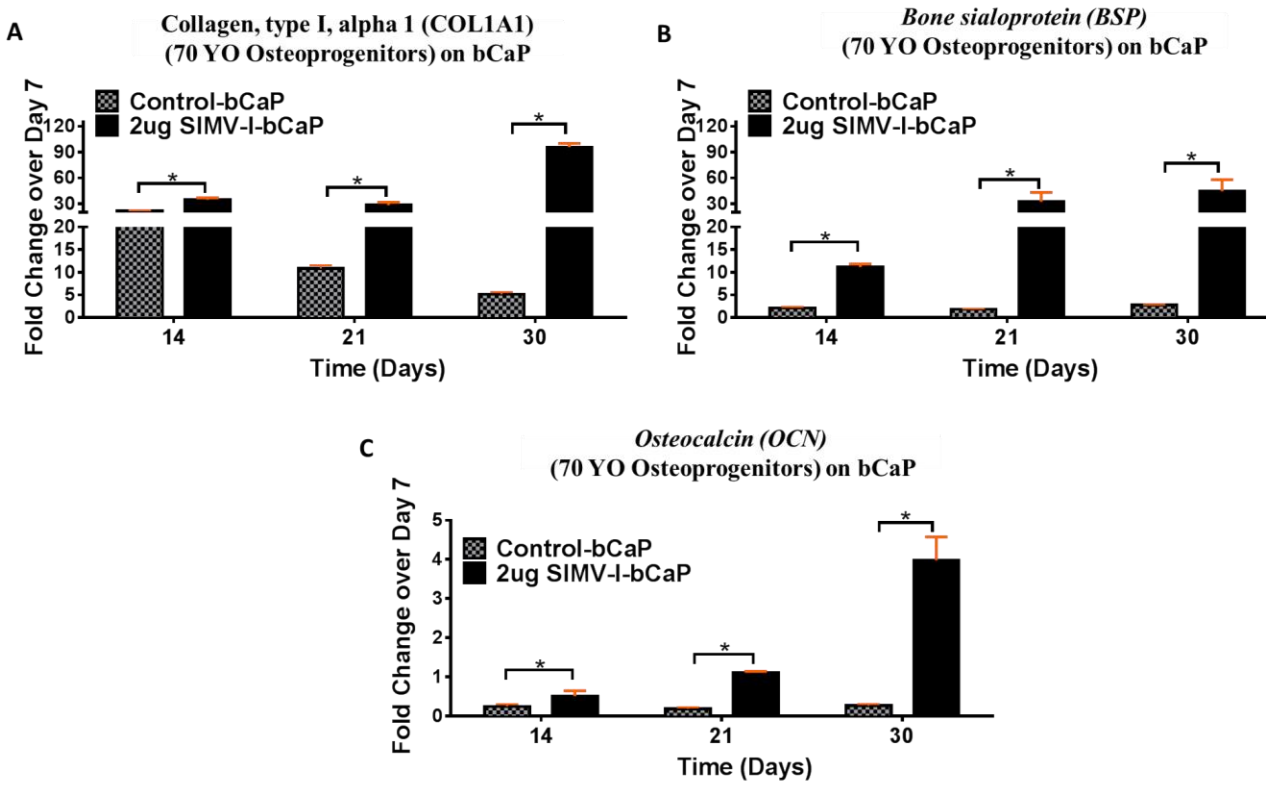

Appendix 1-Figure 9: Enhanced osteogenic effect of Older human osteoprogenitor (70 YO) with delayed delivery of 2 μg SIMV from bCaP. Simvastatin in prodrug form was delayed delivered from bCaP older human osteoprogenitors and enhanced osteogenic response as measured by osteogenic genes (A) *COL1A1*. (B) *BSP* and (C) *OCN*. QPCR data presented in fold change over day 7 (baseline) using 2-ΔΔCT. Statistical analysis was performed using GraphPad software. t: test analysis of each time point was performed and a $P < 0.05$ was considered Significantly different.

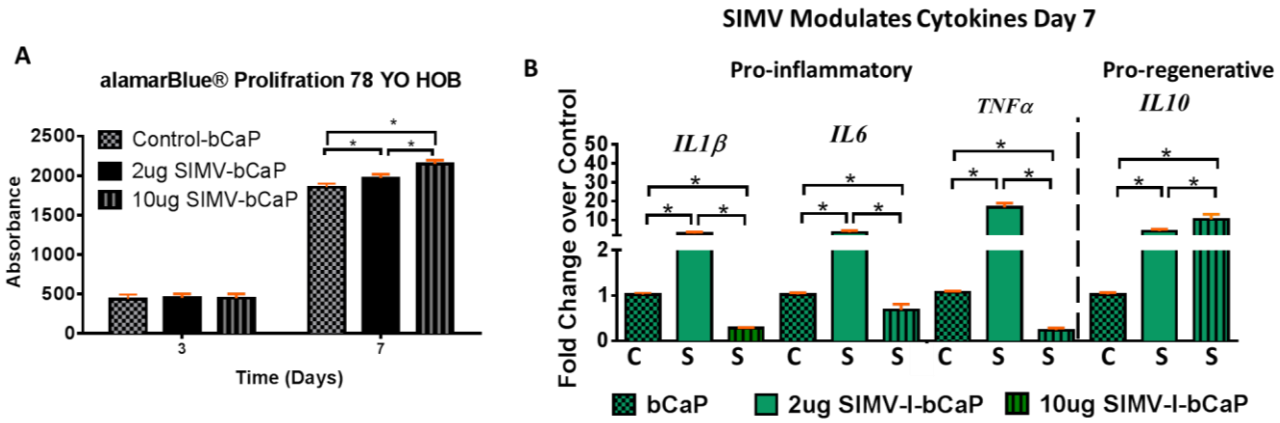

Appendix 1-Figure 10: Human osteoprogenitors from a 78 years old female, passage 2, cells seeded at 30,000 cells/cm^2 on C: bCaP coated disks or S: 2 μg or 10 μg SIMV-bCaP. (A) Enhanced proliferation in a dose dependent manner when cultured on 2 or 10 μg SIMV-bCaP coated disks as compared to control (bCaP only). (B) 10 μg SIMV decreased in anti-inflammatory markers (IL1b, *IL6* and TNFalpha) , (significant increase was observed with 2 μg SIMV-bCaP coated disks), with elevation in pro-reparative *IL10* on day 7 when cultured on both 2 μg and 10 μg SIMV-bCaP. Data presented as fold-change compared to control. Statistical analysis was performed using GraphPad software. Two-way ANOVA multiple comparison analysis of each gene was performed and a $P < 0.05$ was considered significantly different.

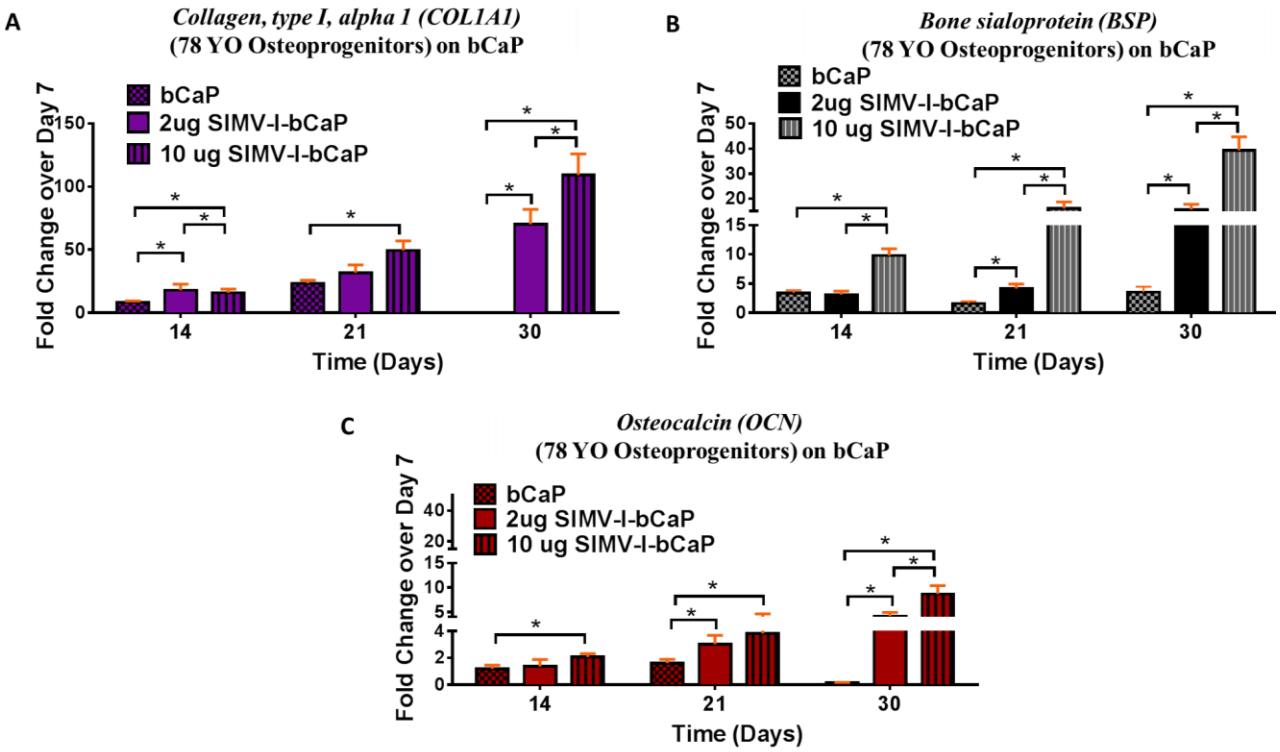

Appendix 1-Figure 11: Enhanced osteogenic effect of older human osteoprogenitors (78 YO female) with delayed delivery of 2 μg or 10 μg SIMV from bCaP. Simvastatin in prodrug form was delayed delivered from bCaP to older human osteoprogenitors and enhanced osteogenic response in a dose dependent manner as measured by osteogenic genes (A) *COL1A1*. (B) *BSP* and (C) *OCN*. QPCR data presented in fold change over day 7 (baseline) using 2-ΔΔCT. Statistical analysis was performed using GraphPad software. t: test analysis of each time point was performed and a $P < 0.05$ was considered Significantly different.

Appendix 2: Older Human Macrophage Data

This appendix represents the in vitro assessment of macrophages derived from peripheral blood of older donors (59 and 67 year old females).

A- Macrophages grown on bCaP as compared to cells grown on polystyrene no drugs.

B- Single factor delivery from bCaP: either the immediate delivery of 250ng IFNγ or the delayed delivery of 10 μg SIMV from bCaP was investigated.

C- Sequential delivery of 250ng IFNγ-bCaP- 10 μg SIMV was also examined as compared to cells grown on bCaP.

Method Primary Older Human Macrophage Isolation:

Macrophages derived from older human peripheral blood (hPB): Human peripheral blood (from females 59 and 67 years old) was used and monocyte were isolated following previously described method using double density gradient centrifugations employing Ficoll Isopaque (40, 41). Briefly, the blood in 50 mL conical tubes was stratified onto Ficoll-Paque PLUS (Fisher Scientific 45-001-749) then centrifuged at 400G for 45 minutes at room temperature. The peripheral blood mononuclear cell (PBMC), at the interface between plasma and Ficoll, were then collected and diluted in EDTA/PBS and centrifuged twice at 200 g for 15 min. The PBMC cells were then plated in RPMI media containing 20% human serum, 1%Pen/Strep in non-treated tissue culture dish. After two hours of initial platting, PBMCs were washed with PBS and and 50 ng/ml human M-CSF was added. Prior to culture on bCaP coated disks, hPBMCs cells were cultured for 7 days to allow for monocyte attachment and differentiation to macrophages. After 7 days, macrophages were gently scrapped and plated on coated disks with or without stimuli

(SIMV or IFNγ or both) at a density of 1 $x10^6$ cells/disk. RPMI media containing 10% heat-inactivated FBS,1%Pen/Strep and 50 ng/ml human M-CSF was used and cells were harvested for gene expression on day 1 and day 6 of culture.

Results Primary Older Human Macrophage on bCaP:

To further examine the effect of bCaP coating on primary macrophages derived from older donor, cells behavior grown on bCaP coating was compared to cells grown on polystyrene non-treated tissue PS. bCaP alone did not affect either M1 or M2 markers as compared to hPB derived macrophages on PS as measured M1 or M2 genes expression of both donors (appendix 2-Figure 1,2).

To examine the effects of delivery from bCaP on primary older human macrophage phenotypes, either the immediate delivery of 250ng IFNγ or delayed delivery of 10 μg SIMV from bCaP was investigated. The delivery of IFNγ alone from bCaP resulted in elevation of *CCL1* (M1 marker) during the course of the study day 1 as compared to day 6. However, *CXCL11* (another M1 marker) was not significantly elevated over time (appendix 2-Figure 3,4 A and B). The delayed delivery of 10 μg SIMV from bCaP resulted in elevation in M2 markers only on day 6 of culture, not seen with IFNγ delivery (appendix 2-Figure 3,4 C and D).

To further investigate older human primary macrophage transition from M1 to M2 state, the sequential delivery of the two factors (250ng IFNγ followed by 10 μg SIMV) from bCaP was also tested using cells from either 59 years old or 67 years old females. The delivery of IFNγ from bCaP before SIMV resulted in elevation of both M1 genes tested, *CCL1* and *CXCL11*, on

day 1 of culture as compared to cells grown on bCaP without drugs with cells from 59 years (appendix 2-Figure 5 A and B). Only *CCL1* , M1 marker, was elevated with IFNγ delivery to macrophages derived from 67 years old female but not *CXCL11* (appendix 2-Figure 6 A and B). The delyed delivery of SIMV after IFNg from bCaP resulted in elevation of both *CD206* and *CD163* (M2 markers) only on day 6 of culture on day 6 of culture indicating the delivery of SIMV happened in delayed manner (appendix 2-Figure 5 and 6).

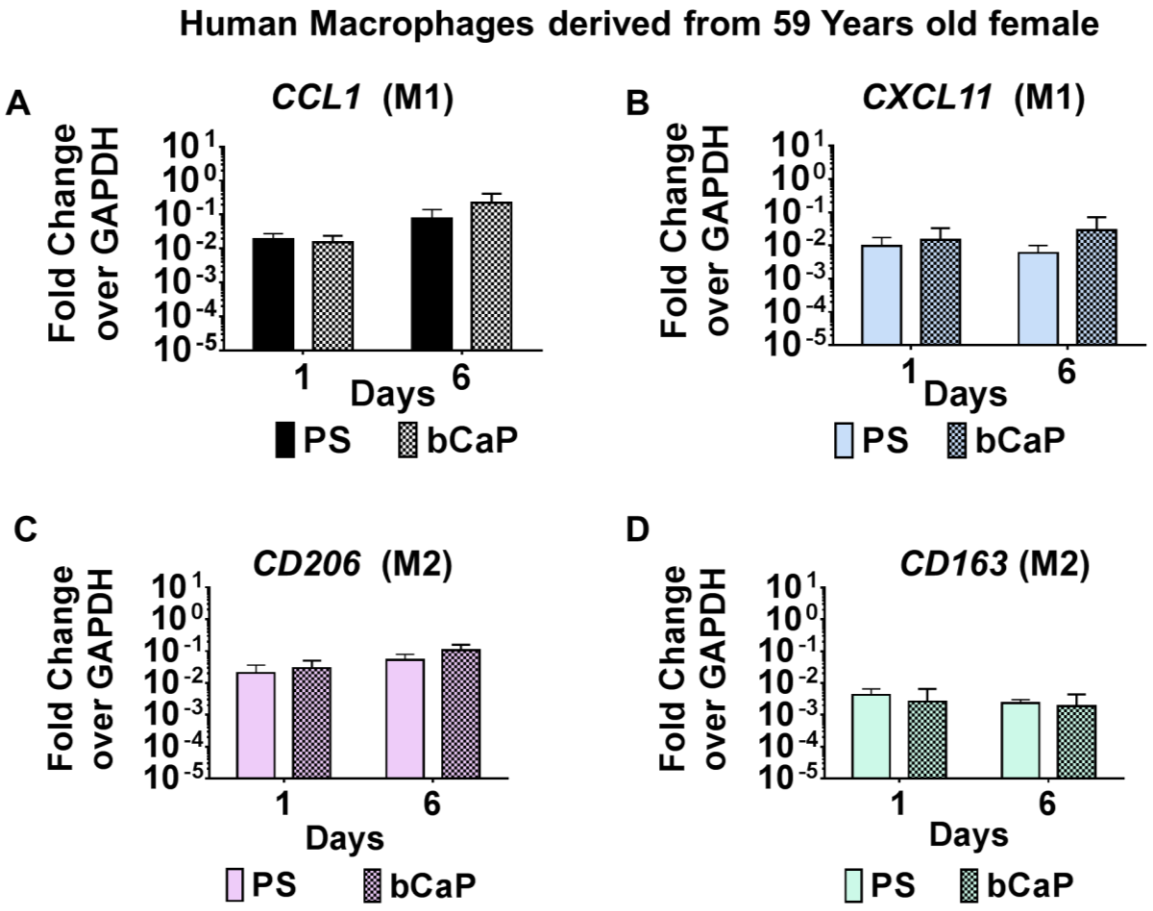

Appendix 2- Figure 1: Gene expression of human primary macrophages derived from a 59 years old female and cultured on bCaP as compared to non-tissue culture-treated polystyrene (PS) on day 1 and day 6 of culture. (A and B) M1 macrophage markers. (C and D) M2 macrophage markers. qRT-PCR data presented as fold change over the housekeeping gene GAPDH.

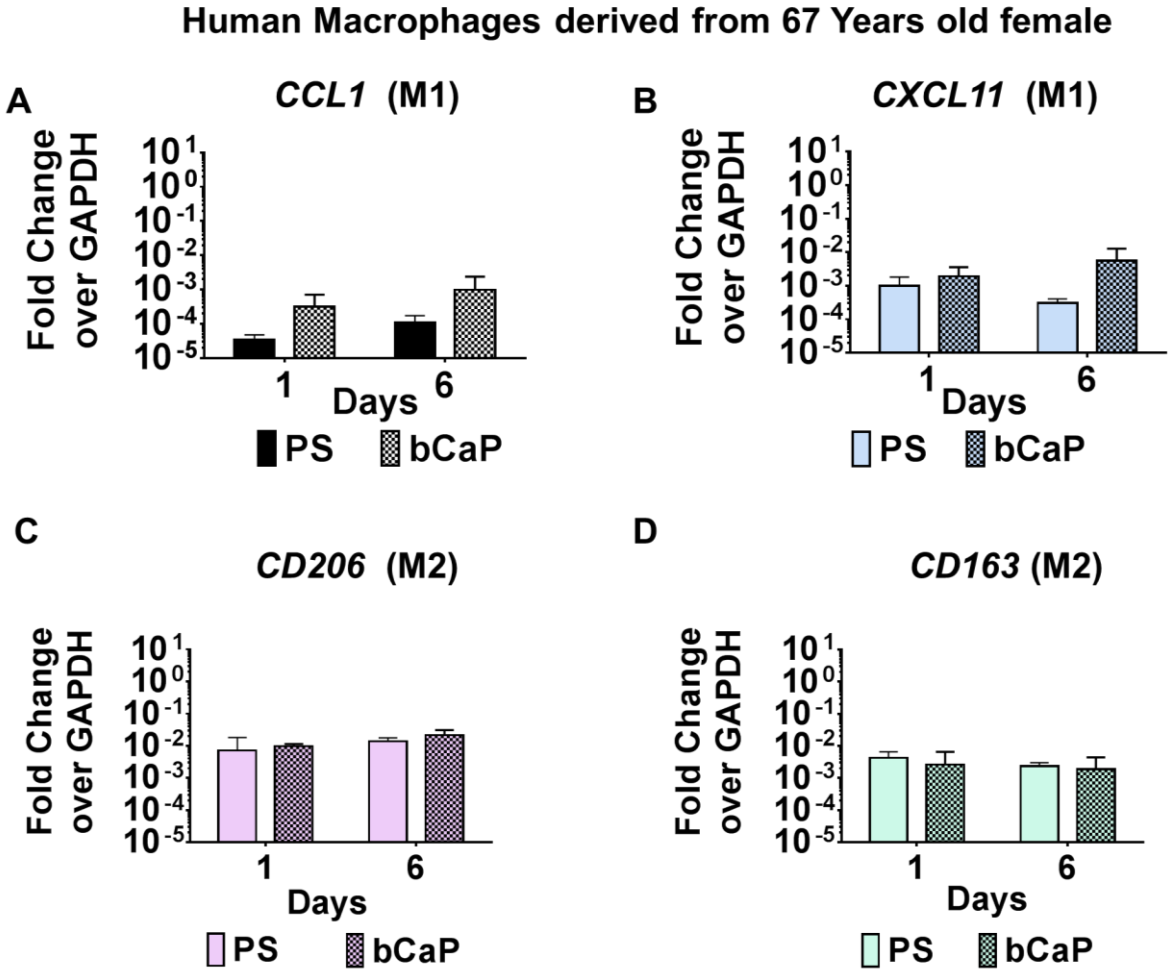

Appendix 2- Figure 2: Gene expression of human primary macrophages derived from a 67 years old female and cultured on bCaP as compared to non-tissue culture-treated polystyrene (PS) on day 1 and day 6 of culture. (A and B) M1 macrophage markers. (C and D) M2 macrophage markers. qRT-PCR data presented as fold change over the housekeeping gene GAPDH.

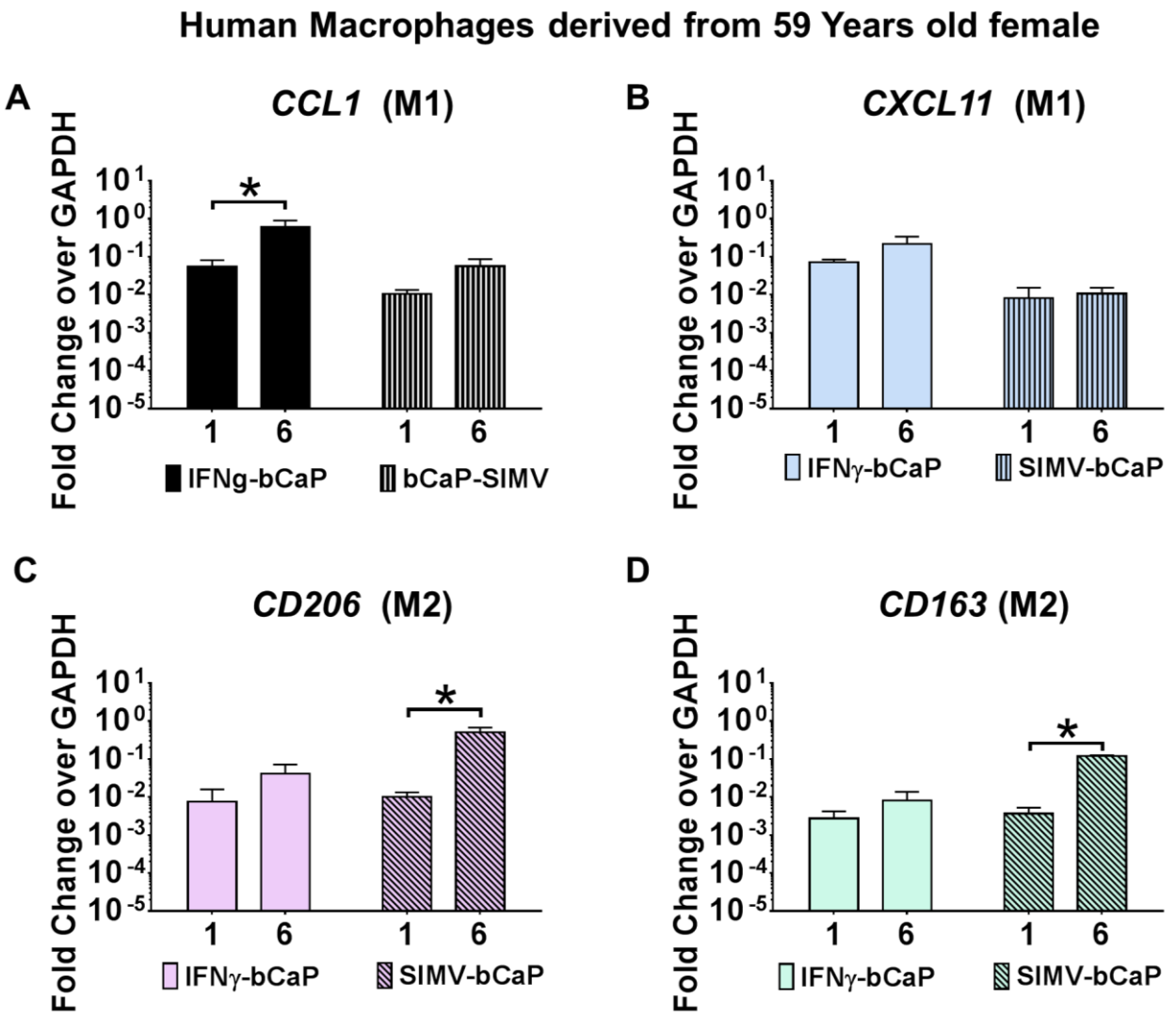

Appendix 2- Figure 3: Single factor delivery study. Gene expression of older human primary macrophage (59 years old female) cultured on bCaP with either IFNγ on the exterior or SIMV below the bCaP barrier layer. (A and B) M1 macrophage markers. (C and D) M2 macrophage markers. Data presented as fold change over the housekeeping gene GAPDH. * $P< 0.05$.

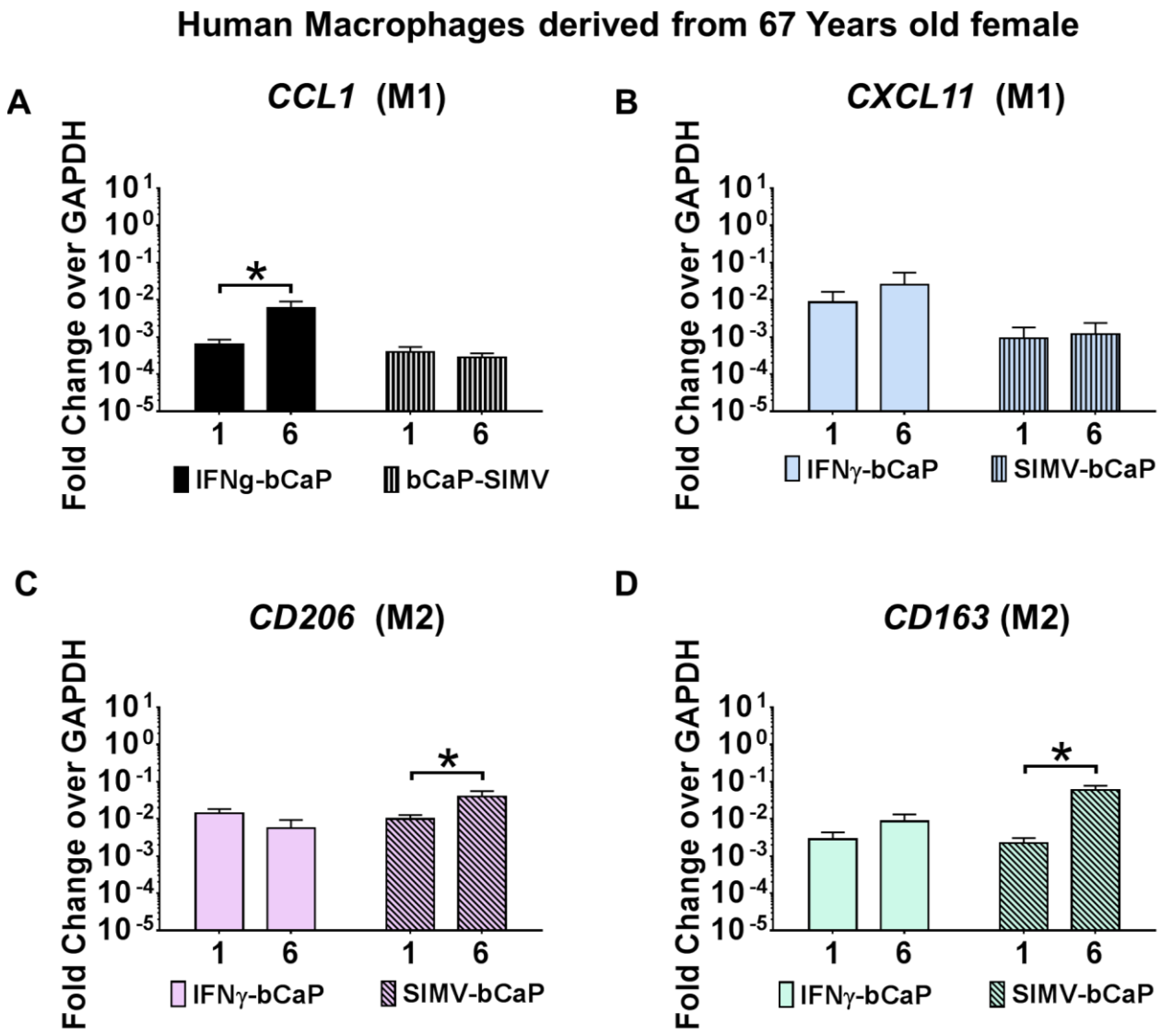

Appendix 2- Figure 4: Single factor delivery study. Gene expression of older human primary macrophages (from a 59 year old female) cultured on bCaP with either IFNγ on the exterior or SIMV below the bCaP barrier layer. (A and B) M1 macrophage markers. (C and D) M2 macrophage markers. Data presented as fold change over the housekeeping gene GAPDH. * P< 0.05.

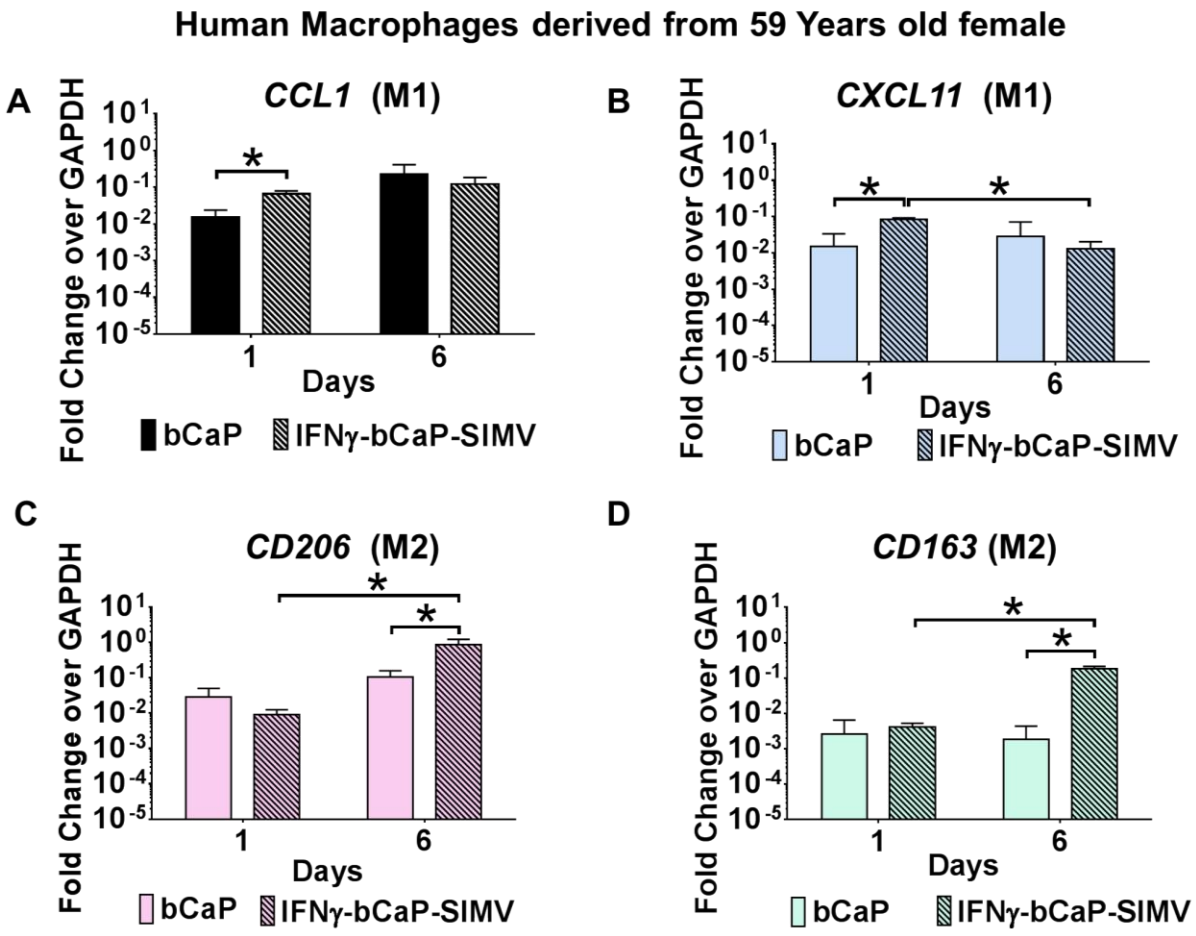

Appendix 2- Figure 5: Gene expression for older human primary macrophage (59 years old female) cultured on bCaP surface with or without 250 ng IFNγ or 10 μg SIMV sequentially delivered from bCaP over 6 days. (A and B) M1 macrophage markers and (C and D) M2 macrophage markers. (F) Schematic representation of the sequential delivery system. * P< 0.05.

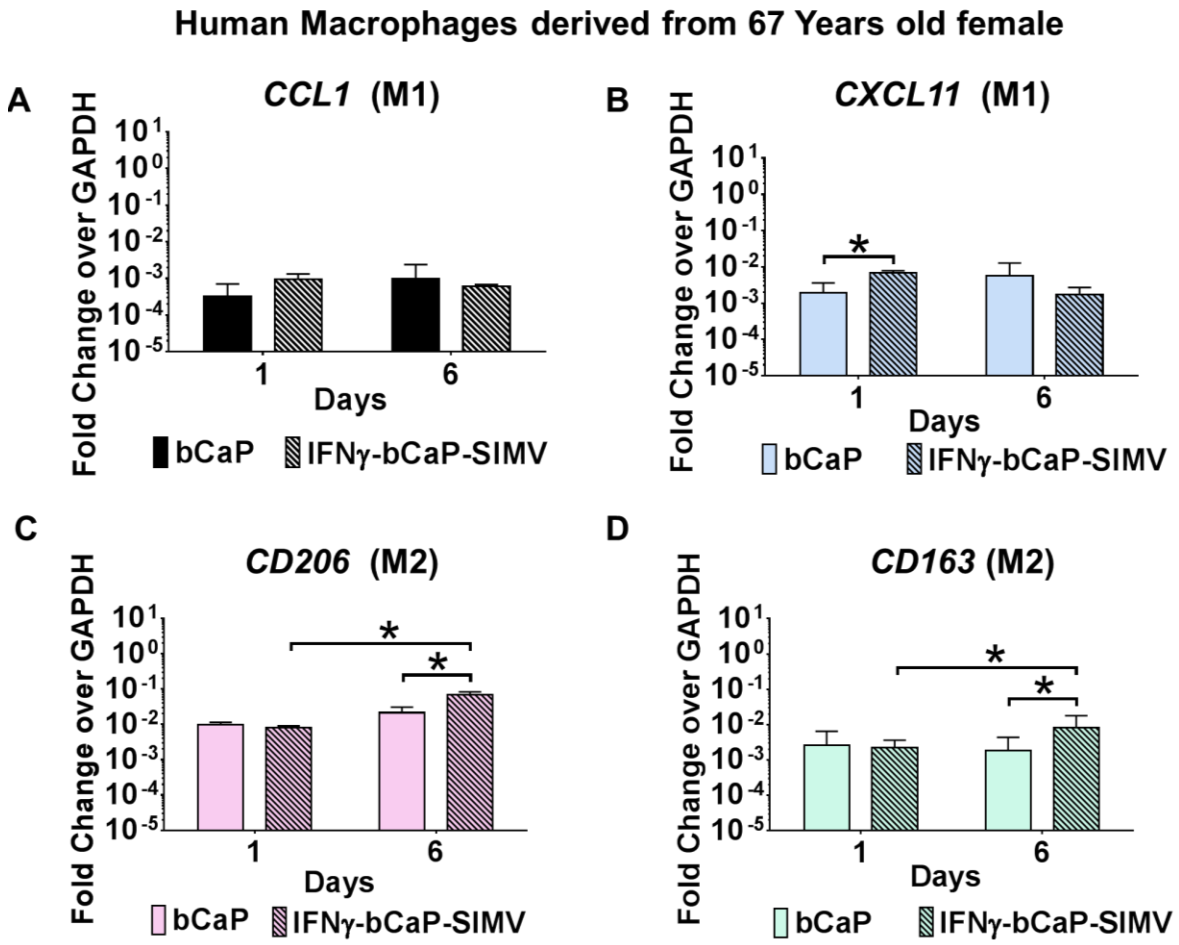

Appendix 2- Figure 6: Gene expression for older human primary macrophage (59 years old female) cultured on bCaP surface with or without 250 ng IFNγ or 10 μg SIMV sequentially delivered from bCaP over 6 days. (A and B) M1 macrophage markers and (C and D) M2 macrophage markers. (F) Schematic representation of the sequential delivery system. * P< 0.05.